NASA CR-175029

CONSTITUTIVE MODELLING OF LUBRICANTS IN CONCENTRATED CONTACTS AT HIGH SLIDE TO ROLL RATIO

By:
Joseph L. Tevaarwerk
Transmission Research Inc.

Dec. 1985

(NASA-CR-175029) CONSTITUTIVE MODELLING OF LUBRICANTS IN CONCENTRATED CONTACTS AT HIGH SLIDE TO ROLL RATIOS Interim Report (Transmission Research, Inc., Cleveland, Ohio.) 85 p HC A05/MF A01 CSCL 11H G3/37

N86-17748

Unclas 05307

Prepared for:

NATIONAL AERONAUTICS AND SPACE ADMINISTRATION
Lewis Research Centre
Cleveland OH 44135
Under Contract DEN 3-35

CONSTITUTIVE MODELLING OF LUBRICANTS IN CONCENTRATED CONTACTS AT HIGH SLIDE-TO-ROLL RATIOS.

By:
Joseph L. Tevaarwerk
Transmission Research Inc.
Dec. 1985.

Prepared for:
NATIONAL AERONAUTICS AND SPACE ADMINISTRATION
Lewis Research Centre
Cleveland, Ohio 44135

1. Report No.	2. Government Accession No.	3. Recipient's Catalog No.
NASA CR-175029		

4. Title and Subtitle	5. Report Date
CONSTITUTIVE MODELLING OF LUBRICANTS IN CONCENTRATED CONTACTS AT HIGH SLIDE TO ROLL RATIOS.	Dec. 1985.
	6. Performing Organization Code

7. Author(s)	8. Performing Organization Report No.
J.L. Tevaarwerk, Applied Tribology RR3 Stokes Lane , Shelburne, VT 05482	10. Work Unit No.

9. Performing Organization Name and Address	11. Contract or Grant No.
Transmission Research Inc. 10823 Magnolia Dr, Cleveland, OHIO 44106	DEN 3-35
	13. Type of Report and Period Covered
12. Sponsoring Agency Name and Address	Contractor Report.
NASA Lewis Research Center. Cleveland OH 44135	14. Sponsoring Agency Code

15. Supplementary Notes

Fourth Interim Report:
Project Manager, D.A. Rohn, Advanced Concepts and Mechanisms Section,
NASA Lewis Research Center, Cleveland, Ohio 44135.

16. Abstract

A constitutive lubricant friction model for rolling/sliding concentrated contacts such as gears and cams was developed, based upon the Johnson and Tevaarwerk fluid rheology model developed earlier. The friction model reported herein differs from the earlier rheological models in that very large slide to roll ratios can now be accommodated by modifying the thermal response of the model. Also the elastic response of the fluid has been omitted from the model, thereby making it much simpler for use in the high slide to roll contacts. The effects of this simplification are very minimal on the outcome of the predicted friction losses (less than 1%). In essence then the lubricant friction model developed for the high slide to roll ratios treats the fluid in the concentrated contact as consisting of a non-linear viscous element that is pressure, temperature and strain rate dependent in its shear response. The fluid rheological constants required for the prediction of the friction losses at different contact conditions were obtained by traction measurements on several of the currently used gear lubricants.

An example calculation, using this model and the fluid parameters obtained from the experiments, shows that it correctly predicts trends and magnitude of gear mesh losses measured elsewhere for the same fluids tested here.

17. Key Words (Suggested by Author(s))	18. Distribution Statement
Gear Mesh friction; Cam sliding friction; Constitutive models; Concentrated Contacts friction; High Slide to Roll Ratios, Traction, Mesh losses.	Unclassified. Unlimited. Star Category 37

19. Security Classif. (of this report)	20. Security Classif. (of this page)	21. No. of pages	22. Price*
Unclassified	Unclassified	VII + 81 pp	

*For sale by the National Technical Information Service, Springfield, Virginia 22161

SUMMARY

A constitutive lubricant friction model for rolling/sliding concentrated contacts such as gears and cams was developed, based upon the Johnson and Tevaarwerk fluid rheology model developed earlier. The friction model reported herein differs from the earlier rheological models in that very large slide to roll ratios can now be accommodated by modifying the thermal response of the model. Also the elastic response of the fluid has been omitted from the model, thereby making it much simpler for use in the high slide to roll contacts. The effects of this simplification are very minimal on the outcome of the predicted friction losses (less than 1%). In essence then the lubricant friction model developed for the high slide to roll ratios treats the fluid in the concentrated contact as consisting of a non-linear viscous element that is pressure, temperature and strain rate dependent in its shear response. The fluid rheological constants required for the prediction of the friction losses at different contact conditions were obtained by traction measurements on several of the currently used gear lubricants. In these tests the contact pressure was varied from 1 to 1.9 GPa, the rolling speed from 10 to 30 m/sec and the fluid inlet temperature from 30 to 80°C. The range of these test conditions corresponds to those encountered in gears and cams. The fluid constants were extracted from the measured traction results by fitting the rheological model against it.

An example calculation, using this model and the fluid parameters obtained from the experiments, shows that it correctly predicts trends and magnitude of gear mesh losses measured elsewhere for the same fluids tested here.

TABLE OF CONTENTS

APPENDICES:

NOMENCLEATURE.

Below follows a list of symbols used in the text and their units.

Sym.	DESCRIPTION	Units
a,b	Semi Hertzian contact size in the x and y direction	[m]
A	Fluid viscosity temperature parameter	[°C]
B	Fluid viscosity pressure parameter	[°C/Pa]
C_s	Specific heat of the disc material	[J/kg.°C]
C	Shear stress temperature constant	[°C/Pa]
C1,2	Number of counter pulses	[-]
C_d	Operating centre distance of gear set	[m]
D_p	Pressure solidification temperature	[°C]
D_v	Viscosity solidification temperature	[°C]
D_s	Shear stress solidification temperature	[°C]
De	Deborah number	[-]
E	Viscosity constant for non linear thermal model	[Pa.sec]
E'	Composite elastic modulus for the disc material	[Pa]
E0	Experimental traction viscosity constant	[Pa.sec]
E1	Experimental traction stress constant	[°C/Pa]
E2	Experimental time delay constant	[-]
F( )	Dissipative function for traction model	[sec^{-1}]
F_s	Dimensionless thermal resistance of the film	[-]
F_x	Contact force in the x direction	[N]
F_y	Contact force in the y direction	[N]
F_z	Normal force on the contact	[N]
F'_z	Contact force per unit length	[N/m]
G	Fluid shear modulus (uncorrected)	[Pa]
Ge	Johnsons elasticity parameter	[-]
$\dot{g}$	Fluid shear strain rate	[1/sec]
h	Central film thickness in contact	[m]
I	Gear ratio	[-]
J1	Dimensionless longitudinal slip variable	[-]
J4	Dimensionless longitudinal traction variable	[-]
$J4_e$	Elastic stress portion of J4	[-]
$J4_p$	Plastic stress portion of J4	[-]
$J4_t$	Thermal dimensionless longitudinal traction	[-]
k	Contact aspect ratio (b/a)	[-]
k_f	Thermal conductivity of fluid	[N/sec °C]
k_s	Thermal conductivity of disc material	[N/sec °C]
k'	Fluid thermal conductivity constant	[N/sec.°C]
k"	Fluid thermal conductivity constant	[°C]
K	Calibration constant in side slip measurement	[m]
K_t	Thermal resistance of gears to ambient	[°C.sec/N.m]
N_p	Number of pinion teeth	[-]

N_g	Number of gear teeth	[-]
p	pressure	[Pa]
P	Mean Hertz contact pressure	[Pa]
P_o	Hertzian peak contact pressure	[Pa]
P_e	Psuedo Peclet number	[-]
P_r	Reduced Hertz pressure	[Pa]
q	Thermal heat flux due to traction	[N/m sec]
Q	Total heat flow due to traction	[N.m/sec]
R_{xe}	Equivalent radius of curvature in x direction	[m]
R_e	Equivalent radius of curvature for discs	[m]
Rb_p	Base radius of the pinion	[m]
Rb_g	Base radius of the gear	[m]
S	Auxiliary variable used in elastic/plastic model	[-]
S	Roller slip	[-]
T	Fluid shear stress	[Pa]
T_s	Non linear shear stress parameter	[Pa]
T_c	Limiting shear strength of fluid	[Pa]
T_o	Limiting shear strength at inlet temperature	[Pa]
t	time	[sec]
U	Rolling speed	[m/sec]
ΔU	Slip velocity in x direction	[m/sec]
V	Viscosity	[Pa.sec]
V0	Viscosity constant	[Pa.sec]
Δv	Side slip velocity of the discs	[m/sec]
w_p	Angular velocity of the pinion	[rad/sec]
X	Dimensionless mesh point distance	[-]
Δx	Small displacement of the displacement transducer	[m]
YI	Inlet shear heating factor	[-]
Z_i	Dimensionless inlet temperature	[-]

GREEK SYMBOLS.

β	Side slip angle	[rad]
θ	Temperature of the fluid	[°C]
θ_c	Shearplane temperature	[°C]
θ_o	Inlet or blank temperature	[°C]
θ_i	Inlet temperature of oil into gear box	[°C]
Θ	Operating pressure angle for gearset	[rad]
Φ	Time delay parameter	[-]
ρ_s	Density of the disc material	[kg/m^{-3}]
χ ψ	Hertzian contact shape parameters	[-]

LIST OF FIGURES:

PHOTOGRAPHS

FIGURES

1-0 INTRODUCTION

Gears play a major role in today's society in that they are one of the most common forms used for the transmission of power. It is therefore important that they operate under conditions of low power loss and long life. The power that is lost in a gear system may consist of several components. These are the losses due to the churning of the gears in the oil, the losses due to the momentum transfer of oil that is flung off the gears, the losses due to the rotation of the gears in the oil air mixture, the losses at the contact location between the gears, and losses due to support bearings and seals. In this report we will concentrate on one particular aspect of the losses namely the contact losses. To achieve this we will use the traction prediction techniques as developed previously, but modified such that the high slide to roll ratios as encountered in gears can be accommodated in the calculations. While this report concentrates on using this model for gears it is equally applicable to cams where one also encounters high slide to roll ratios and concentrated contacts.

1-1 MESH LOSSES IN GEARS

A pair of teeth in contact may be modelled as the contact between two truncated sections of circular discs or rollers. The actual radius of curvature of each equivalent roller would vary as the tooth pair moves through its mesh, that is from the point of initial contact to the final loss of contact. The power transmitted from one gear to the other results in a normal load between the two teeth in contact. This causes a local elastic deformation of the surfaces and the generation of a high interface stress. For most gears a lubrication fluid is introduced into the mesh to prevent surface damage, to reduce the friction, and to provide for some form of cooling. The rolling motion of the teeth draws this fluid into the contact zone and a thin layer of this fluid will separate the actual contact area. One of the mesh losses results from this film forming action and can be thought of as the power required to pump this thin layer of fluid through the contact zone. From first principles it can be shown that this loss is directly proportional to the thickness of the fluid layer in the contact. This loss is often called the rolling friction loss.

At the point of contact the surface velocities of each tooth is dictated by its own base geometry and the distance away from the pitch point. For all but the pitch point these velocities are different so that the layer of fluid trapped in the contact is sheared. The level of resistance that is encountered due to this shear gives rise to the contact sliding friction loss. The magnitude of this level of friction depends on the amount of contact stress, the sliding velocities, the local temperatures, the rolling velocities, and last but not least the nature of the lubricating fluid. The actual shear or rheological behavior of the fluid in the contact gap has been the subject of a great deal of research in recent times, and is very complex in nature because of the extreme conditions in the contact zone. Close examination of the fluid history as it passes through the contact gap reveals that it experiences a sudden pressure pulse from atmospheric to possibly several Giga Pascal in a time period of 1 to .1 m/sec. The shearing of the fluid in the contact results

in a resisting shear stress through the thickness of the fluid layer. This in turn will lead to heat generation and from simple calculations, temperatures in the center of the film can easily reach several hundred degrees Centigrade.

To be able to predict the gear mesh losses it is therefore imperative that we fully understand and model the behaviour of the fluid under the conditions as present in the gear mesh. Yet to study the rheological properties of the fluid under these conditions precludes the use of most of the conventional instruments used for steady state measurements. In fact the only suitable type of instrument for the study is a disc traction or friction test machine where most of the conditions are the same or similar to those in gear teeth in contact.

1-2 PRIOR INVESTIGATIONS.

The topic of power losses in gears has concerned researchers from the very beginning of the introduction of gears. Notable contributions are those by Buckingham [1963], Merrit [1972], Shipley [1962], and Chiu [1975]. A very complete review of the of friction prediction techniques available to gearing engineers is given by Martin [1978]. Anderson and Loewenthal [1981] did a very detailed review of the methods used by the above references and included their own. They state that the major differences between the various methods is in the treatment of the sliding losses in the mesh.

Anderson and Loewenthal [1981] tried to use the various gear efficiency models on data from the literature. This data is however quite scarce and also it was not possible to use the most recent traction theories for the sliding loss because no traction data was available for the fluids used. The comparison between the predicted and measured results from the Anderson and Loewenthal [1981] investigation is therefore subject to the possible errors introduced due to the lack of good traction data for the lubricants. The opportunity to remove some of the uncertainty from the prediction methods came with the work of Mitchell and Coy [1982] , where the effect of the various lubricants on the power efficiency of a helicopter transmission were measured. The data was taken under very carefully controlled conditions and with well known fluids. Upon the request of Anderson and Loewenthal the transmission efficiency was measured for a traction fluid. Traction fluid is normally used in traction drives because it has much higher slip traction characteristics than conventional fluids. This fluid indicated a very much lower power efficiency than other fluids of comparable viscosity. It should also be mentioned here that the observed trends in efficiency with temperature were unexpected in that some of the fluids showed a higher loss at higher fluid temperatures. This indicates that the losses cannot simply be viscosity related.

An attempt by Coy, Mitchell and Hamrock [1984] to explain the trends in the measured efficiencies on the basis of viscosity and pressure viscosity data was not successful. They could not predict the temperature efficiency trend or the correct order for the efficiency as measured for the fluids. It was clear that some other parameters played a role in the gear efficiency.

1-3 CURRENT RESEARCH PROGRAM.

As pointed out by Anderson and Loewenthal [1981] the traction characteristics of the lubricating fluid are very important in predicting overall mesh efficiencies. Since the fluids used in the Mitchell and Coy [1982] were all readily available, it was decided that these fluids would be tested for their traction characteristics and that the resulting experimental traction data would be analyzed on the basis of recent thermal traction theories. In order to shed some light on the observed efficiency trends as reported by Mitchell and Coy [1982] it was agreed that a select number of the fluids as used there would be tested for their traction. The selected fluids are;

Designation in Mitchell & Coy	Commercial name
F	Mobil RL-71
K	Royco 555
E	Syntech NS-6774
A	Kendall ATF-220
I	Mobil Jet II
X	Santotrac 50 (not shown in Mitchell and Coy)
Y	Sunoco TDF88 (not shown in Mitchell and Coy)

The efficiencies as measured by Mitchell and Coy [1982] are shown in Fig 1 below as a function of inlet oil temperature. Note the trends of the efficiency with inlet temperature for the fluids E and X.

The investigation reported herein was performed by Transmission Research, Inc of Cleveland, Ohio, under contract to the NASA Lewis Research Center. The NASA technical project manager was D.A. Rohn of the Advanced Concepts and Mechanisms Section.

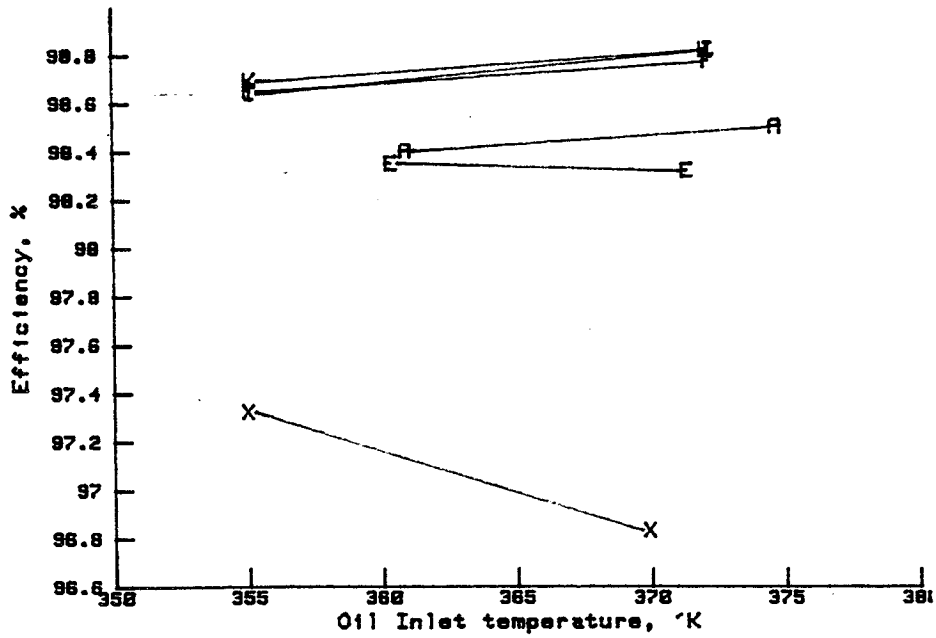

Fig 1: Experimental Effic. vs. Oil Inlet temp.

2-0 EXPERIMENTS

The various traction experiments were carried out on an existing twin disc test facility, shown in figure 2-1, 2-2 and 2-3. The test facility was also used for the traction test results as reported in Tevaarwerk [1985]. This test facility was modified such that it would be capable of measuring the longitudinal slip occurring in the contact, and to extend the range of sideslip. Traction curves are obtained by using a combination of longitudinal and the side slip techniques; so that large traction transfer can be measured without the need for a large motor generator set. It also has the advantage that the effects of bearing friction and rolling traction can be corrected for by the simple measurement of the longitudinal slip. This is particularly important when the expected levels of fluid friction are low, as is the case with some of the lubricant tested here. With longitudinal traction measurements the correction for bearing friction and rolling traction is often of the same magnitude as the measured friction with these lubricants.

2-1 DESCRIPTION OF TWIN DISC MACHINE.

For an extensive description of twin disc traction testers the reader is referred to the literature; Smith [1965] and Johnson and Roberts [1974]. Basically the machine consists of two discs, called the upper and lower disc. The lower disc is mounted in rolling element bearings through shafts and the only degree of freedom is one of rotation about this axis. The lower disc always has a transverse radius of curvature of infinity. The upper disc is contained in bearings that are mounted in the upper assembly. This upper assembly is suspended with elastic hinges such that only direct normal motion or axial motion is possible. The assembly will however always stay horizontal. The upper disc (or toroid) has curvatures so that the desired contact geometry is arrived at. The upper assembly is constructed such that the toroidal axis can be tilted relative to the horizontal plane so as to introduce spin on the contact. It can also be skewed about the normal to the contact to introduce a side slip velocity. To introduce longitudinal slip it is possible to attach a electro mechanical brake to the toroid and extract torque from this system. Control of the amount of slip resulting from this however is difficult because of the nature of the traction slip response of the fluids.

In order to achieve the range of pressures required for the traction data a set of discs with a nominal aspect ratio of 1.7 is used. These discs are made of AISI-01 steel, hardened to 7.00 GPa, ground and polished to a surface finish of less than .05 μm RMS and with an out of roundness error of less than 5 μm. Between tests the discs are inspected for surface damage and if needed, reground and polished to bring them back up to specifications. The required normal load, obtained by a dead loading technique, can be calculated from the Hertz theory for elastic bodies in contact. The maximum contact normal stress P_o is given by;

$$P_o = \frac{1}{2\pi\varphi\chi}\sqrt[3]{\frac{3F_z E'^2}{R_e^2}} \qquad (2\text{-}1)$$

where F_z= contact normal load [N]
P_o= Hertzian contact stress [Pa]
E'= composite elastic modulus [Pa] ;(231 GPa for steel)
R_e= equivalent disc radius [m]
$= (1/R_x + 1/R_y)^{-1}$
φ, χ = Hertzian contact shape factors [-]

2-2 INSTRUMENTATION OF THE TRACTION TESTER.

By suitably instrumenting the disc machine the relevant experimental parameters can be measured. In the experiments reported here the sideslip, sideways traction force, toroid surface temperature, rolling velocity, the amount of longitudinal slip, and the degree of asperity contact are measured. The technique of measuring each of these variables will be discussed next.

2-2-1 THE MEASUREMENT OF THE TRACTION FORCE.

A ring dynamometer type load cell is used to measure the side slip force of the upper toroid assembly. The electrical signal from the load cell is conditioned for noise and amplified using common mode rejection techniques. The gain on the amplifier is adjusted so that a good range on the signal is measured for each test. Calibration of the load cell is done in situ by dead loading. This calibration is checked periodically.

2-2-2 THE MEASUREMENT OF SIDE SLIP.

The skew angle is measured by using a direct current displacement transducer on the upper assembly and thereby measuring the rotation angle of this assembly. This skew angle gives the amount of side slip/roll ratio through the relationship;

(2-2) $$\Delta v/U = \tan(\beta)$$

where β = side slip angle [rad]
Δv = side slip velocity [m/sec]
U = rolling velocity [m/sec]

By measuring the amount of skew with the displacement transducer the side slip/roll ratio is obtained directly through;

(2-3) $$\Delta v/U = K\Delta x$$

where Δx is the displacement of the transducer and K a scale factor. The electrical output of the displacement transducer is filtered in an R-C network to provide a low-pass signal. The maximum frequency response of the R-C network is .1 sec. The displacement transducer is calibrated by rotating the upper assembly through a known angle and then calculating the amount of side slip for this angle.

2-2-3 THE MEASUREMENT OF ROLLING VELOCITY AND LONGITUDINAL SLIP.

The rotational velocity of both the disc on the toroid are measured by using a MC 6840 frequency counter. The proximity probes for the control of the counters are mounted near the support bearings, see Fig. 2-3. Each shaft had a simple protrusion on it that would produce a pulse once per revolution. This pulse is used to turn countdown counters on when controlled to do so. The next successive pulse from the proximity probe would stop the countdown. When each of the two counters had completed their cycle a flag is set and the register contents are read. From the difference between the original and the final contents of the registers the amount of time for a single revolution of each shaft is calculated. From this the angular speed for each shaft is calculated, and hence the peripheral velocity of each roller can be calculated if the roller radius is known. The countdown frequency on the counters is selected such that an accuracy of at least 1 : 10000 is obtained. By employing this method the slip of the rollers could be measured every 5 or six revolutions of the shafts. From the count down and the undeformed roller radii the slip is calculated as follows;

$$(2\text{-}4) \quad S = 2\,\frac{(U2 - U1)}{(U2 + U1)} = 2\left(\frac{R2}{R1} - \frac{C2}{C1}\right) / \left(\frac{R2}{R1} + \frac{C2}{C1}\right) \qquad [-]$$

This can be approximated if the amount of slip is small by the following;

$$(2\text{-}5) \qquad S = \left(\frac{R2}{R1} - \frac{C2}{C1}\right)$$

where S = roller slip [-]
U = rolling velocity [m/sec]
C = number of count down pulses [-]
R = roller radius [m]

Suffix 1 denotes the toroid and suffix 2 denotes the disc.

It should be stressed that the actual amount of slip will be somewhat different when two different roller materials are in contact because of the deformation of the rollers themselves. The errors introduced by this problem can be removed by measuring the rolling slip at very low rolling speeds.

2-2-4 THE MEASUREMENT OF THE TOROID SURFACE TEMPERATURE.

In the analysis and reduction of the test data it is important that the disc temperature be used as the reference inlet temperature for the film thickness. This temperature can be measured by embedding a thermocouple directly below the surface of the toroid and then to take this signal out through mercury slip rings. This method

is however not very practical when a number of different toroids are involved and is also very costly from an installation point of view. With care the surface temperature can also be measured by using a trailing thermocouple that rides on the disc surface. The disadvantage of this technique is that it can be speed sensitive in its response because of frictional heating.

The latter technique is employed here and care is taken to ensure that the contact force on the thermocouple is not excessive. A temperature reference bath junction ensures that the same reference level for the thermocouple is used at all times. The signal from the thermocouple is amplified using common mode rejection techniques to minimize the influence of electrical noise and other disturbances. Calibration is done by the boiling water method adjusted for sea level differences. This calibration is checked periodically. Only slight deviations are encountered. Because of the frictional heating at the junction/toroid interface a variation of about 2 °C is found in the signal between stationary discs and those rotating at a surface velocity of 120 m/s. The overall reproducibility of the temperature measurement is better than 2°C.

The temperature on the machine is regulated through the use of heaters and coolers on the test fluid. This test fluid would be allowed to circulate freely before the start of a test series in order to bring the machine up to a uniform temperature. No specific effort is made however to maintain a given set point temperature during the test and the reason for this will become clear in the analysis of the results.

2-2-5 CONTACT RATIO MEASUREMENT.

In order to measure the degree of asperity contact that took place at any one time an electrical conductance circuit as shown below is employed.

The selection of the various electrical components is such that only very low voltages are applied across the two discs to minimize the risk of surface damage through arcing. The output signal of network is essentially DC in nature with only slow fluctuations in the contact conditions being recorded.

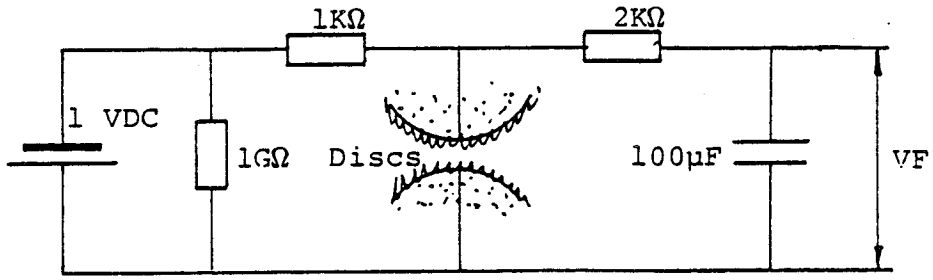

Schematic of the contact ratio measuring circuit.

2-3 TRACTION MEASUREMENTS.

Traction curves are obtained by the slow rotation of the upper assembly from a positive value of side slip/roll ratio to a negative value. The signals from the above discussed transducers are fed into a digitizer from where they are led into an

Apple II+ computer for plotting and storage on magnetic media for future use. The computer would automatically trace the force versus slip curve on the screen. By reversing the direction of rotation of the machine, a duplicate set of curves can be obtained. For each experiment 500 data points are taken at fixed time periods of .2 seconds. Multiple data points would be stored as separate entries.

After the completion of a test series the data would be recalled into memory of the computer and further manipulated. This manipulation consisted of the averaging of the multiple entries, the filling in of any gaps in the data through forward and backward interpolation, the comparison of the traces for the forward and reverse rolling direction and the centering of the traces about the center lines. After the centering operation the data would be smoothed by a 'N' point averaging technique for traction points after the peak traction points. For storage a geometric series is used so that the total traction trace is now represented by 40 data points for each measured variable. These traces are then stored on magnetic media and used for further manipulation and data extraction at a later point

2-3-1 TRACTION TEST RESULTS

In order to shed some light on the observed efficiency trends as reported by Mitchell and Coy [1982] it was agreed that a select number of the fluids as used there would be tested for their traction. The selected fluids are;

Designation in Mitchell & Coy	Commercial name
F	Mobil RL-71
K	Royco 555
E	Syntech NS-6774
A	Kendall ATF-220
I	Mobil Jet II
X	Santotrac 50 (not in Mitchell and Coy)
Y	Sunoco TDF88 (not in Mitchell and Coy)

Ideally these above lubricants should have come from the same batch as those used for the reported gear efficiency measurements. Unfortunately this was not possible. It should be stressed that while the designation may be the same, the actual fluid may not be.

The viscosity temperature and the viscosity pressure behaviour of these fluids are shown in Figs 2-4 and 2-5. These results are from Present et al [1983], and will be used for the filmthickness calculations for the analysis of the various tests. The dependence of the fluid thermal conductivity on temperature is shown in Fig 2-6. While attempts were made to measure this property by an external source, it was found that the results showed too much uncertainty to be useful here. The dependency of the thermal conductivity on temperature was estimated by the method as used by Jackson [1980].

To get adequate traction data on the above fluids for the purposes of traction prediction it was decided to test in under the following conditions;

Mean Contact Pressure	.7 - 1.3 GPa in 4 steps
Mean rolling Velocity	10, 20 and 30 m/sec
Mean inlet temperature	30 and 80°C
Slip levels	-.20 to .20

Traction test on the first five fluids indicated above were taken under these conditions. The traction test results for the last two fluids were taken from earlier reported data. In total close to 200 traction tests are taken. These traces and a summary of all the test conditions may be found in Appendix I.

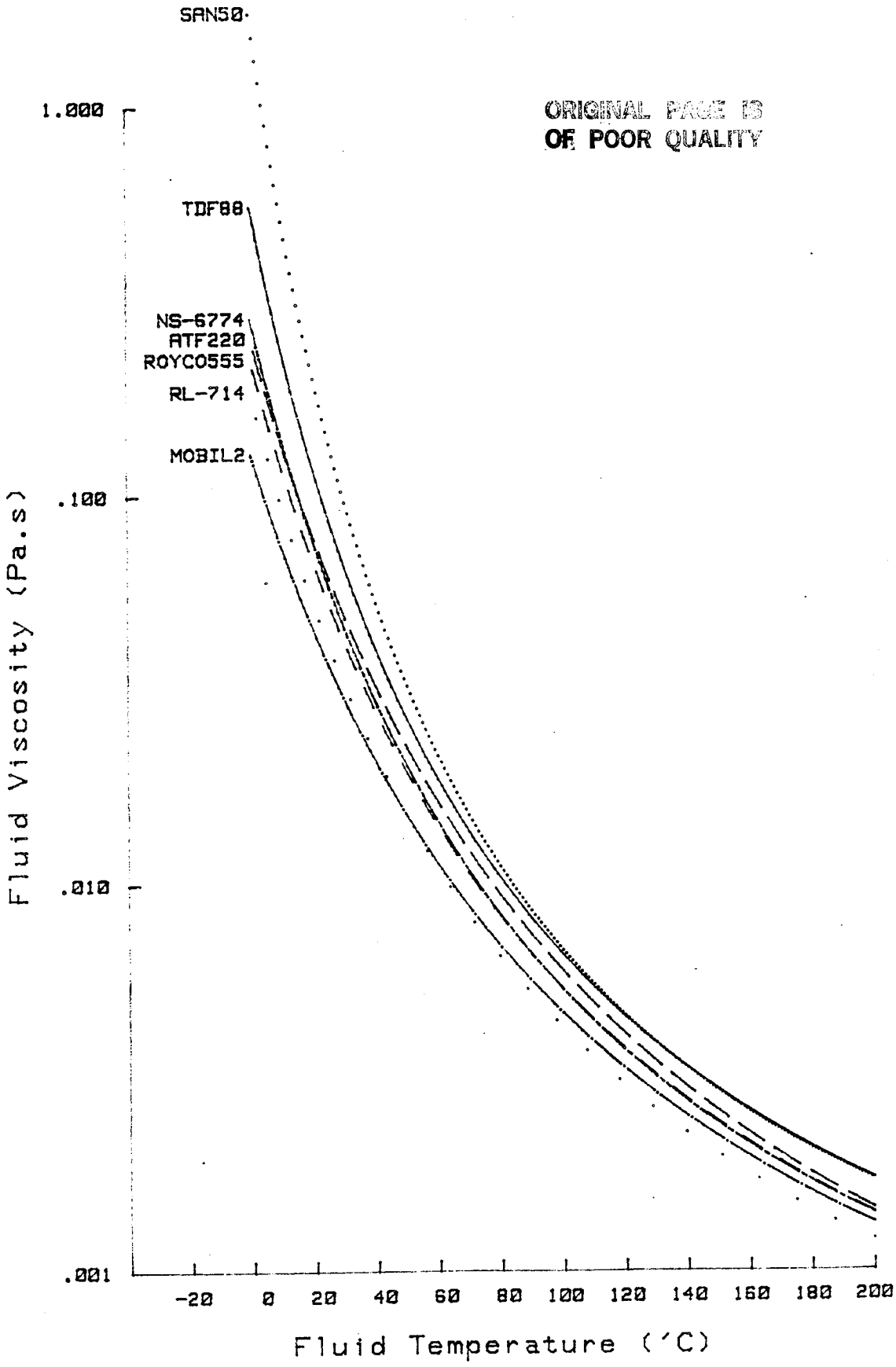

Fig. 2-4 Fluid temperature viscosity traces for the test fluids.

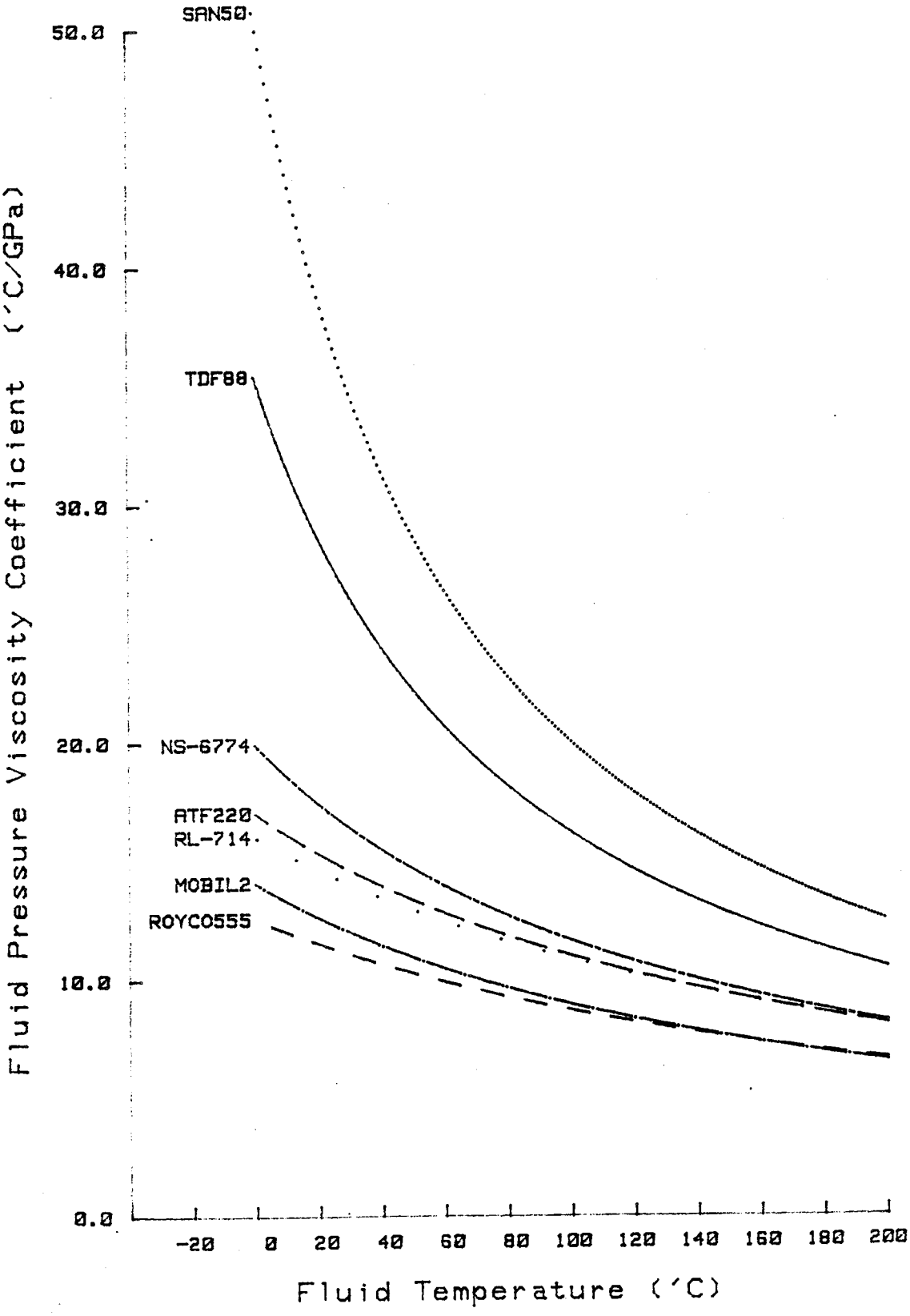

Fig. 2-5 Fluid pressure viscosity coefficient for the tests fluids.

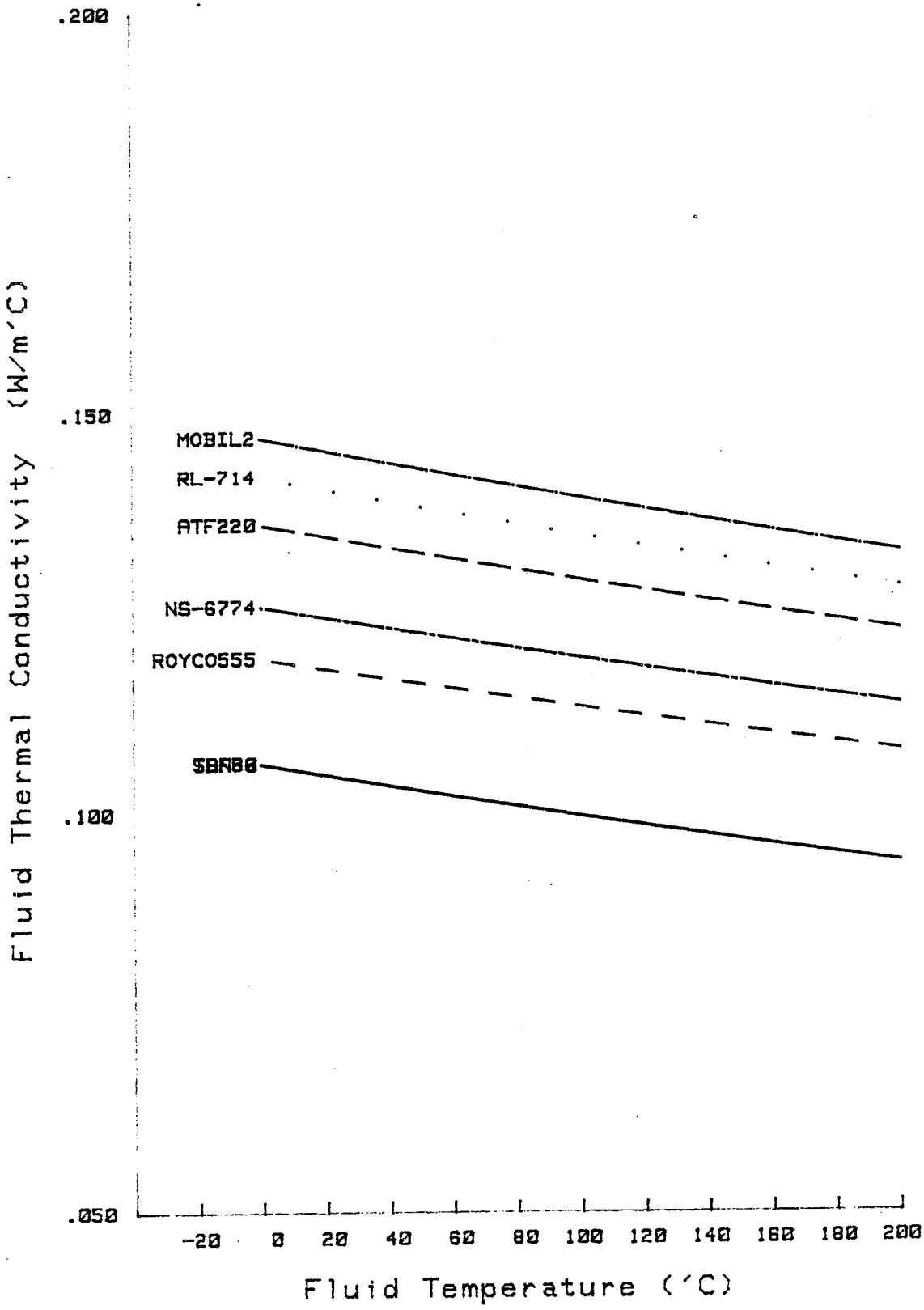

Fig. 2-6 Thermal conductivity of the test fluids as a function of temperature.

3-0 THEORETICAL ANALYSIS

In order to understand the required analysis of the experimental data it will be helpful to consider the following discussion of traction.

The ability of a fluid film, trapped under high pressure in the elastically deformed region of two loaded curved elements, to transmit a tangential force from one element to the other, is commonly referred to as friction or traction. The magnitude of this force depends on several variables such as :1) the contact kinematic conditions of slip, spin and sideslip, 2) the fluid present, 3) temperature, pressure and operating speeds. We will examine the traction behaviour under simple slip only.

Under conditions of increasing slip between the two elements an increasing traction force is transmitted up to a certain limit at which point it will decrease with further slip. See Fig. 3-1

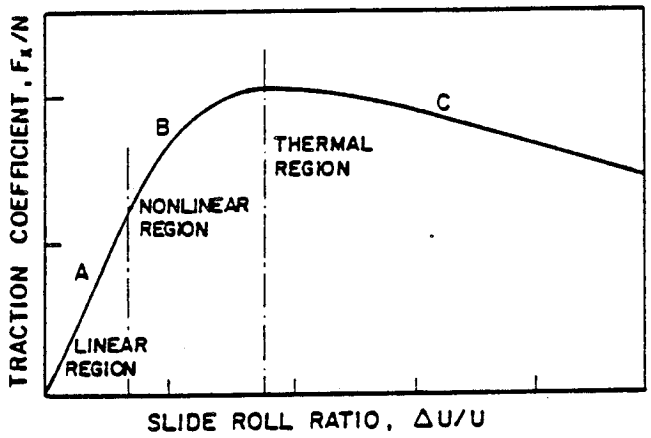

Fig. 3-1 Typical traction /slip curve.

There are three regions identified on this traction curve and the behaviour in each of these regions can best be described by the Deborah number. For a simple Maxwell viscoelastic model this number is the ratio of the relaxation time and the mean transit time, see Johnson and Tevaarwerk [1977].

(A) The linear low slip region. Thought to be isothermal in nature, it is caused by the shearing of a linear viscous fluid (low De) or that of a linear elastic solid (high De).

(B) The nonlinear region. Still isothermal in nature but now the viscous element responds nonlinearly. At low De this portion of the traction curve can be described by a suitable nonlinear viscous function alone, while at high De a linear elastic element interacts with the nonlinear viscous element.

(C) At yet higher values of slip the traction decreases with increasing slip and it is no longer possible to ignore the dissipative shearing and the heat that it generates in the film. Johnson and Cameron [1967] showed that the shear plane hypothesis advanced by Smith [1965] does account for most of their experimental observations in this region. More recently Conry et al [1979] have shown that a nonlinear viscous element together with a simple thermal correction can also describe this region.

3-1 ISOTHERMAL TRACTION ANALYSIS.

The rheological model that describes the traction under simple slip in all three regions of operation fairly well is the J & T traction model as presented by Johnson and Tevaarwerk [1977];

$$(3\text{-}1) \qquad \frac{1}{G}\frac{dT}{dt} + F(T) = \dot{\overset{o}{g}}$$

where T = shear stress [Pa]
G = shear modulus [Pa]
t = time [sec]
$\dot{\overset{o}{g}}$ = shear strain rate [1/sec]

The dissipative function F(T) is open to the choice of the researcher to fit the observed traction but Johnson and Tevaarwerk [1977] found that the hyperbolic sine;

$$(3\text{-}2) \qquad F(T) = \frac{T_S}{V} \sinh\left(\frac{T}{T_S}\right)$$

where T_S = non-linear shear stress parameter. [Pa]
V = local viscosity [Pa.sec]

described all of their experimental results in regions (A) and (B) very well. At higher pressures and for fluids with high traction coefficients this dissipative function may be replaced by the purely plastic behaviour of the material;

$$(3\text{-}3) \qquad F(T) = 0 \text{ for } T < T_C \;;\; F(T) = \dot{\overset{o}{g}} \text{ for } T = T_C$$

where T_C = limiting shear strength of the fluid [Pa].

Whether the perfectly plastic behaviour of the material is intrinsic is not clear. Work by Johnson and Greenwood [1980] suggests that it is possibly the result of thermal behaviour of the sinh model. For many applications the elastic/plastic traction model is adequate. It was used by Tevaarwerk and Johnson [1979c] and Tevaarwerk [1979b] to predict traction under various conditions of slip and spin. The analysis is completely isothermal in nature and for simple slip the traction is given by;

$$(3\text{-}4) \qquad J4 = \frac{2}{\pi}\left[\tan^{-1}S + \frac{S}{(1+S^2)}\right]$$

where $S = \frac{2}{3}\frac{J1}{\sqrt{k}}$

The shear strain rate in the fluid was taken to be the same everywhere in the contact and assumed to be constant throughout the film thickness. Its magnitude was taken to be;

$$\overset{o}{g} = \frac{\Delta v}{h}$$

Equation (3-4) results from the integration of stresses, caused by the shearing of an elastic element of pressure independent average shear modulus G, and the plastic stresses proportional to the local Hertzian pressure. The predicted traction from an elastic/plastic model compares very well with the experimentally observed values for combinations of slip and spin, provided that the spin or slip are not too large. Large slip or spin results in almost purely dissipative stresses over the contact area and hence non-isothermal behaviour. Traction prediction under these conditions is still possible but the thermal effects need to be brought into the picture. Tevaarwerk [1981],[1979d] presents two techniques for calculating such spin traction curves. The latter technique requires the shape of the traction curve in the large slip regime to provide a simple correction to the isothermally predicted spin traction.

Isothermal traction analysis was used in the reduction of traction data for the report on the results of the traction measurement, Tevaarwerk [1981b].

3-2 THERMAL TRACTION ANALYSIS.

The ability to separate the elastic stresses from the plastic ones can now be used to perform a thermal traction calculation. The analysis presented here follows the technique outlined by Tevaarwerk [1980] and [1982].

Equation (3-4) resulted from the integration of isothermal elastic and plastic stresses over the contact area of an ellipse. For the region of contact under elastic stress the shear energy is conserved and therefore does not give rise to temperature increases. The plastically deforming region however, is non-conservative and a temperature rise in the fluid is expected. This will lead to a reduction in the local plastic strength of the fluid. Equation (3-4) may therefore be better written in its elastic and plastic parts;

$$J4 = J4_p + J4_e \tag{3-5}$$

$$J4_e = \frac{4\,S}{(1+S^2)^2} \tag{3-6}$$

$$J4_p = \frac{2}{\pi}\left[\tan^{-1}S + \frac{S(S^2-1)}{(1+S^2)^2}\right] \tag{3-7}$$

This modification is given by T_c/T_o where T_c is the average stress under thermal conditions and T_o is the average stress under isothermal conditions. We are dealing therefore with averaged stresses in the plastic region of the contact even though the isothermal stress distribution is according to the Hertzian pressure. This seemingly contradictory assumption is supported by

theoretical evidence by Tevaarwerk [1979d]. The modified equation would therefore be;

$$(3\text{-}8) \qquad J4_t = J4_e + \frac{T_c}{T_o} J4_p$$

The modification term T_c/T_o can be found from a thermal balance over the contact region under plastic stress. This region can be thought of as a thermal source whose heat is conducted/convected away. The length of the source is a function of the location of the onset of plastic deformation after the initial elastic region, however in this simple model we will take the source length to be "a" where this is the semi contact length in the running direction. As a simple thermal balance we will use the expression reported by Johnson and Cameron [1967] for the shear plane temperature;

$$(3\text{-}9) \qquad \theta_c - \theta_o = q \frac{h}{k_f} \left[Fs + \frac{.5}{\sqrt{P_e}} \right]$$

where;

$$(3\text{-}10) \qquad P_e = \frac{a \rho_s C_s U}{k_s} \left\{ \frac{k_s\ h}{k_f\ a} \right\}^2 \quad [-]$$

and

q = average thermal strength of the source [W/m^2]
θ_c = shearplane temperature in the contact [°C]
θ_o = inlet temperature of the fluid [°C]
k_f = thermal conductivity of fluid in the contact [W/m°C]
h = central film thickness in the contact [m]
k_s = thermal conductivity of the roller material [W/m°C]
C_s = specific heat of the roller material [J/kg°C]
ρ_s = density of the roller material [kg/m^3]
F_s = thermal resistance of the film [-]

This expression is only valid when the heat is <u>conducted</u> through the film and <u>convected</u> away by the discs, a condition that is true for most traction drive contacts. The strength q of the source is given by;

$$(3\text{-}11) \qquad q = T \Delta U$$

The thermal resistance of the film F_s may be calculated from the following expression by Tevaarwerk [1985];

$$(3\text{-}12) \qquad F_s = .07675 + .003455\, Z_i + .0000325\, Z_i^2 - .016\, \mathrm{Ln}(30/P_e)$$

$$\text{where } Z_i = \frac{A + B\,P}{\theta_o + D}$$

In order to proceed any further we need a relationship between temperature and the shear strength of the fluid. A typical relationship that has its roots in the Eyring theory of fluid transport is given by;

$$(3\text{-}13) \qquad T(\theta) = \frac{1}{C}\left[A + BP + (\theta+D)\ \mathrm{Ln}\ \left(\frac{2\,CE}{\theta+D}\right)\right]$$

where ; A = viscosity temperature constant [°C]
B = pressure viscosity constant [°C/Pa]
C = non-linear shear stress constant [°C/Pa]
D = fluid solidification temperature [°C]
E = fluid viscosity [Pa.sec]
P = pressure of the fluid in the contact [Pa]

At first sight it seems that this equation has five disposable constants in it, however two of these constants (A and D) may be obtained from the atmospheric viscosity temperature relationship, and one more (B) can be obtained from the Barus viscosity pressure relationship. The constant D is known as the solidification temperature; the temperature to which the fluid should be cooled to become solid like under atmospheric pressure. Only the constants C and E need to be determined experimentally from the traction results and this will be done in the next chapter. It should be noted here that the ultimate aim is to derive the fluid traction parameters such that they apply for all the experimental conditions reported here.

By using equations (3-9), (3-10), (3-11) and (3-13) the average thermal shear stress can be obtained for a given set of conditions. In equation (3-8) we need the ratio of the average contact shear stress under thermal conditions to that under isothermal conditions. This is really the ratio of the shear stress given by equation (3-13) evaluated at the shearplane temperature θ_c (from equation 3-9) and the shear stress as evaluated at the inlet temperature conditions θ_o. The other contact conditions remain the same for this ratio calculation.

The method that is outlined above was used for the traction data analysis as reported by Tevaarwerk [1985] , with the exception of equation (3-12). Previously the value of F_s was fixed at .1 . For the analysis of the traction data as reported here, several improvements were made in the model and these changes are outlined in the next chapter.

4-0 EXTRACTION OF THE TRACTION PARAMETERS.

In order to use the traction model to calculate the level of traction in a given contact condition, the relevant traction parameters need to be extracted. In equation (3-1) we saw that both the elastic effects and the nonlinear viscous effect account for the behaviour of the fluid. Elastic effects are typically only felt under conditions of high contact pressure, low temperature and low slip. These conditions are not typical of those occurring in gear tooth contacts, so it would seem safe that we ignore any of the elastic fluid effects for the present analysis. This means that we only need to know the large strain viscous effects.

4-1 EXTRACTION OF THE LARGE STRAIN PARAMETERS.

The large slip region , that is the region beyond the traction peak, is exclusively governed by the dissipative element in the rheological equation. All the elastic effects have completely disappeared so that it is now quite easy to extract the governing parameters for this region. In essence what is required is a reverse analysis of the traction calculation normally used for the calculation of the traction curves. When the elastic response of the fluid is no longer dominant all the shear strain rate in the film is taken by the viscous element and we may express equation (3-1) as;

$$F(T) = \dot{\bar{g}} = \frac{T_S}{V} \operatorname{Sinh}\left(\frac{T}{T_S}\right) \tag{4-1}$$

When the argument T/T_S is larger than 1 this may be further simplified to the following;

$$F(T) = \dot{\bar{g}} = \frac{T_S}{2V} \operatorname{Exp}\left(\frac{T}{T_S}\right) \tag{4-2}$$

This expression relates the stress to strain response for a small element of fluid that is subjected to a shear strain rate $\dot{\bar{g}}$, is at a given pressure and a given temperature. Each of the parameters in this equation can be a function of temperature or pressure or both. In the analysis of traction it is normally sufficient to treat the fluid viscosity as a function of temperature and pressure and to make the non linear stress parameter a function of temperature only. The following relationships will be used here:

--- for the viscosity we will combine the Vogels temperature viscosity and the Barus pressure viscosity relationships as follows;

$$V(\theta,p) = V_o \exp\left(\frac{A}{\theta+D_V} + \frac{pB}{\theta+D_p}\right) \tag{4-3}$$

where V_o = viscosity constant [Pa.sec]
A = temperature viscosity constant [°C]
D_V = solidification constant for Vogels equation [°C]

B = pressure viscosity constant [°C/Pa]
D_p = solidification constant for Barus equation [°C]
θ = local temperature [°C]
p = local pressure [Pa]

--- for the temperature dependence of T_s on the local temperature we will use the following;

(4-4) $$T_s = \frac{\theta + D_s}{C}$$

where C = non linear shear stress constant [°C/Pa]
D_s = solidification constant for Eyring equation [°C]

These parameters (except for the temperature and the pressure) are all constants for a given fluid.

In order to proceed any further we have to make some assumptions about the conditions within the contact. Firstly we will assume that average conditions exist for the contact. Hence temperature and pressure are are only mean temperatures and pressures. Also we will assume that the important temperature for the analysis is the shear plane temperature as given by equation (3-9). Furthermore the shear strain rate $\dot{\gamma}$ will be assumed to be constant throughout the film and in the case of the traction experiments it is constant over the contact area. Its magnitude is given by;

(4-5) $$\dot{\gamma} = \Delta v/h \qquad [sec^{-1}]$$

where h = central filmthickness [m]

The central filmthickness is calculated from the expressions by Hamrock and Dowson [1977]. Further modifications to this film thickness to allow for inlet shear heating are made by using the Murch and Wilson [1975] approach.

Hence in total we will make the following simplifications;

(4-6)

	local	average	equation #
temperature	θ	θ_c	(3-9)
shear strain rate	$\dot{\gamma}$	$\Delta v/h$	(3-4b)
pressure	p	$P=2P_o/3$	(2-1)
shear stress	T	$T = F_x/F_z$	

By substituting the expressions from equation (4-3) to (4-6) into equation (4-2) we obtain;

$$(4\text{-}7) \qquad \frac{\Delta v}{h} = \frac{1}{2CVo(\theta_c+D_s)} \text{Exp} \left(\frac{T\,C}{\theta_c+D_s} - \frac{A}{\theta_c+D_v} - \frac{B\,P}{\theta_c+D_p} \right)$$

At a first glance there appear to be 7 parameters that can be used to fit the data. This is not the case however because several of these are determined by the results from other experiments. For example by the correlation of the viscosity data for the lubricants to equation (4-3) solves for the constants A, B, D_v , V_o and D_p. It remains therefore to find the constants D_s and C. These can be derived from the thermal region of the traction curve itself by curve fitting equation (4-7) to it. For this purpose it is better to write this equation in a slightly different form;

$$(4\text{-}8) \qquad \frac{T}{\theta_c+D_s} = \frac{1}{C} \left[\frac{A}{\theta_c+D_v} + \frac{BP}{\theta_c+D_p} + \text{Ln} \left(\frac{2CVo\ \Delta v}{(\theta_c+D_s)\ h} \right) \right]$$

From the above equation it is apparent that if this relationship holds then the results from the traction measurements should form a straight line when plotted in the above fashion. The slope of this line gives the value for C while the value of D_s can be calculated by adjusting it until the best fit is obtained.

4-2 REDUCED PRESSURE EFFECTS.

When a fluid film is present in the contact zone the pressure distribution is not strictly Hertzian but modified by the fluid. Due to the hydrodynamic action the pressure distribution is more peaky, and is spread over a broader area. This will lead to a reduction in the mean pressure in the contact. The reduced pressure may be calculated from the pressure ratio as given below;

$$(4\text{-}9) \qquad P_r = P \left[1 - 4\, G_e^{-.25}\, YI^{-3}\, e^{(-2.3/k)} \right]$$

where
G_e = Johnsons elasticity constant [-]
P = mean Hertz contact pressure [Pa]
YI = Inlet shear heating factor [-]
k = aspect ratio (b/a) [-]
P_r = reduced contact pressure [Pa]

4-4 TRANSIT TIME DEPENDENCE.

The fluid in the contact is subjected to very high pressure gradients for a very short time duration. It is therefore not likely that the viscosity in the contact has reached equilibrium conditions. How near equilibrium that it is will depend on several factors such as the time it is subjected to the pressure and the easy with which the molecules can rearrange themselves.

A suitable dimensionless grouping that takes these various factors into account is given as;

$$\Phi = \frac{U\, V(\theta_o)}{a\, P_o} \qquad (4\text{-}10)$$

where Φ = dimensionless time delay parameter [-]
U = mean roller speed [m/sec]
$V(\theta_o)$ = viscosity at inlet temperature [Pa.sec]
a = semi Hertz contact length [m]
P_o = Hertz contact pressure [Pa]

This parameter is used in conjunction with the viscosity constant in the following way;

$$Vo = E0\ \Phi^{E2} \quad [Pa.sec] \qquad (4\text{-}11)$$

where E0 = equilibrium viscosity [Pa.sec]
E2 = time delay exponent [-]

The single constant V_o has now been replaced by this two constants equation so we have increased our degree of freedom by one for the system.

4-5 THERMAL CONDUCTIVITY TEMPERATURE DEPENDENCE

As shown in Fig 2-6 the thermal conductivity of the fluid is a function of the temperature. This has a direct influence on the thermal resistance of the fluid in the contact. In order to take this effect into account the thermal conductivity was fitted to the following equation;

$$k_f = \frac{k'}{\theta_c + k''} \qquad (4\text{-}12)$$

Since the shear plane temperature occurs in equation (4-12) and the thermal conductivity occurs in equation (3-9) the solution to both the thermal conductivity and the shear plane temperature must be done on an iterative basis.

4-6 ANALYSIS OF THE EXPERIMENTAL RESULTS.

By combining the above equations (4-8), (4-9) and (4-10) the traction data may be fitted to the following equation;

$$\frac{T}{\theta_c+D_s} = \frac{1}{C}\left[\frac{A}{\theta_c+D_v} + \frac{BP_r}{\theta_c+D_p} + \mathrm{Ln}\left(\frac{2\ C\ E0\Phi^{E2}\ \Delta v}{(\theta_c+D_s)\ h}\right)\right] \qquad (4\text{-}13)$$

where the shear plane temperature is calculated from equation (3-9) as;

$$(3\text{-}9) \qquad \theta_c - \theta_o = T\,\Delta v\,\frac{h}{k_f}\left[\,Fs + \frac{.5}{\sqrt{P_e}}\,\right]$$

and P_e is given by;

$$(3\text{-}10) \qquad P_e = \frac{a\,\rho_s C_s U}{k_s}\left\{\frac{k_s\,h}{k_f\,a}\right\}^2 \quad [-]$$

and F_s is;

$$(3\text{-}12) \qquad F_s = .07675 + .003455\,Z_i + .0000325\,Z_i^2 - .016\,\mathrm{Ln}(30/P_e)$$

the dimensionless temperature Z_i is modified somewhat now to take the two different solidification temperatures into account;

$$(4\text{-}11) \qquad Z_i = \left\{\frac{A}{\theta_o + D_v} + \frac{B\,P_r}{\theta_o + D_p}\right\}$$

From the experimental traction data as reported in Chapter 2 the curves where no asperity contact took place were used in a multiple curve regression analysis to determine the parameters C, E0 and E2. A summary of the traction curves used in the regression and the resulting fit of the traction data to equation (4-10) is shown in Appendix II for the 7 fluids investigated here.

The regression constants for each of the fluids are given at the end of the summary sheet for each fluid. The variable E1 corresponds to C in the above equations.

5-0 PREDICTION OF THE GEAR MESH FRICTION LOSSES.

The action of gear teeth that are transmitting power from one gear to the next may be modelled as a pair of rollers in contact. This modelling has allowed us to use traction test machines so that the essential rolling and slip traction data and models can be extended to the prediction of the gear mesh losses. What we have done so far is to take the traction data and to reduce all of it to a few fixed parameters through the traction modelling. With this model we should now be able to predict the level of traction for a given fluid when the contact pressure, rolling velocity, slip velocity and temperatures are known. While in the traction testers the parameters such as load, speed and contact radii are essentially constant during a given test, this is by no means the case in the contact of gear teeth, so we need to develop the proper equations for these first. After that we can then apply the traction prediction technique to a typical set of gears.

In this chapter we will gradually work towards this goal and demonstrate how this is done for spur gears. The technique will only be demonstrated for spur gears here but is not limited to these alone, since it contains all the essential details needed for friction prediction in other types of gears.

5-1 CONTACT CONDITIONS IN A PAIR OF SPUR GEARS

In order to predict the local traction at the contact formed between two gear teeth in load bearing we need to know the local curvatures and the velocities. These can be obtained from the basic gear parameters such as the operating centre distance, the gear ratio and the operating pressure angle, provided that the gear form is of the involute type.

Consider a pair of spur gears as shown below.

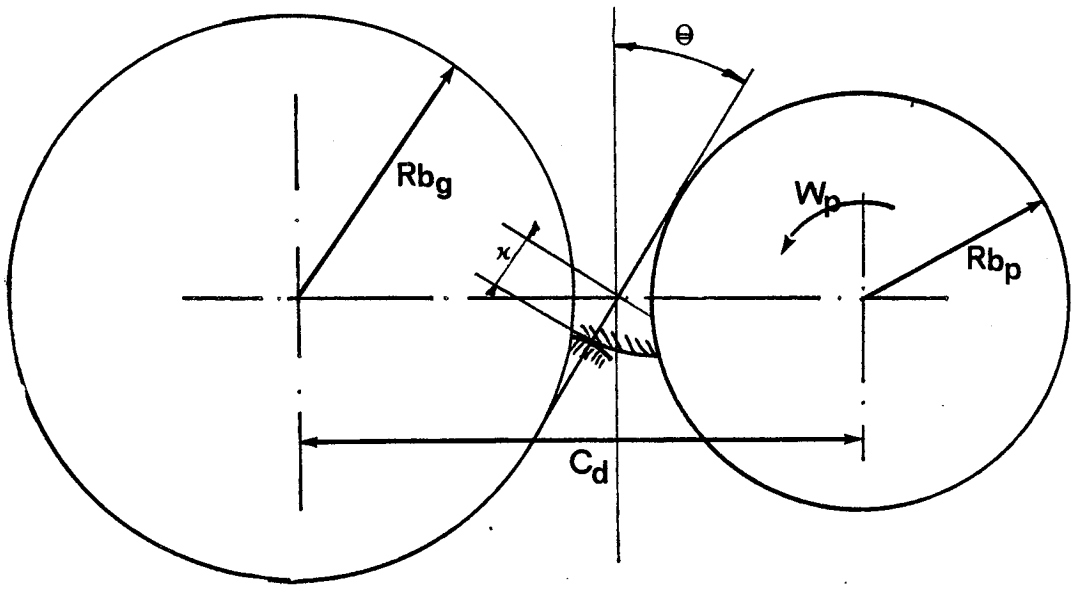

If we assume that the tooth profile is of the involute form over the region that contact takes place than we may write the following relationships;

(5-1) $$C_d = (Rb_p + Rb_g)/\cos \Theta$$

where Θ = operating pressure angle [rad]
C_d = operating centre distance [m]
Rb_p = base radius of the pinion [m]
Rb_g = base radius of the gear [m]

The instantaneous contact radii for the gear and pinion to the mesh point are given by;

(5-2) instantaneous radius for gear $= Rb_g \tan \Theta - x$
instantaneous radius for pinion $= Rb_p \tan \Theta + x$

where the location of the mesh point is measured a distance x away from the pitch point in the direction of motion of the gear teeth. From these we may calculate the equivalent contact radius as used in the Hertz contact calculations;

(5-3) $$R_{xe} = \frac{Cd \sin \Theta}{(I+1)^2} \quad [(I - X)(1 + X)]$$

where R_{xe} = equivalent contact radius in the rolling direction [m]
$I = Ng/Np$ = gear ratio [-]
Ng = number of gear teeth [-]
Np = number of pinion teeth [-]

and $$X = \frac{x(I+1)}{C_d \sin \Theta}$$ = dimensionless mesh point distance [-]

This value of the equivalent contact radius may now be used to calculate the Hertz contact pressure P_o and the contact dimension 'a' in the rolling direction. These quantities are needed in equations (4-9) to calculate the reduced contact pressure P_r and for calculating the Peclet number in equation (3-10). Also needed for this is the normal load F'_z on the tooth. This load depends on the location of x and other gear parameters. It will be assumed here that its magnitude has been established by the user. Assuming that the teeth have no crowning so that line contact will occur, we write the Hertz equation for contact pressure and size as follows;

$$(5\text{-}4) \qquad a = \sqrt{\frac{8\ F'_z\ R_{xe}}{\pi\ E'}}$$

and

$$(5\text{-}5) \qquad P_o = \sqrt{\frac{E'\ F'_z}{2\ \pi\ R_{xe}}}$$

5-2 INSTANTANEOUS ROLLING AND SLIDING VELOCITIES.

The thickness of the film that is formed in between the two teeth in contact depends upon the local conditions of viscosity and surface velocity. Also the amount of sliding velocity at any given instant is needed to calculate the level of the mean shear strain rate in the film. Hence, needed are the instantaneous rolling velocity and the velocity difference at the contact location. Assuming that we have rigid body rotation for the two gears these velocities are given as;

$$(5\text{-}6) \qquad U = w_p \frac{C_d \sin \Theta}{(I+1)} [\ 1 + X(I-1)/2I\ ]$$

and

$$(5\text{-}7) \qquad U_p - U_g = (\ X\ w_p\ C_d \sin \Theta\ )/I$$

where

U_p = rolling velocity for the pinion [m/sec]
U_g = rolling velocity for the gear [m/sec]
U = mean rolling velocity $(U_p+U_g)/2$ [m/sec]
w_p = angular velocity of the pinion [rad/sec]

5-3 GEAR TOOTH TEMPERATURES.

In all the equations dealing with the shear plane temperature predictions we used the inlet temperature of the fluid. This is really the temperature of the bodies in contact in the immediate vicinity of the contact. In the traction tests this temperature was measured with the riding thermocouple so that the traction results were corrected for this on a point by point basis. In the case of gears however we normally have no direct control over this temperature, but rather control the fluid inlet temperature to the transmission itself. The tooth temperature, which corresponds more directly to our inlet temperature θ_o , is determined by the amount of thermal resistance that it encounters in sheding the heat from the frictional losses at its surface. The exact determination of this resistance is too

complicated for analysis here. Suffice it to say that a very good estimate of this inlet temperature may be obtained by the following;

(5-8) $$\theta_o = \theta_i + K_t Q$$

where θi = inlet temperature of the fluid into the gearbox [°C]
Kt = thermal resistance of gear tooth to ambient [°C.sec/N.m]
Q = total amount of heat generated during a mesh cycle [N.m/sec]

Since the amount of heat generated during a given mesh cycle depends on the traction of the fluid, which in turn depends on the local tooth temperature, it is easy to see that an iterative type solution is required to obtain θ_o.

5-4 FRICTION EQUATION

In chapter 4 we analyzed the traction data with the hyperbolic sine as the principle non-linear viscous element. In order to extract the fundamental constants from the traction data we had to make some assumptions about the magnitude of the term T/T_s. When this term was much bigger than unity we approximated the hyperbolic sine with the exponential form. This allows us to use very simple regression techniques to find the fundamental constants for the given fluid by using equation (4-13). When dealing with traction drives where the traction is such that this stress ratio T/T_s is always greater than 1 we can use equation (4-13) or the simpler form (3-13) directly to predict the traction as well. It is only when the slip velocities are high and when the traction properties of the fluid are such that we might violate the stress ratio condition , that we have to return to the original form of the Eyring non-linear viscous function. What this really means is that we have to substitute the traction constant that we solved for into equation (4-1). If we don't do this we will not be able to predict the linear thermal viscous regime of the traction curve correctly.

Starting now with equation (4-1) and backsubstituting the constants that we solved for we may write the following equation for the contact shear stress;

(5-9) $$T = \left(\frac{\theta_c + D_s}{E1}\right) \operatorname{Sinh}^{-1}\left[\frac{\overset{\circ}{g}\, E1\, E0\, \Phi^{E2}\, \exp\left(\frac{A}{\theta_c + D_v} + \frac{B\, P_r}{\theta_c + D_p}\right)}{\theta_c + D_s}\right]$$

5-5 OUTLINE OF THE CALCULATION PROCEDURE.

We are now in a position to calculate the traction (or friction) from the equations developed so far. Because of the nature of the process we will indicate the variables that are solved for in a form of flowchart. This flowchart will consist of three levels of calculations. These are;

1) variables only dependent on the geometry
2) variables dependent on the above and θ_o
3) variables dependent on the above and θ_c

Since there are two levels of iterations required at steps 2 and 3 these will become the inner most loops. Table 5-1 shows the flowchart that outlines the level at which each variable is calculated and the appropriate equation to be used.

INPUT ⟶ Fixed parameters

Gearing data : C_d, Θ, I, w_p, θ_i, F'_z, X, K_t
Material data : E', k_s, C_s, s
Fluid data : A, B, V0, D_v, D_p, K', K'', θ_i
Traction data : D_s, E0, E1, E2

LEVEL 1 ⟶ Variables dependent on geometry alone

Symbol:	Equation:
R_{xe}	5-3
a	5-4
P_o	5-5
U	5-6
U_p-U_g	5-7

LEVEL 2 ⟶ Variables dependent on θ_o

Symbol:	Equation:
θ_o	5-8
Φ	4-10
h	Hamrock-Dowson
P_r	4-9
$\overset{o}{g}$	4-5
Z_i	4-11
P_e	3-10
F_s	3-12

LEVEL 3 ⟶ Variables dependent on θ_c

Symbol:	Equation:
θ_c	3-9
k_f	4-12
T	5-9

Table 5-1 : Flowchart of the traction calculation and the variables associated.

5-6 EXAMPLE TRACTION PREDICTION.

As an example of the traction predicted by the method as outlined in Table 5-1, it was decided to do this for each of the fluids that were used in this investigation. Ultimately such a traction prediction would be an essential step in the prediction of the overall powerloss in a given transmission. Since we have not concerned ourselves with losses other than those caused by the sliding action of the gears it does only predict the sliding losses. Depending on the conditions in the transmission these losses may dominate or simply be a part of the overall.

Here we will try to predict the powerloss for the fluids tested in traction and to see how these predicted losses compare with those measured by Mitchell and Coy [1982]. Since none of the gearing details are known to us we will have to make some assumptions about the geometry needed in our calculations. For simplicity we will make these predictions at the following conditions;

(5-10)

R_{xe} = .025 [m]
U = 10 [m/sec]
Po = 1 [GPa]
θ_i = 80 and 100 [°C]
Up-Ug $\longrightarrow$ 0 to U [m/sec]
Kt = 0 [°C.sec/N.m]

As a first prediction the amount of sliding traction is shown in Fig 5-1. This is for all the fluids tested here. The traction is plotted as the traction coefficient here which is defined as;

(5-11) Traction coeff. = T/P = F_x/F_z

These curves show the level of traction at a given value of slip. They do reveal that the traction for fluids X and Y are much higher than for the others. The next highest traction is revealed by fluid B. This order corresponds to the order in which the efficiencies measurements of Mitchell and Coy [1982] went. The curves in Fig 5-1 look like ordinary traction curves to us but this is misleading. Since only the viscous model is retained for the traction prediction done here, the initial slope is viscous in nature and not elastic as might be expected for some of the fluids. All this is not very important in the prediction of gear efficiencies because we want the total slip losses in the mesh. The instantaneous powerloss at a given value of slip is the product of the traction force and the slip velocity. In dimensionless form this is given as;

(5-12) Instantaneous loss $= 2\left(\frac{F_x}{F_z}\right)\cdot\left(\frac{U_p-U_g}{U_p+U_g}\right)$

The curves of the instantaneous loss for the seven fluids are shown in figures 5-2 and 5-3 for the two different temperatures. Again the order of the instantaneous losses are as those observed in the full transmission test particularly for the traction fluids at the higher temperature. These show a higher loss at the higher temperatures as was observed in the real transmission test.
A yet more indicative parameter that shows the power loss in a mesh cycle would be the total of all the power loss from the starting slip till the current value of the slip. Essentially the area under the Instantaneous loss curves of figures 5-2 and 5-3. These curves are shown in figures 5-4 and 5-5 for the two different inlet temperatures.

5-7 THE CONSTANT FRICTION COEFFICIENT CONCEPT.

Some of the gear friction models that are used in the prediction of mesh losses employ a constant friction coefficient. This friction coefficient provides for an easy method to calculate the losses if so desired. It also gives a very simple method for estimating the effect of the sliding friction loss on the overall losses of the powertrain. In order to use this method however we must have access to the average friction coefficient. This value may be calculated by the methods presented above because it is nothing more than the integral of the instantaneous losses divided by the current level of slip. For the example data as used above, these resulting constant friction coefficient curves are shown in figures 5-6 and 5-7. At sufficiently large values if slip it is indeed clear that the friction coefficient by this method is about constant.

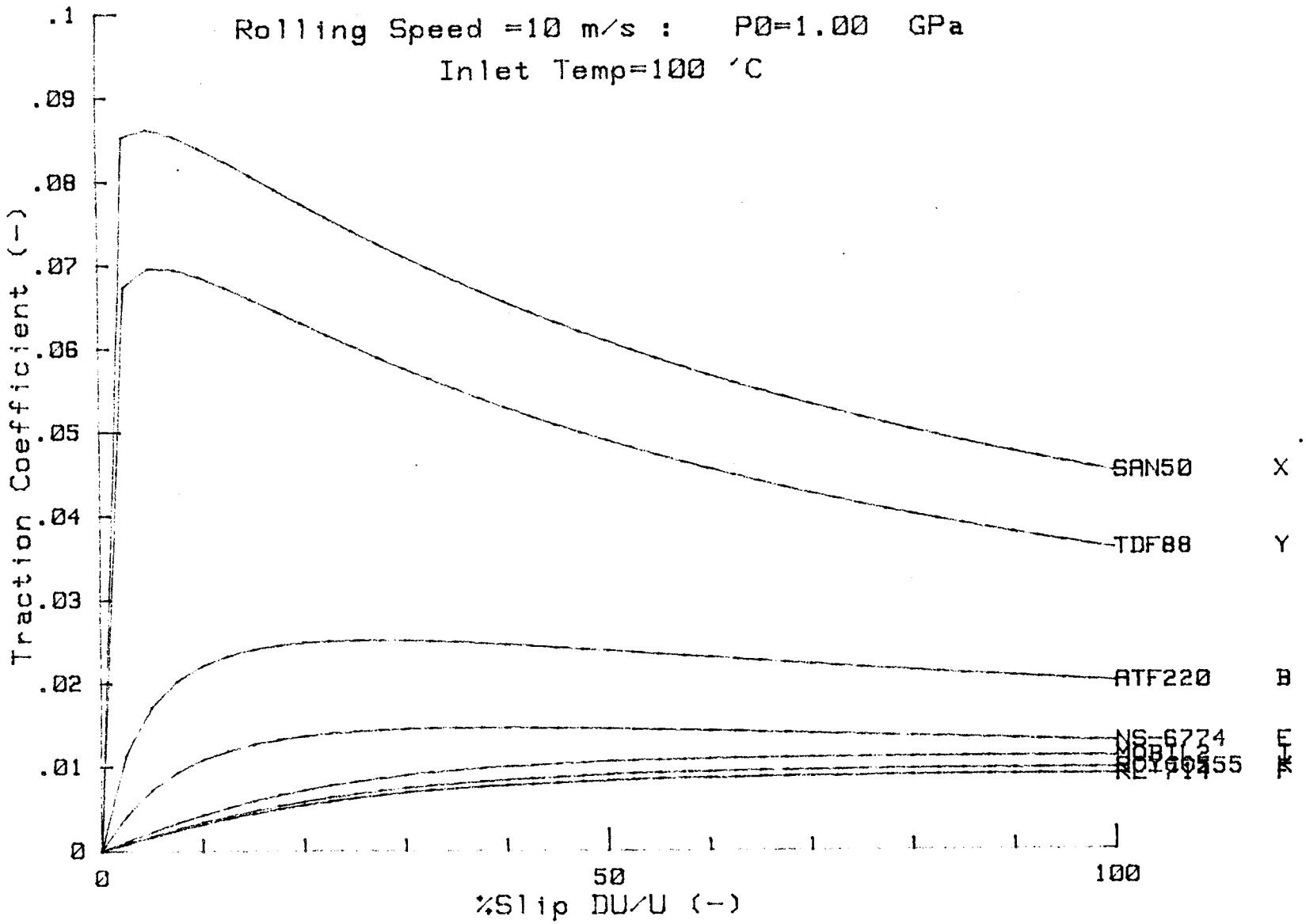

Fig. 5-1 Predicted traction coefficients for the tests fluids as a function of the slip. At constant speed, pressure and inlet

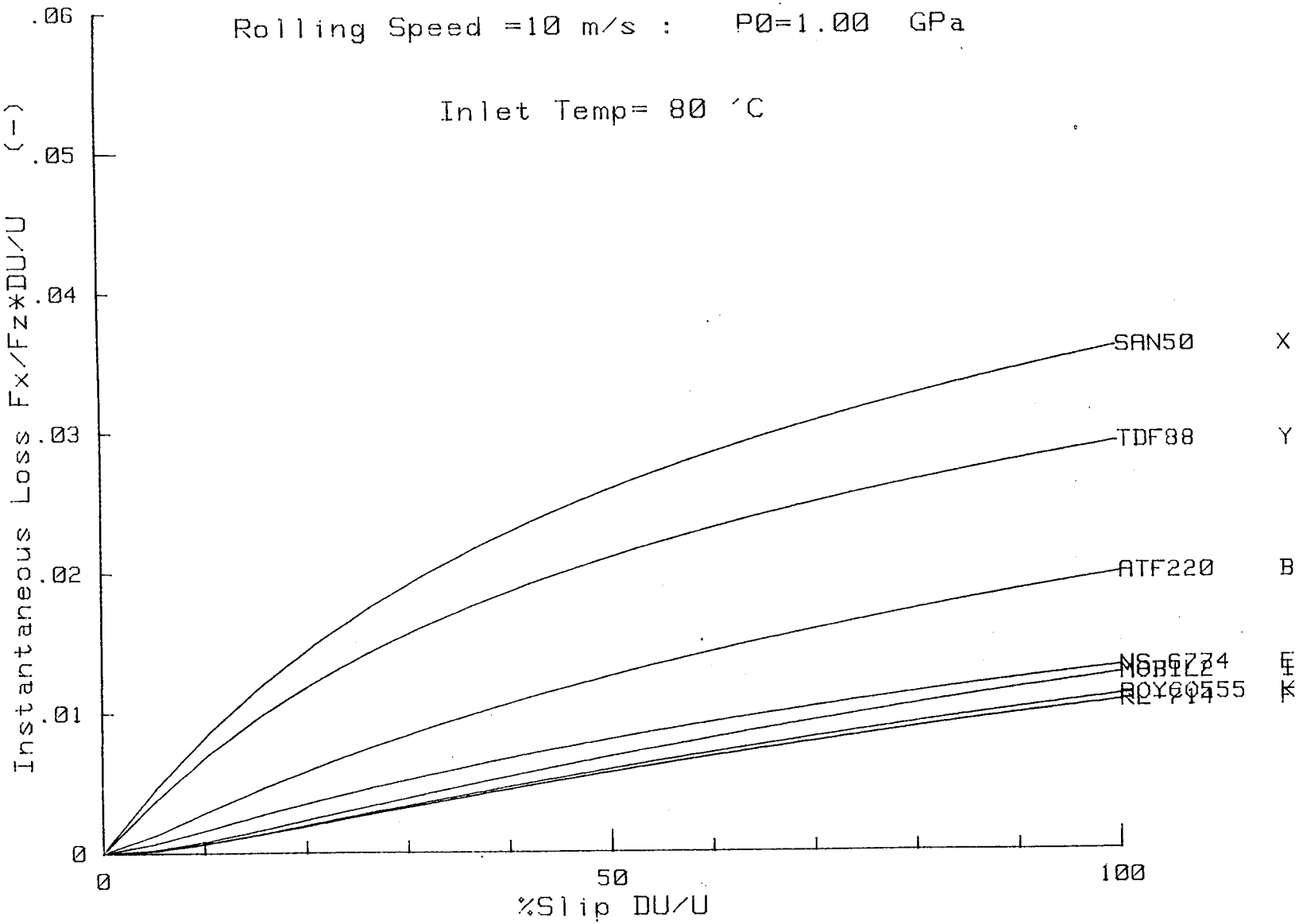

Fig. 5-2 **Dimensionless instantaneous loss factor for the test fluids as a function of slip. Inlet temperature = 80 °C.**

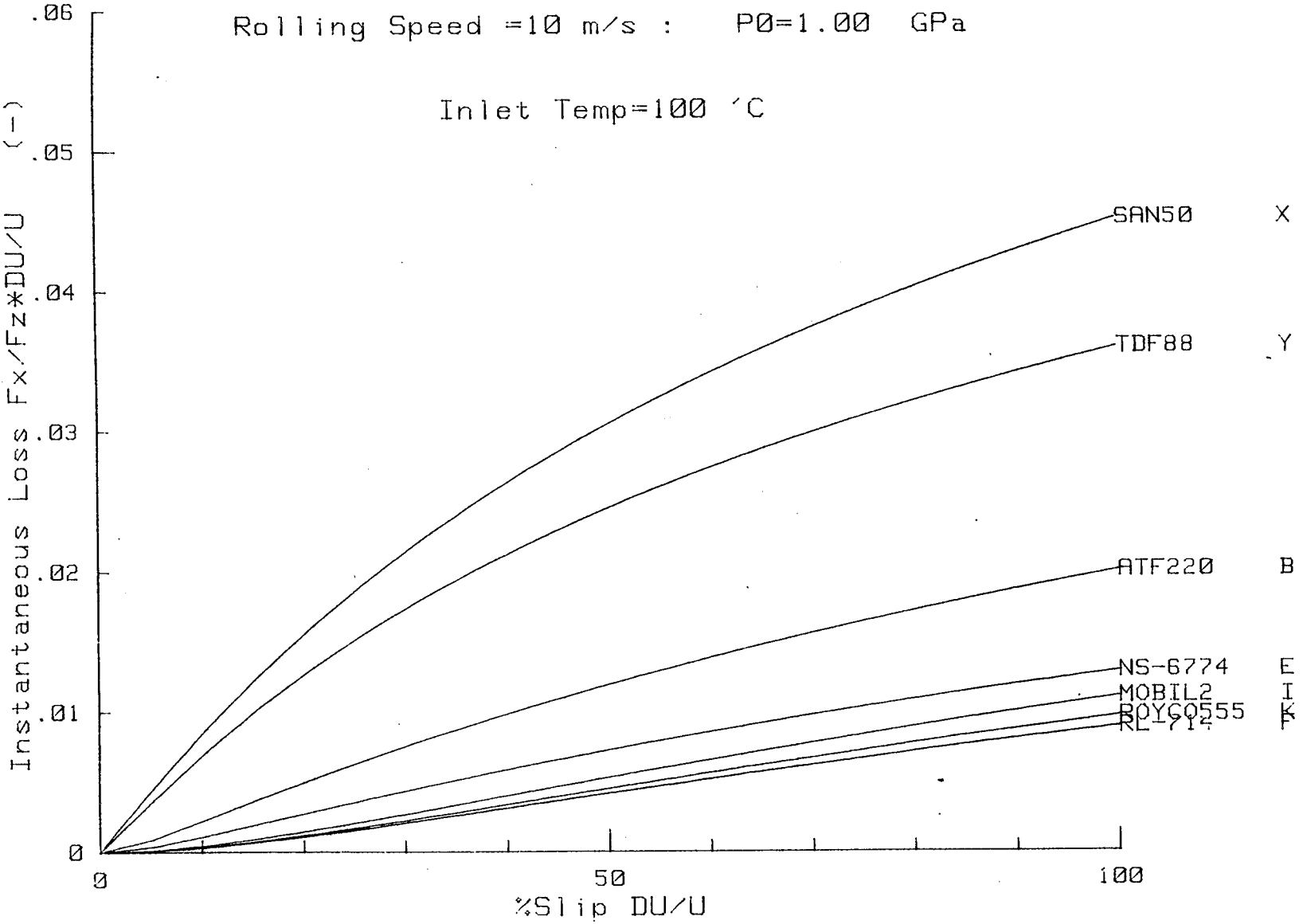

Fig. 5-3 **Dimensionless instantaneous loss factor for the test fluids as a function of slip. Inlet temperature = 100 °C.**

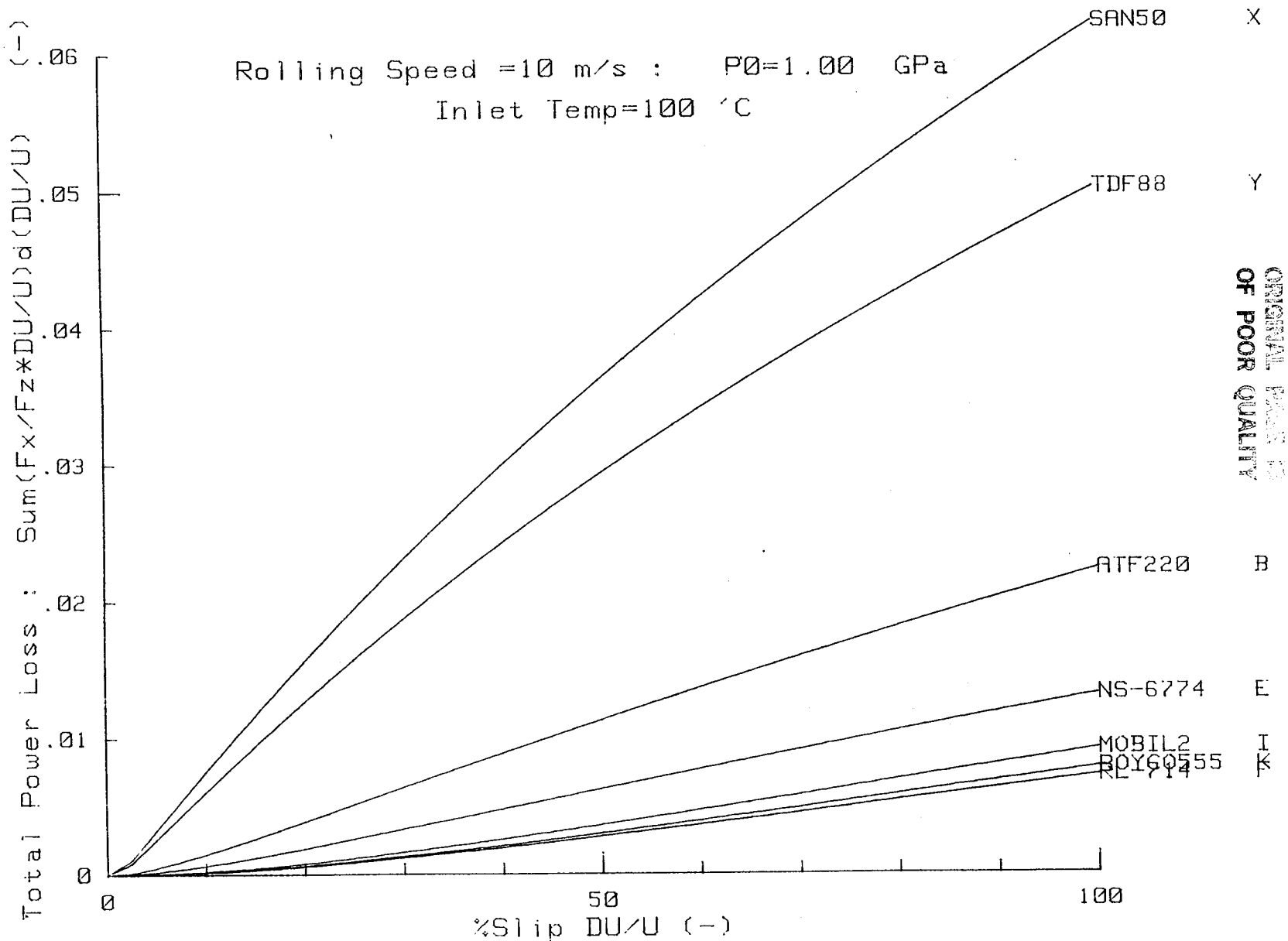

Fig. 5-5 **Dimensionless total power loss factor for the test fluids as a function of slip. Inlet temperature = 100 °C.**

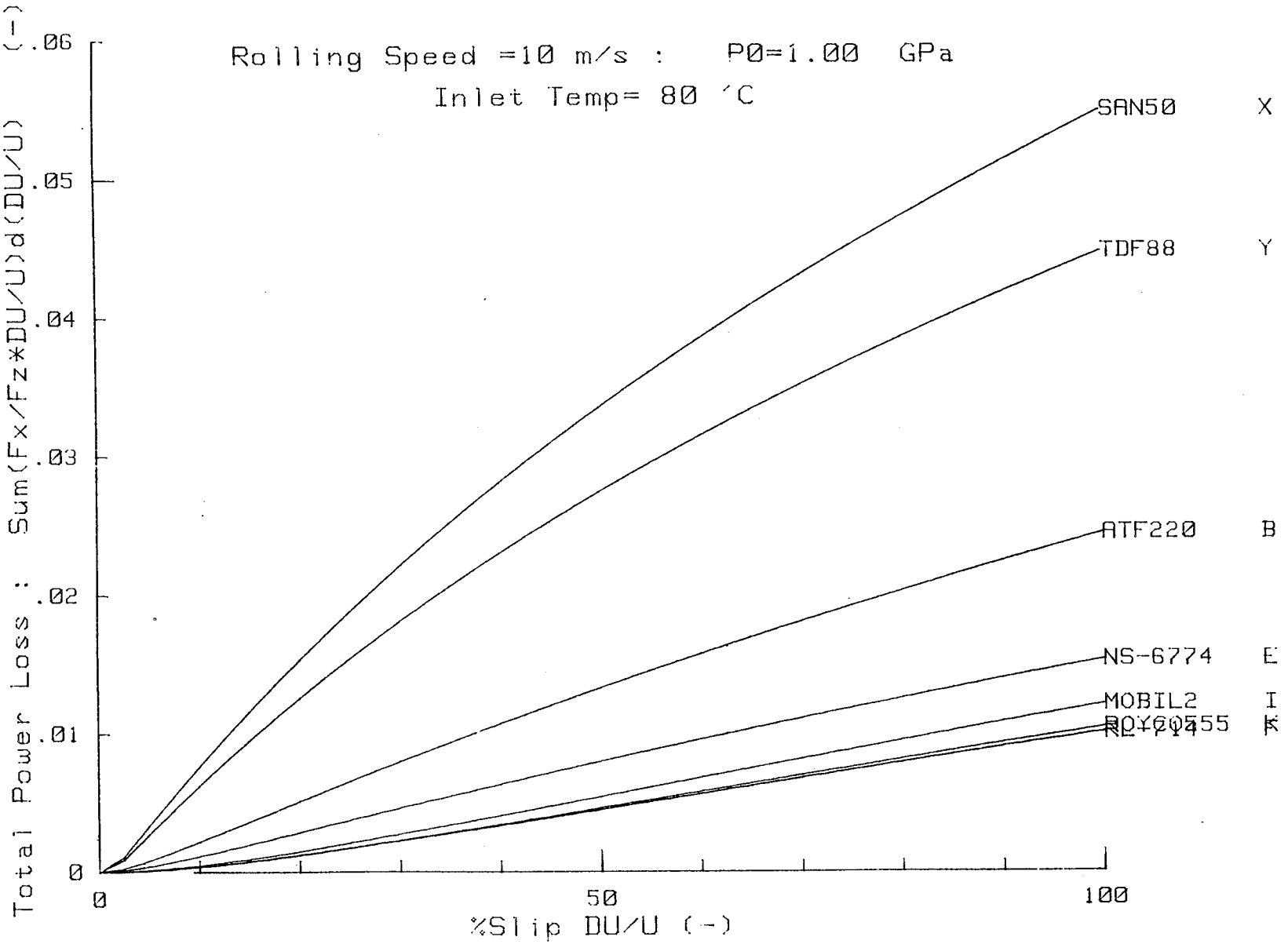

Fig. 5-4 **Dimensionless total power loss factor for the test fluids as a function of slip. Inlet temperature = 80 °C.**

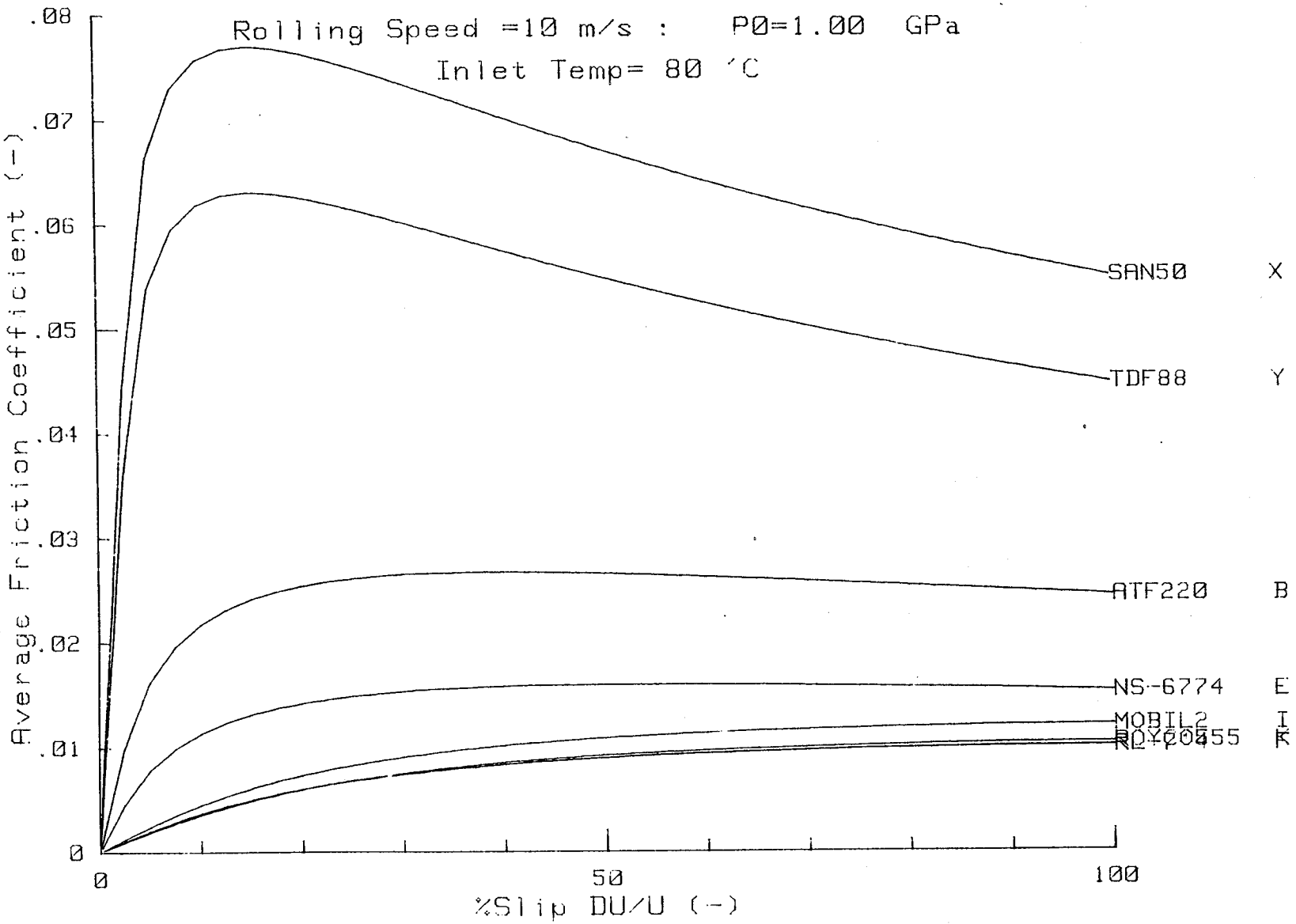

Fig. 5-6 **The average mesh friction coefficient for the test fluids as a function of slip. Inlet temperature = 80 °C.**

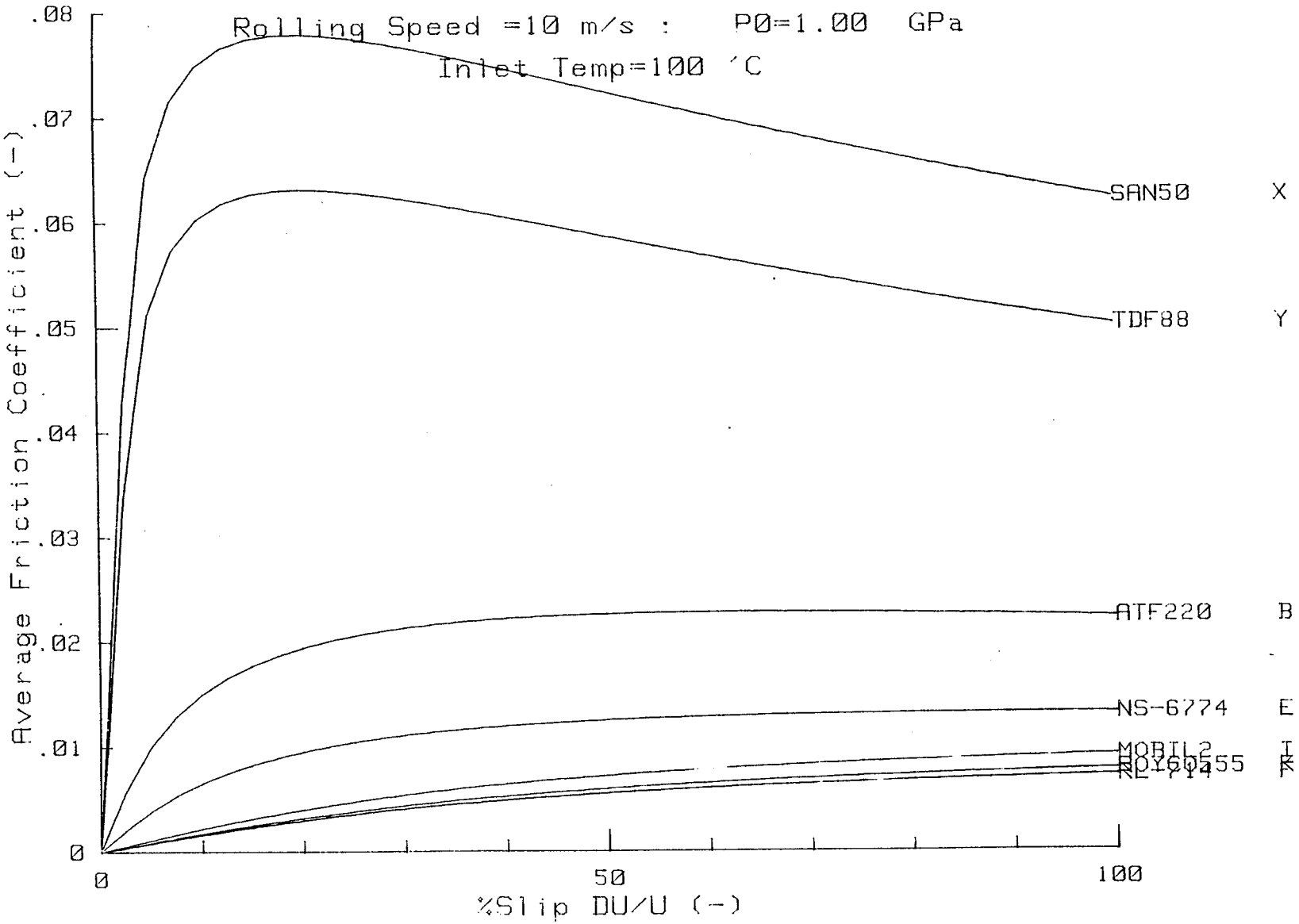

Fig. 5-7 **The average mesh friction coefficient for the test fluids as a function of slip. Inlet temperature = 100 °C.**

6 REFERENCES

Anderson, N.E. and Loewenthal, S.H. [1981] "Comparison of Spur Gear Efficiency Prediction Methods." Pro. of Advanced Power Transmission Technology, Nasa Lewis 1981. NASA CP 2210, pp 365-382.

Buckingham, E. [1963] "Analytical Mechanics of Gears.", Dover Publications, Inc. 1963, pp395-425.

Chiu, Y.P. [1975] "Approximate Calculation of Power loss in Involute Gears." ASME paper #75-PTG-2, Oct 1975.

Conry, T.F., Johnson, K.L. and Owen, S. [1979] "Viscosity in the Thermal Regime of Traction". Proc. of the Leeds-Lyon Conference, Lyon 1979, pp. 219-227.

Coy, J.J., Mitchell, A.M. and Hamrock, B.J. [1984] "Transmission Efficiency Measurements and Correlations with Physical Charactersistic of the Lubricant." , presented at the AGARD meeting Lisbon, Oct 8-12, 1984, Portugal.

Hamrock, B.J. and Dowson, D. [1977] "Isothermal Elastohydrodynamic Lubrication of Point Contacts, Part III - Fully Flooded Results." , J. Lubr. Technol. Trans. ASME., 99 , #2, pp. 264-276.

Jackson, A. [1980] "A Simple Method for Determining Thermal EHL Correction Factors for Rolling Element Bearings and Gears.", Trans. ASLE #24,2. pp 159-163

Johnson, K.L. and Cameron, R. [1967] "Shear Behaviour of Elastohydrodynamic Oil Films at High Rolling Contact Pressures". Proc. Inst. Mech. Eng. (London), 182 , pt. I, #14, pp. 307-319.

Johnson, K.L. and Roberts, A.D. [1974] "Observations of Viscoelastic Behaviour of an Elastohydrodynamic Lubricant Film". Proc. Roy. Soc. (London), Series A, 337 , #1609, (1974), pp. 217-242.

Johnson, K.L. and Tevaarwerk, J.L. [1977] "Shear behaviour of Elastohydrodynamic Oil Films". Proc. Roy. Soc. (London), Series A, 356 , #1685, pp. 215-236.

Johnson, K.L., and Greenwood, J.A. [1980] "Thermal Analysis of an Eyring fluid in EHL Traction", Wear, 61 (1980), p 353.

Martin, K.F. [1978] "A Review of Friction Predictions in Gear Teeth." , Wear, 49 , pp 201-238.

Merrit, H.E. [1972] "Gear Engineering." John Wiley & Sons, Inc., 1972, pp. 345-357.

Mitchell, A.M. and Coy, J.J. [1982] "Lubricant effects on Efficiency of a Helicopter Transmission." NASA TM 82857, (1982).

Murch, L.E. and Wilson, W.R.D. [1975] " A Thermal Elastohydrodynamic inlet zone analysis." , J. Lubr. Technol. Trans. ASME. , 97 , #2, p212.

Present, D.L., Newman, F.L., Tyler, J.C. and Cuellar, J.P. [1983] "Advanced Chemical Characterization and Physical Properties of Eleven Lubricants." AFLRL # 166, NASA LeRC CR 168187.

Shipley, E.E. [1962] "Loaded Gears in Action." in Gear Handbook by D.W. Dudley, ed. McGraw Hill Book Co. Inc., pp 14-1 to 14-60.

Smith, F.W. [1965] "Rolling Contact Lubrication-The Application of Elasto hydrodynamic Theory". Trans . Am. Soc. Mech. Engrs. 87 , (1965), Series D, p. 170 .

Tevaarwerk, J.L. [1979b] "Traction Drive Performance Prediction for the Johnson and Tevaarwerk Traction Model". NASA TP-1530.

Tevaarwerk, J.L. and Johnson, K.L. [1979c] "The Influence of Fluid Rheology on the Performance of Traction Drives", J. Lubr. Technol. Trans. ASME., 101 , p 266.

Tevaarwerk, J.L. [1979d] "Traction Calculations using the Shear plane Hypothesis" Proc. of the Leeds-Lyon Conference, Lyon 1979, pp. 201-213.

Tevaarwerk, J.L. [1980] "Thermal Influence on the Traction behaviour of an Elastic/Plastic model" Proc. of the Leeds-Lyon Conference, Leeds 1980, pp. 302-309.

Tevaarwerk, J.L. [1981] "A Simple Thermal Correction for Large Spin Traction Curves" J. Mech. Design. Trans. ASME., 103 , #2, (1981), p440.

Tevaarwerk, J.L. [1981b] "Traction Contact Performance Evaluation at High Speeds". NASA CR-165226, Sept., 1981.

Tevaarwerk, J.L. [1982] "Traction in Lubricated Contacts ". Proc. of the Int. Symposium on Contact Mechanics and Wear of Rail/Wheel systems. Vancouver 1982

Tevaarwerk, J.L. [1985] " Thermal Traction Contact Performance Evaluation under fully Flooded and Starved Conditions.", NASA CR-168173.

Tevaarwerk, J.L. [1985b] "Equivalent Thermal Resistance of an EHL film." In progress.

********** 2.11360752E+11

TRACTION CURVE DATA SUMMARY FOR MOBIL2 :Prog PLOTTER Rev# 1

**********22:03:46

Test # (----)	Po (GPa)	Uo (m/s)	To ('C)	Fz (N)	kk (-)	a (m)
MOBIL5131R	1.01	9.9	32	200	1.7	.00024
MOBIL5132R	1.01	19.9	33	200	1.7	.00024
MOBIL5133R	1.01	30.2	35	200	1.7	.00024
MOBIL5134R	1.27	10.2	34	400	1.7	.00030
MOBIL5135R	1.27	20.3	35	400	1.7	.00030
MOBIL5136R	1.27	30.2	37	400	1.7	.00030
MOBIL5137R	1.60	10.3	35	800	1.7	.00037
MOBIL5138R	1.60	20.2	36	800	1.7	.00037
MOBIL5139R	1.60	29.1	38	800	1.7	.00037
MOBIL513AR	1.93	10.9	37	1400	1.7	.00045
MOBIL513BR	1.93	20.6	38	1400	1.7	.00045
MOBIL513CR	1.93	27.8	41	1400	1.7	.00045
MOBIL5141R	1.01	10.3	77	200	1.7	.00024
MOBIL5142R	1.27	20.3	78	400	1.7	.00030
MOBIL5143R	1.01	29.7	78	200	1.7	.00024
MOBIL5144R	1.27	10.3	77	400	1.7	.00030
MOBIL5145R	1.27	20.3	78	400	1.7	.00030
MOBIL5146R	1.27	29.8	79	400	1.7	.00030
MOBIL5147R	1.60	10.3	80	800	1.7	.00037
MOBIL5148R	1.60	20.2	81	800	1.7	.00037
MOBIL5149R	1.60	30.1	83	800	1.7	.00037
MOBIL514AR	1.93	10.6	82	1400	1.7	.00045
MOBIL514BR	1.93	20.2	84	1400	1.7	.00045

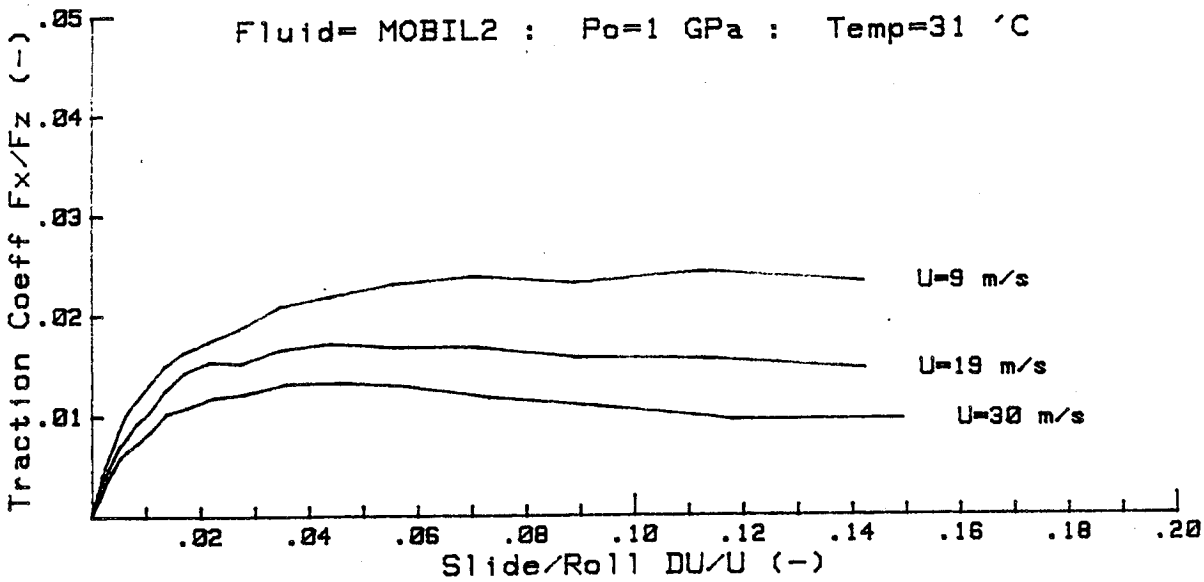
Fluid= MOBIL2 : Po=1 GPa : Temp=31 'C
Traction Coeff Fx/Fz (-)
.05
.04
.03
.02
.01
U=9 m/s
U=19 m/s
U=30 m/s
.02 .04 .06 .08 .10 .12 .14 .16 .18 .20
Slide/Roll DU/U (-)

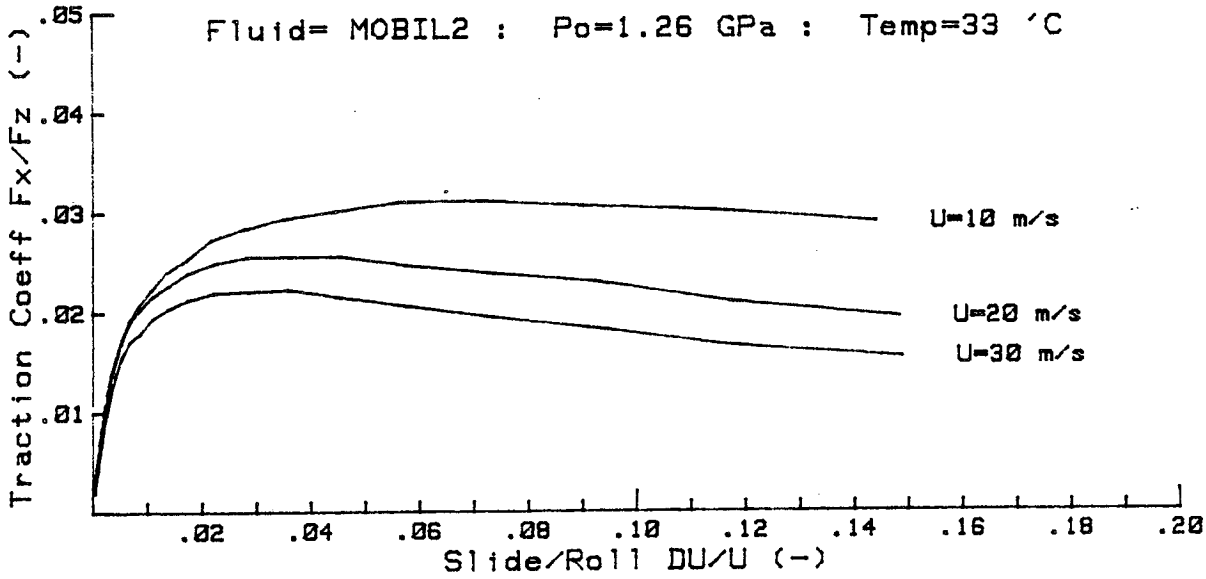
Fluid= MOBIL2 : Po=1.26 GPa : Temp=33 'C
Traction Coeff Fx/Fz (-)
.05
.04
.03
.02
.01
U=10 m/s
U=20 m/s
U=30 m/s
.02 .04 .06 .08 .10 .12 .14 .16 .18 .20
Slide/Roll DU/U (-)

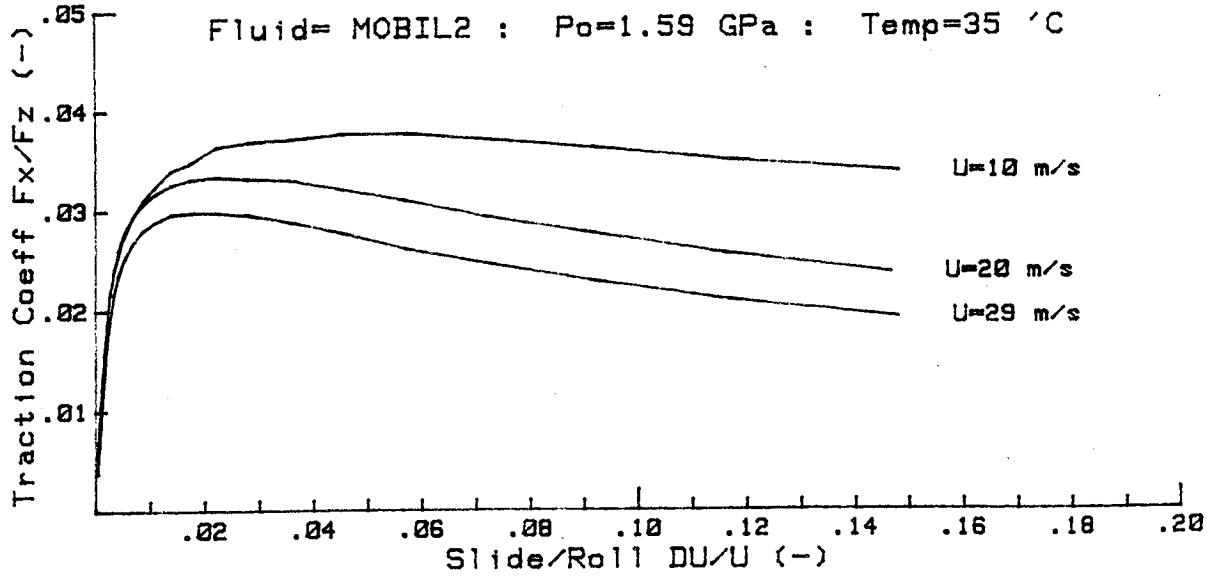
Fluid= MOBIL2 : Po=1.59 GPa : Temp=35 'C
Traction Coeff Fx/Fz (-)
.05
.04
.03
.02
.01
U=10 m/s
U=20 m/s
U=29 m/s
.02 .04 .06 .08 .10 .12 .14 .16 .18 .20
Slide/Roll DU/U (-)

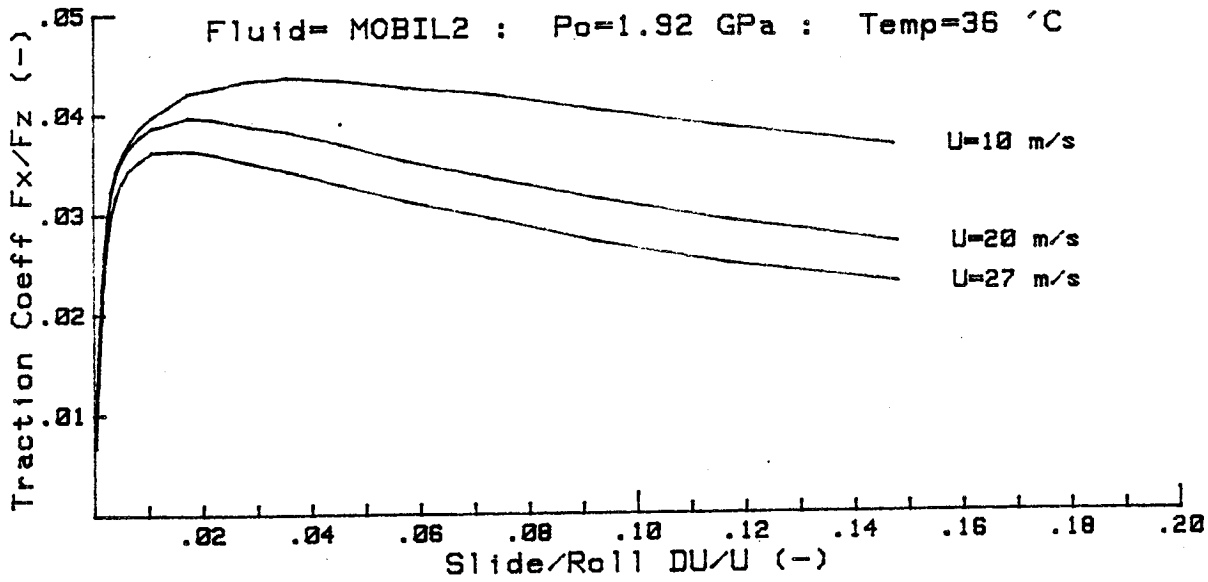
Fluid= MOBIL2 : Po=1.92 GPa : Temp=36 'C
Traction Coeff Fx/Fz (-)
.05
.04
.03
.02
.01
U=10 m/s
U=20 m/s
U=27 m/s
.02 .04 .06 .08 .10 .12 .14 .16 .18 .20
Slide/Roll DU/U (-)

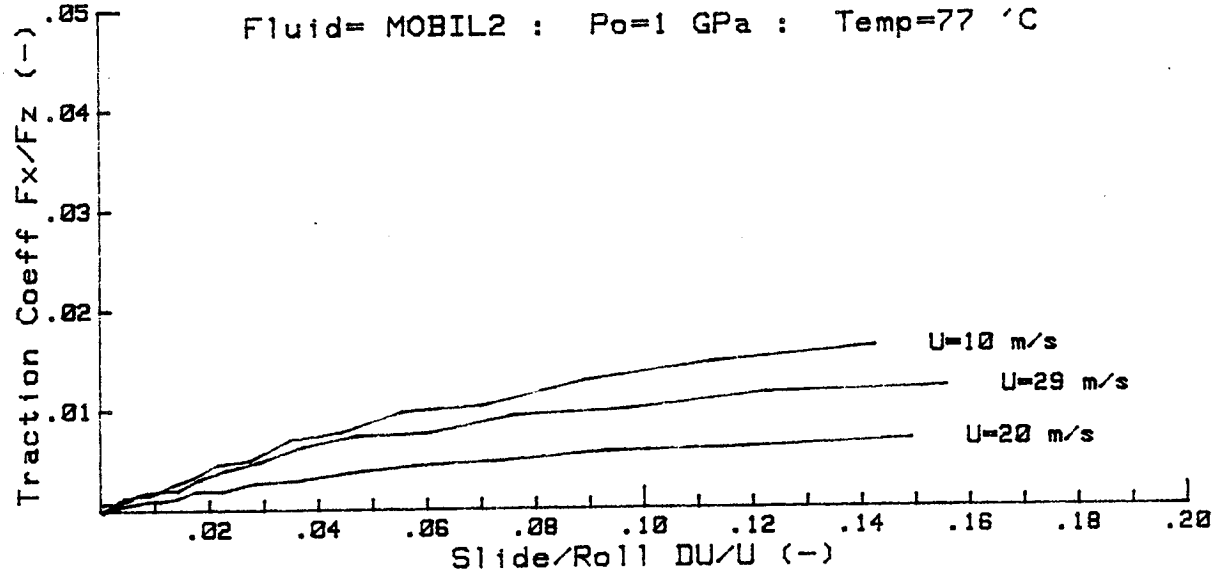
Fluid= MOBIL2 : Po=1 GPa : Temp=77 'C
Traction Coeff Fx/Fz (-)
.05
.04
.03
.02
.01
U=10 m/s
U=29 m/s
U=20 m/s
.02 .04 .06 .08 .10 .12 .14 .16 .18 .20
Slide/Roll DU/U (-)

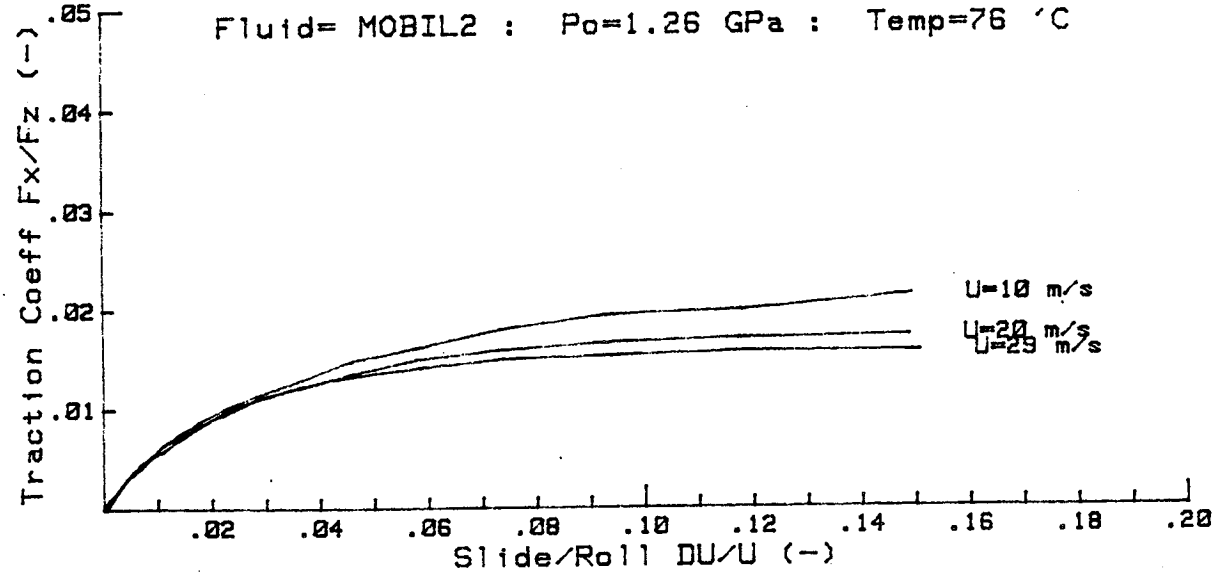
Fluid= MOBIL2 : Po=1.26 GPa : Temp=76 'C
Traction Coeff Fx/Fz (-)
.05
.04
.03
.02
.01
U=10 m/s
U=20 m/s
U=29 m/s
.02 .04 .06 .08 .10 .12 .14 .16 .18 .20
Slide/Roll DU/U (-)

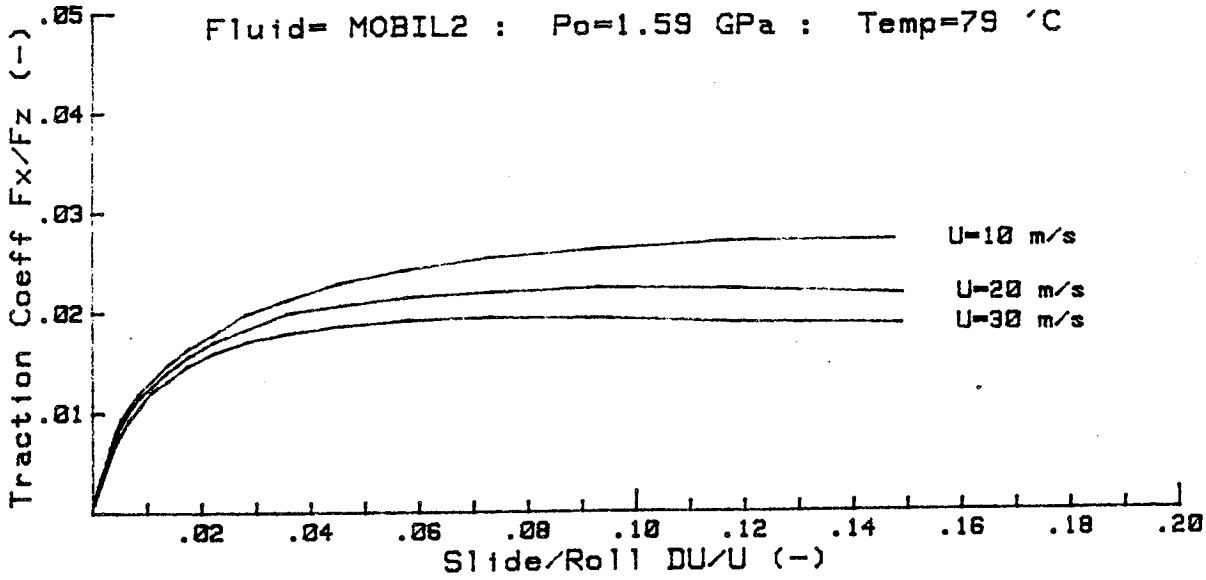
Fluid= MOBIL2 : Po=1.59 GPa : Temp=79 'C
Traction Coeff Fx/Fz (-)
.05
.04
.03
.02
.01
U=10 m/s
U=20 m/s
U=30 m/s
.02
.04
.06
.08
.10
.12
.14
.16
.18
.20
Slide/Roll DU/U (-)

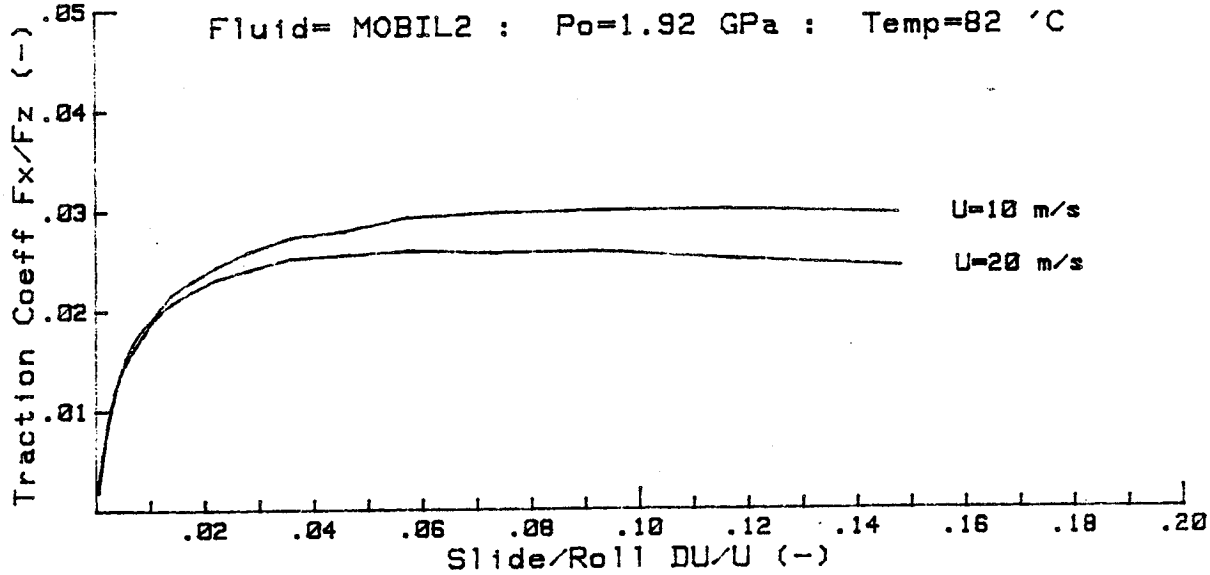
Fluid= MOBIL2 : Po=1.92 GPa : Temp=82 'C
Traction Coeff Fx/Fz (-)
.05
.04
.03
.02
.01
U=10 m/s
U=20 m/s
.02
.04
.06
.08
.10
.12
.14
.16
.18
.20
Slide/Roll DU/U (-)

********** 2.08662912E+11

TRACTION CURVE DATA SUMMARY FOR NS-6774 :Prog PLOTTER Rev# 1

**********04:54:20

Test # (----)	Po (GPa)	Uo (m/s)	To ('C)	Fz (N)	kk (-)	a (m)
NS_675191R	1.01	10.2	34	200	1.7	.00024
NS_675192R	1.01	20.3	36	200	1.7	.00024
NS_675193R	1.01	29.7	38	200	1.7	.00024
NS_675194R	1.27	10.3	37	400	1.7	.00030
NS_675195R	1.27	20.3	37	400	1.7	.00030
NS_675196R	1.27	30.2	40	400	1.7	.00030
NS_675197R	1.60	10.2	38	800	1.7	.00037
NS_675198R	1.60	20.3	39	800	1.7	.00037
NS_675199R	1.60	30.2	41	800	1.7	.00037
NS_67519AR	1.93	11.1	39	1400	1.7	.00045
NS_67519BR	1.93	21.1	41	1400	1.7	.00045
NS_67519CR	1.93	31.3	45	1400	1.7	.00045
NS_67519DR	1.01	10.7	79	200	1.7	.00024
NS_67519ER	1.01	20.8	79	200	1.7	.00024
NS_67519FR	1.01	30.2	80	200	1.7	.00024
NS_67519GR	1.27	20.8	80	400	1.7	.00030
NS_67519HR	1.27	10.7	79	400	1.7	.00030
NS_67519IR	1.27	30.4	79	400	1.7	.00030
NS_67519JR	1.60	10.2	77	800	1.7	.00037
NS_67519KR	1.60	20.3	78	800	1.7	.00037
NS_67519LR	1.60	30.2	81	800	1.7	.00037
NS_67519MR	1.93	11.3	82	1400	1.7	.00045
NS_67519NR	1.93	21.0	84	1400	1.7	.00045
NS_67519OR	1.93	30.5	83	1400	1.7	.00045

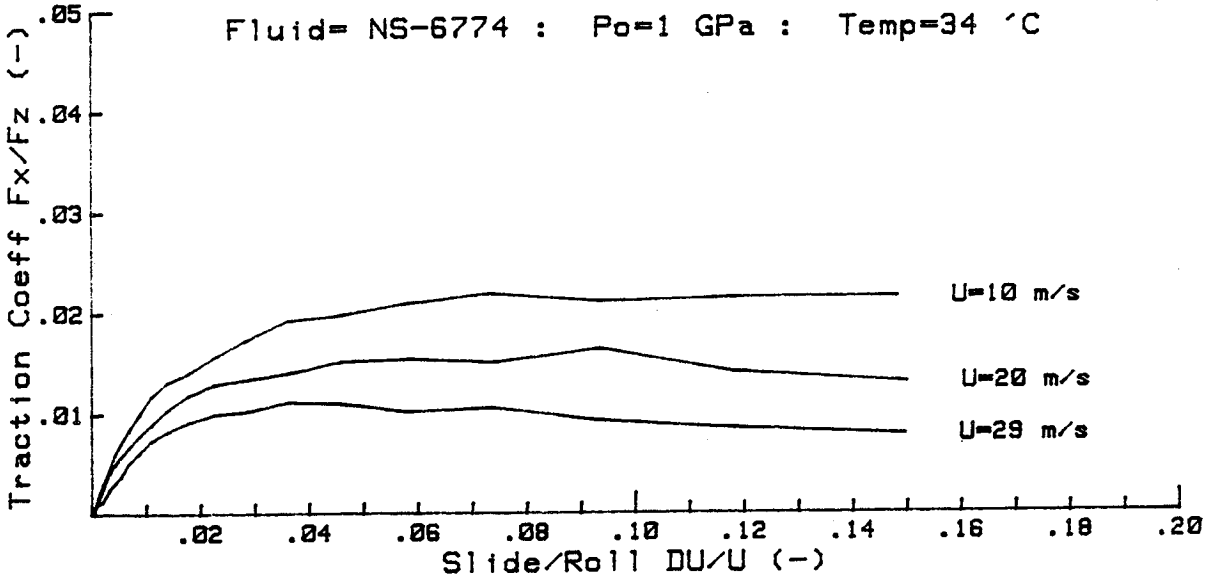
Fluid= NS-6774 : Po=1 GPa : Temp=34 'C
Traction Coeff Fx/Fz (-)
.05
.04
.03
.02
.01
U=10 m/s
U=20 m/s
U=29 m/s
.02 .04 .06 .08 .10 .12 .14 .16 .18 .20
Slide/Roll DU/U (-)

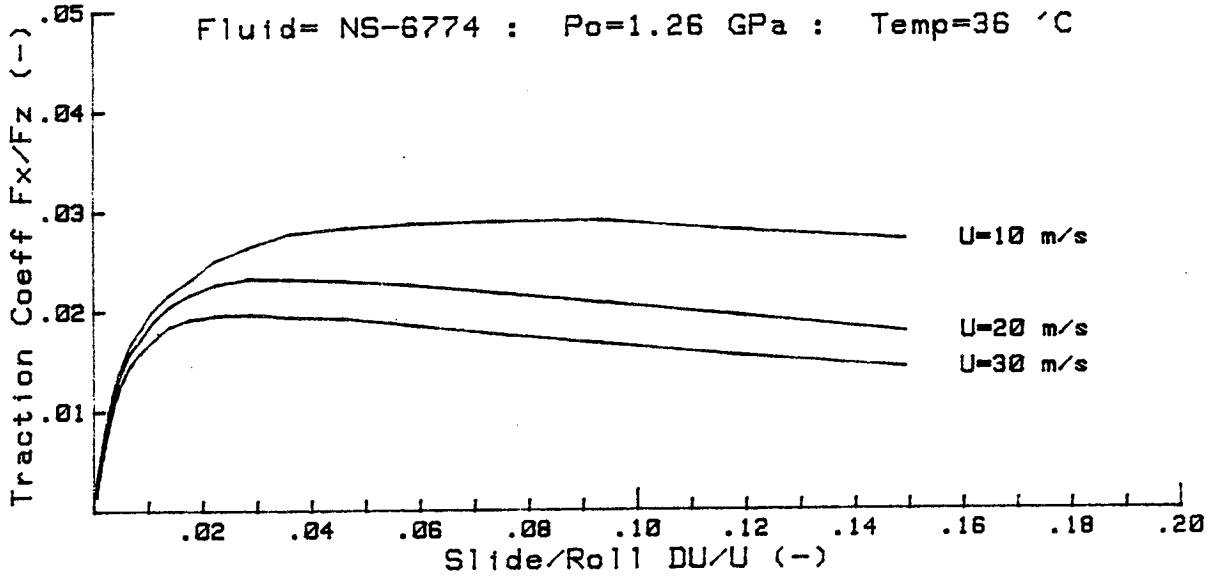
Fluid= NS-6774 : Po=1.26 GPa : Temp=36 'C
Traction Coeff Fx/Fz (-)
.05
.04
.03
.02
.01
U=10 m/s
U=20 m/s
U=30 m/s
.02 .04 .06 .08 .10 .12 .14 .16 .18 .20
Slide/Roll DU/U (-)

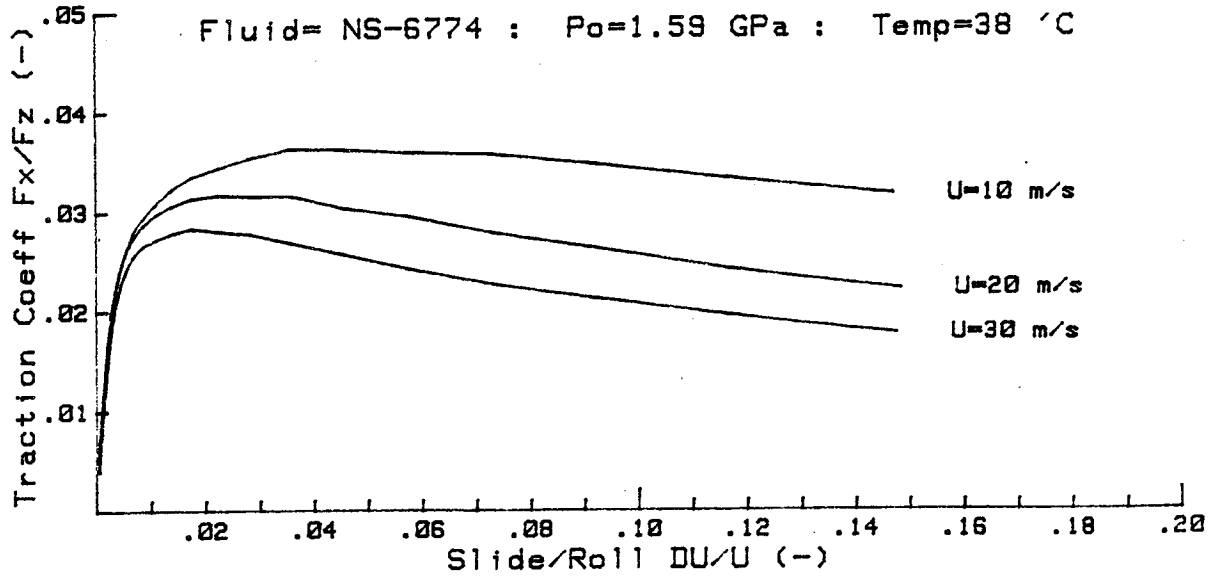
Fluid= NS-6774 : Po=1.59 GPa : Temp=38 'C
Traction Coeff Fx/Fz (-)
.05
.04
.03
.02
.01
U=10 m/s
U=20 m/s
U=30 m/s
.02 .04 .06 .08 .10 .12 .14 .16 .18 .20
Slide/Roll DU/U (-)

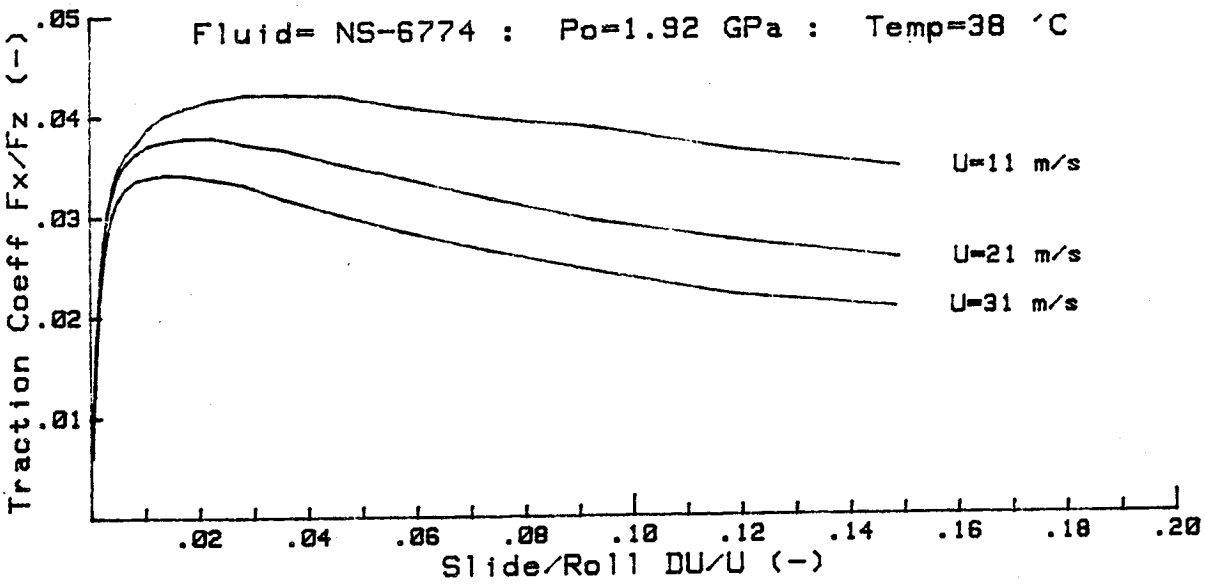
Fluid= NS-6774 : Po=1.92 GPa : Temp=38 'C
Traction Coeff Fx/Fz (-)
.05
.04
.03
.02
.01
U=11 m/s
U=21 m/s
U=31 m/s
.02 .04 .06 .08 .10 .12 .14 .16 .18 .20
Slide/Roll DU/U (-)

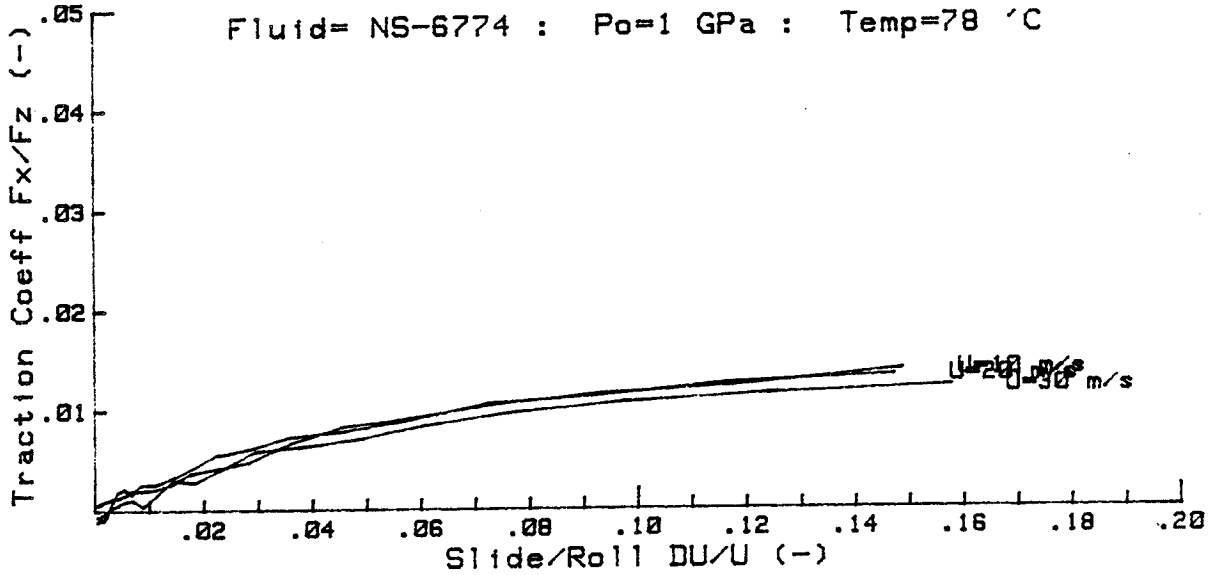
Fluid= NS-6774 : Po=1 GPa : Temp=78 'C
Traction Coeff Fx/Fz (-)
.05
.04
.03
.02
.01
U=10 m/s
U=20 m/s
U=30 m/s
.02 .04 .06 .08 .10 .12 .14 .16 .18 .20
Slide/Roll DU/U (-)

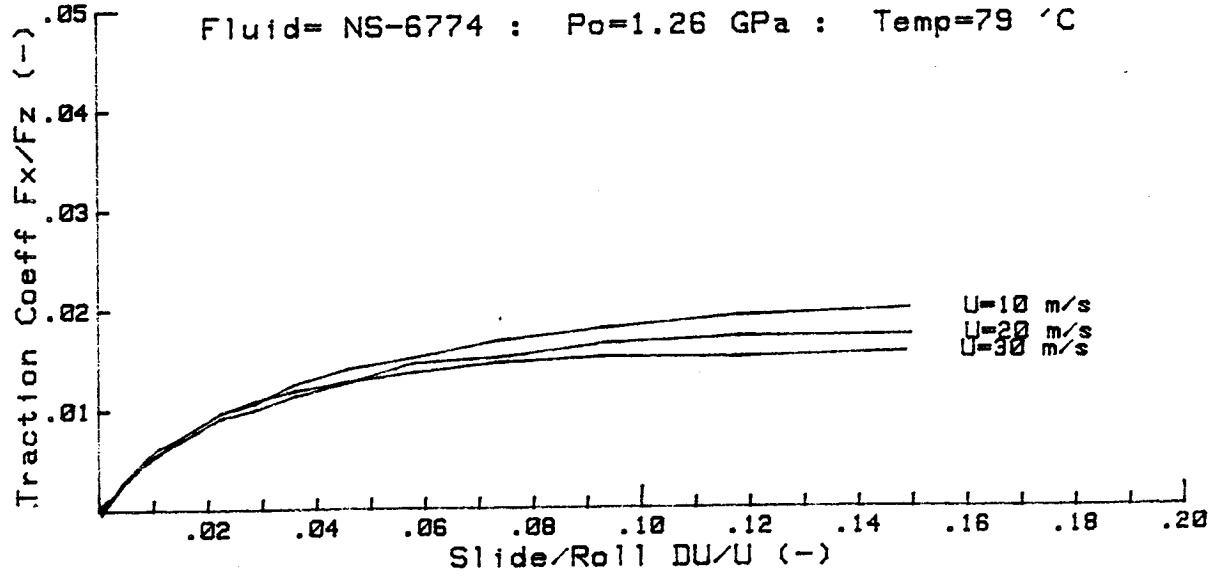
Fluid= NS-6774 : Po=1.26 GPa : Temp=79 'C
Traction Coeff Fx/Fz (-)
.05
.04
.03
.02
.01
U=10 m/s
U=20 m/s
U=30 m/s
.02 .04 .06 .08 .10 .12 .14 .16 .18 .20
Slide/Roll DU/U (-)

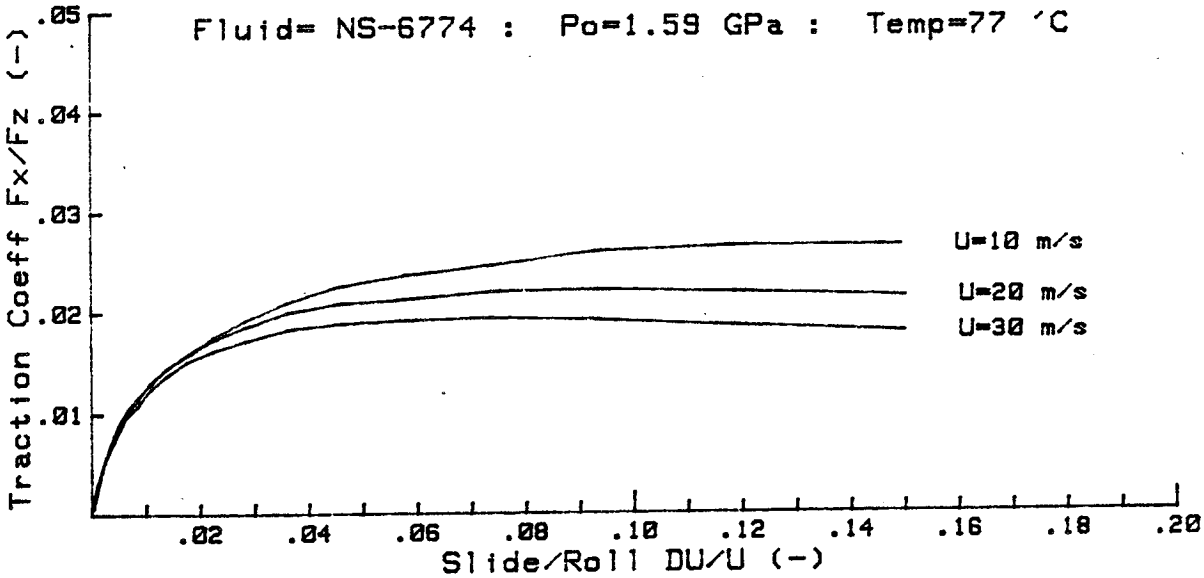
Fluid= NS-6774 : Po=1.59 GPa : Temp=77 'C
Traction Coeff Fx/Fz (-)
.05
.04
.03
.02
.01
U=10 m/s
U=20 m/s
U=30 m/s
.02 .04 .06 .08 .10 .12 .14 .16 .18 .20
Slide/Roll DU/U (-)

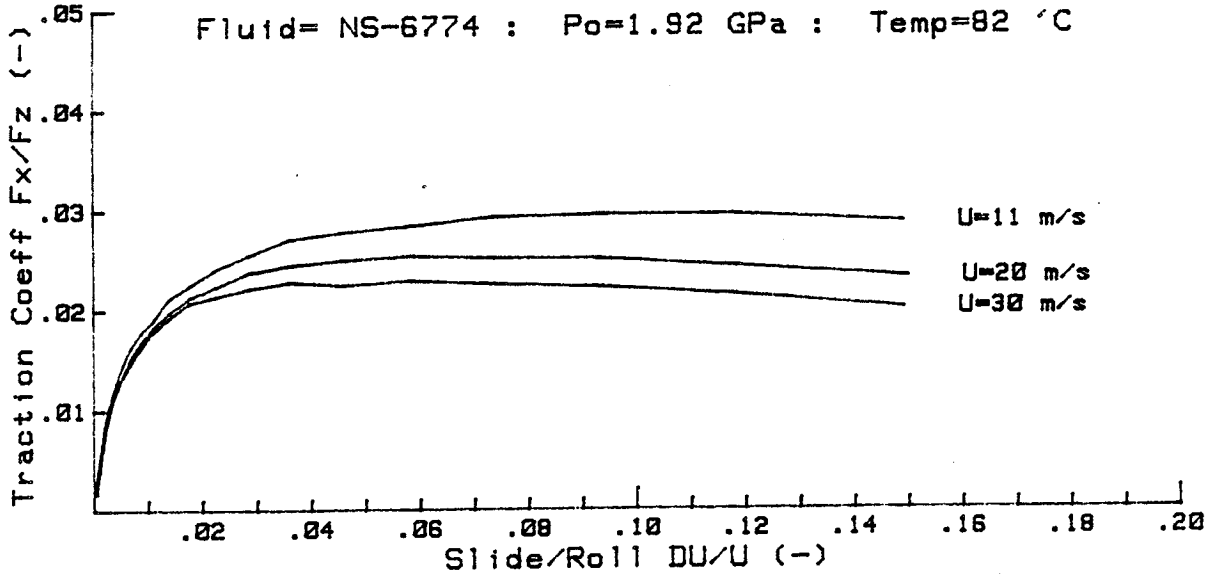
Fluid= NS-6774 : Po=1.92 GPa : Temp=82 'C
Traction Coeff Fx/Fz (-)
.05
.04
.03
.02
.01
U=11 m/s
U=20 m/s
U=30 m/s
.02 .04 .06 .08 .10 .12 .14 .16 .18 .20
Slide/Roll DU/U (-)

********** 2.08662912E+11

TRACTION CURVE DATA SUMMARY FOR ATF220 :Prog PLOTTER Rev# 1

**********00:08:18

Test # (----)	Po (GPa)	Uo (m/s)	To ('C)	Fz (N)	kk (-)	a (m)
ATF224CV1R	1.01	10.2	27	200	1.7	.00024
ATF224CV2R	1.01	20.2	28	200	1.7	.00024
ATF224CV3R	1.01	30.2	30	200	1.7	.00024
ATF224CV6R	1.27	9.8	29	400	1.7	.00030
ATF224CV7R	1.27	20.0	30	400	1.7	.00030
ATF224CV8R	1.27	30.0	31	400	1.7	.00030
ATF224CV9R	1.60	10.2	30	800	1.7	.00037
ATF224CVAR	1.60	20.2	31	800	1.7	.00037
ATF224CVBR	1.60	30.2	33	800	1.7	.00037
ATF224CVCR	1.93	10.9	32	1400	1.7	.00045
ATF224CVDR	1.93	20.6	33	1400	1.7	.00045
ATF224CVER	1.93	30.5	35	1400	1.7	.00045
ATF225131R	1.01	10.0	78	200	1.7	.00024
ATF225132R	1.01	20.0	81	200	1.7	.00024
ATF225133R	1.01	25.3	84	200	1.7	.00024
ATF225134R	1.01	30.1	85	200	1.7	.00024
ATF225135R	1.27	10.3	82	400	1.7	.00030
ATF225136R	1.27	20.2	81	400	1.7	.00030
ATF225137R	1.27	30.0	82	400	1.7	.00030
ATF225138R	1.60	10.5	82	800	1.7	.00037
ATF225139R	1.60	20.3	82	800	1.7	.00037
ATF22513AR	1.60	30.1	84	800	1.7	.00037
ATF22513BR	1.93	20.9	83	1400	1.7	.00045
ATF22513CR	1.93	25.7	83	1400	1.7	.00045
ATF22513DR	1.93	10.9	81	1400	1.7	.00045

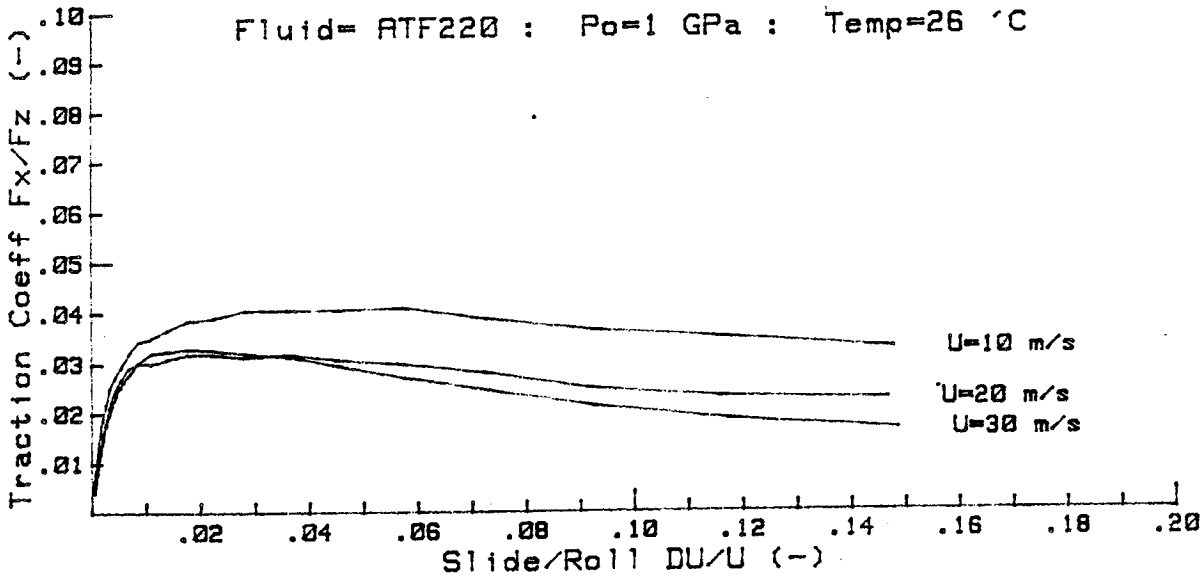
Fluid= ATF220 : Po=1 GPa : Temp=26 'C
Traction Coeff Fx/Fz (-)
.10
.09
.08
.07
.06
.05
.04
.03
.02
.01
U=10 m/s
U=20 m/s
U=30 m/s
.02 .04 .06 .08 .10 .12 .14 .16 .18 .20
Slide/Roll DU/U (-)

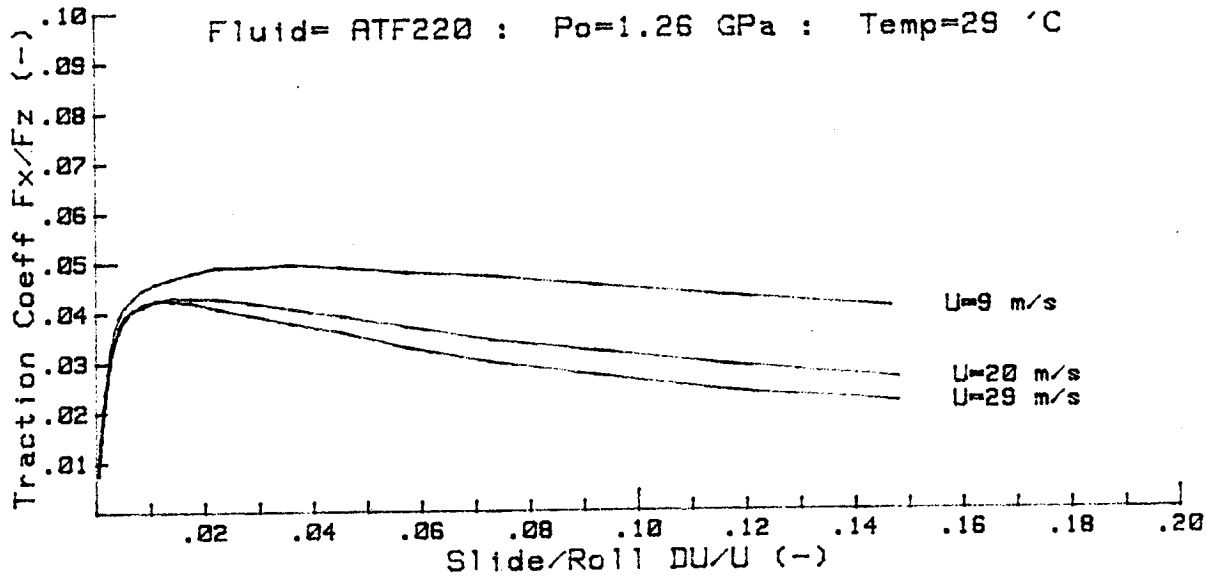
Fluid= ATF220 : Po=1.26 GPa : Temp=29 'C
Traction Coeff Fx/Fz (-)
.10
.09
.08
.07
.06
.05
.04
.03
.02
.01
U=9 m/s
U=20 m/s
U=29 m/s
.02 .04 .06 .08 .10 .12 .14 .16 .18 .20
Slide/Roll DU/U (-)

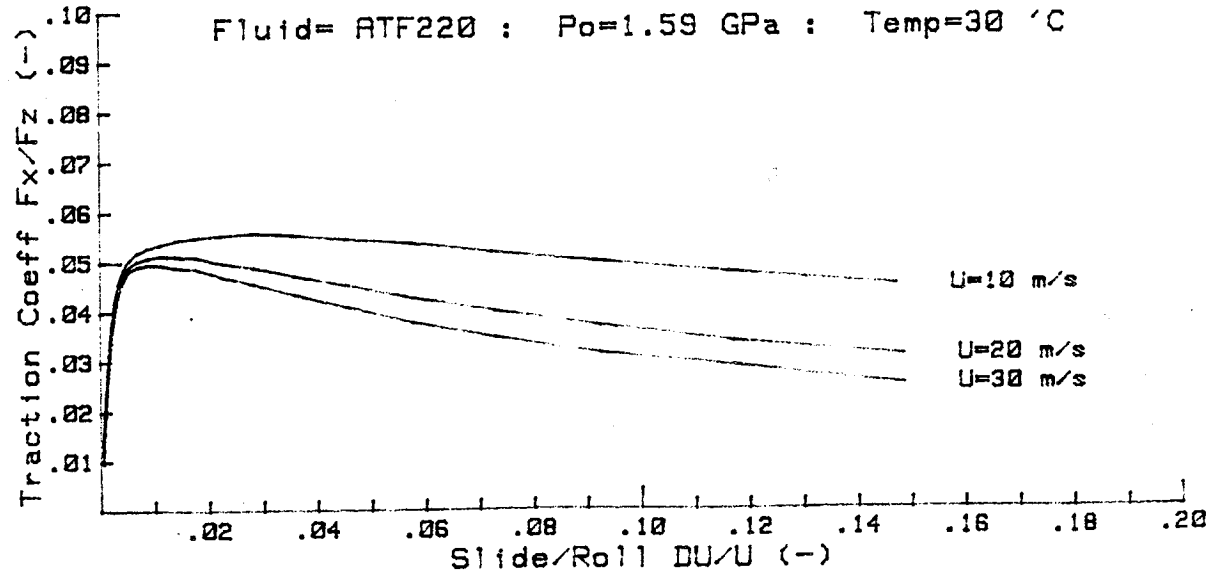
Fluid= ATF220 : Po=1.59 GPa : Temp=30 'C
Traction Coeff Fx/Fz (-)
.10
.09
.08
.07
.06
.05
.04
.03
.02
.01
U=10 m/s
U=20 m/s
U=30 m/s
.02 .04 .06 .08 .10 .12 .14 .16 .18 .20
Slide/Roll DU/U (-)

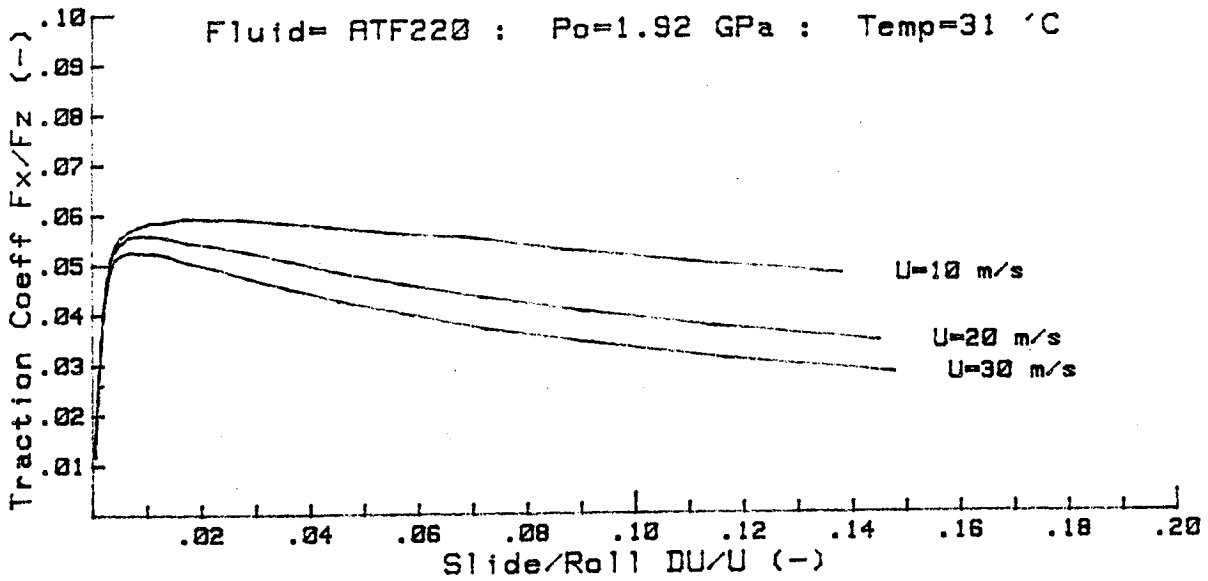
Fluid= ATF220 : Po=1.92 GPa : Temp=31 'C
Traction Coeff Fx/Fz (-)
.10
.09
.08
.07
.06
.05
.04
.03
.02
.01
U=10 m/s
U=20 m/s
U=30 m/s
.02 .04 .06 .08 .10 .12 .14 .16 .18 .20
Slide/Roll DU/U (-)

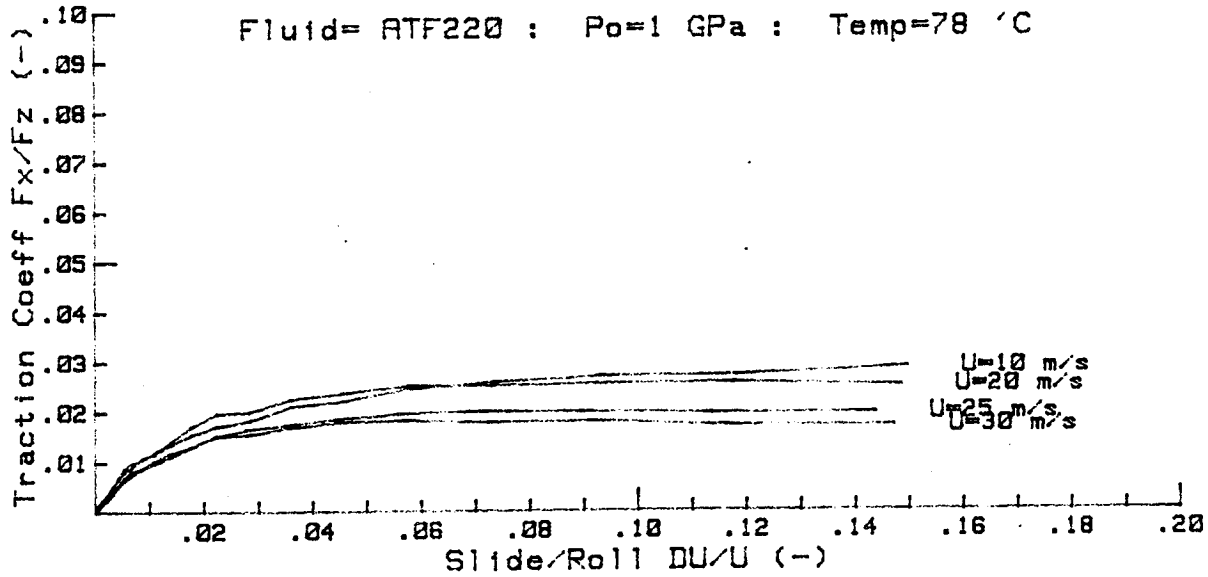
Fluid= ATF220 : Po=1 GPa : Temp=78 'C
Traction Coeff Fx/Fz (-)
.10
.09
.08
.07
.06
.05
.04
.03
.02
.01
U=10 m/s
U=20 m/s
U=25 m/s
U=30 m/s
.02 .04 .06 .08 .10 .12 .14 .16 .18 .20
Slide/Roll DU/U (-)

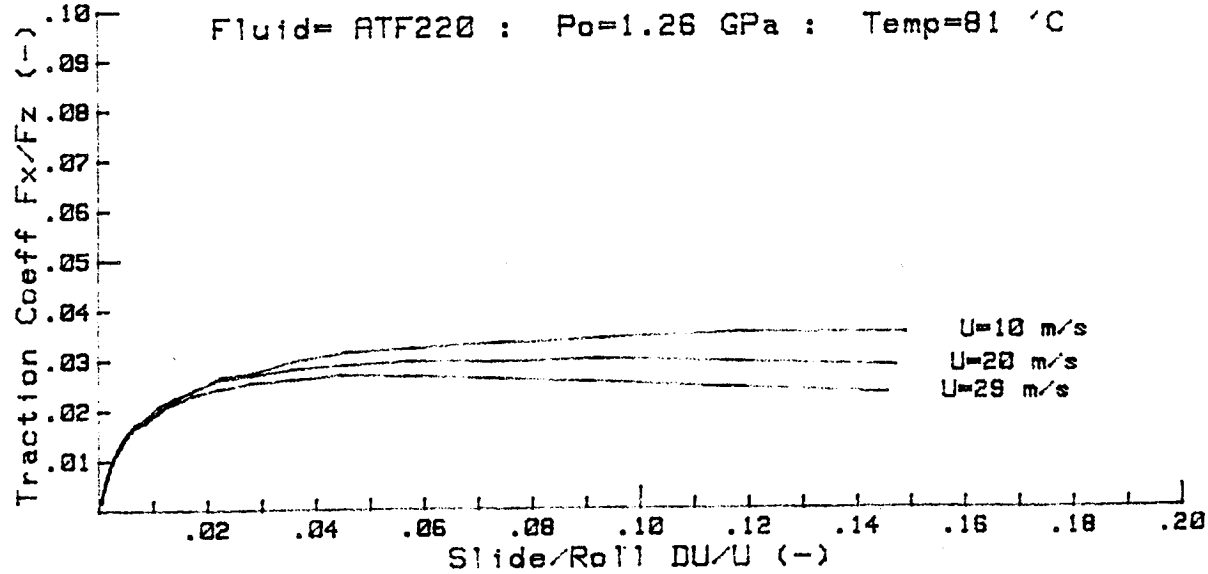
Fluid= ATF220 : Po=1.26 GPa : Temp=81 'C
Traction Coeff Fx/Fz (-)
.10
.09
.08
.07
.06
.05
.04
.03
.02
.01
U=10 m/s
U=20 m/s
U=29 m/s
.02 .04 .06 .08 .10 .12 .14 .16 .18 .20
Slide/Roll DU/U (-)

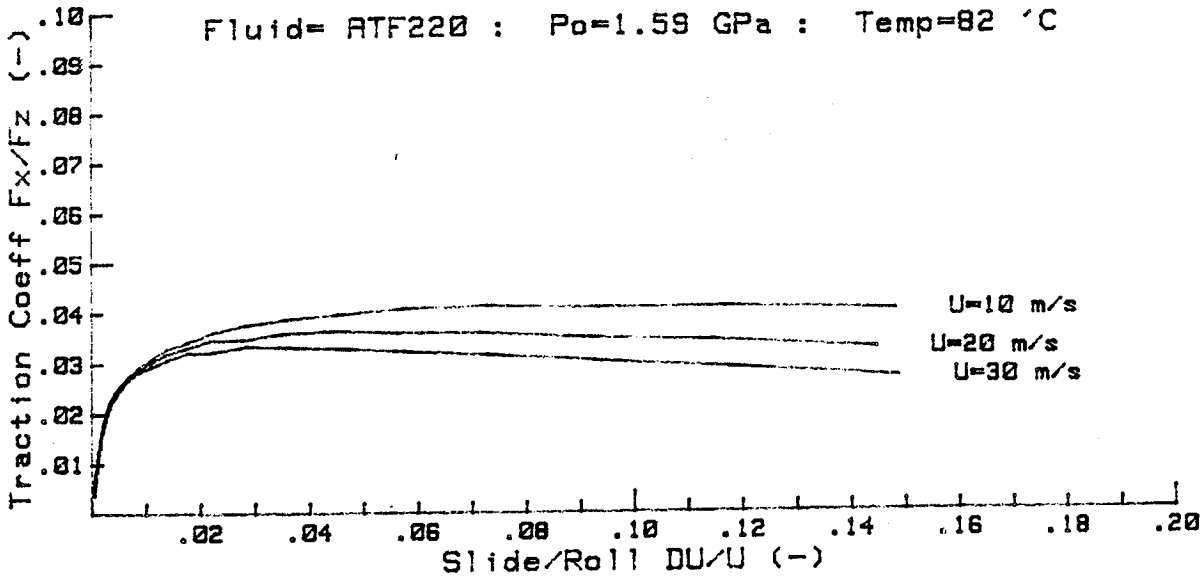

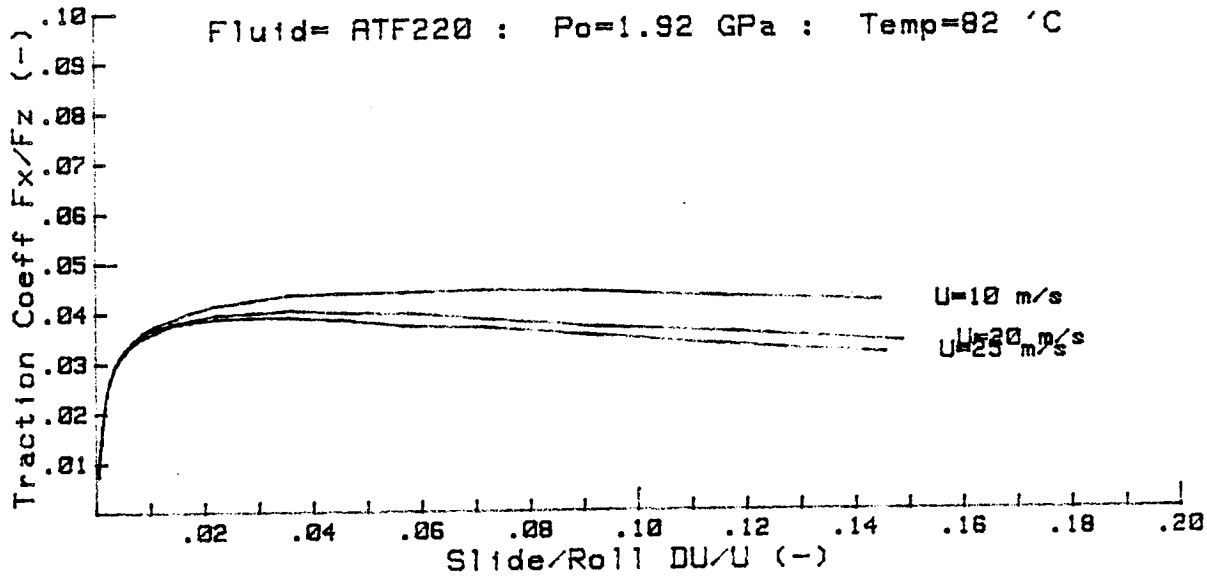

********** 2.08662912E+11

TRACTION CURVE DATA SUMMARY FOR ROYCO555 :Prog PLOTTER Rev# 1

**********00:32:58

Test # (----)	Po (GPa)	Uo (m/s)	To ('C)	Fz (N)	kk (-)	a (m)
ROYCO5141R	1.01	10.3	32	200	1.7	.00024
ROYCO5142R	1.01	20.3	34	200	1.7	.00024
ROYCO5143R	1.01	30.1	36	200	1.7	.00024
ROYCO5144R	1.27	10.3	35	400	1.7	.00030
ROYCO5145R	1.27	20.3	36	400	1.7	.00030
ROYCO5146R	1.27	30.6	39	400	1.7	.00030
ROYCO5147R	1.60	10.2	36	800	1.7	.00037
ROYCO5148R	1.60	20.1	38	800	1.7	.00037
ROYCO5149R	1.60	30.1	40	800	1.7	.00037
ROYCO514AR	1.93	10.5	37	1400	1.7	.00045
ROYCO514BR	1.93	20.4	40	1400	1.7	.00045
ROYCO514CR	1.93	30.2	43	1400	1.7	.00045
ROYCO514DR	1.01	10.7	78	200	1.7	.00024
ROYCO514ER	1.01	20.3	78	200	1.7	.00024
ROYCO514FR	1.01	29.9	79	200	1.7	.00024
ROYCO514GR	1.27	10.3	79	400	1.7	.00030
ROYCO514HR	1.27	20.3	79	400	1.7	.00030
ROYCO514IR	1.27	30.1	80	400	1.7	.00030
ROYCO514JR	1.60	10.4	79	800	1.7	.00037
ROYCO514KR	1.60	20.3	79	800	1.7	.00037
ROYCO514LR	1.60	30.1	79	800	1.7	.00037
ROYCO514MR	1.93	10.6	78	1400	1.7	.00045
ROYCO514NR	1.93	20.2	79	1400	1.7	.00045
ROYCO514OR	1.93	30.1	81	1400	1.7	.00045

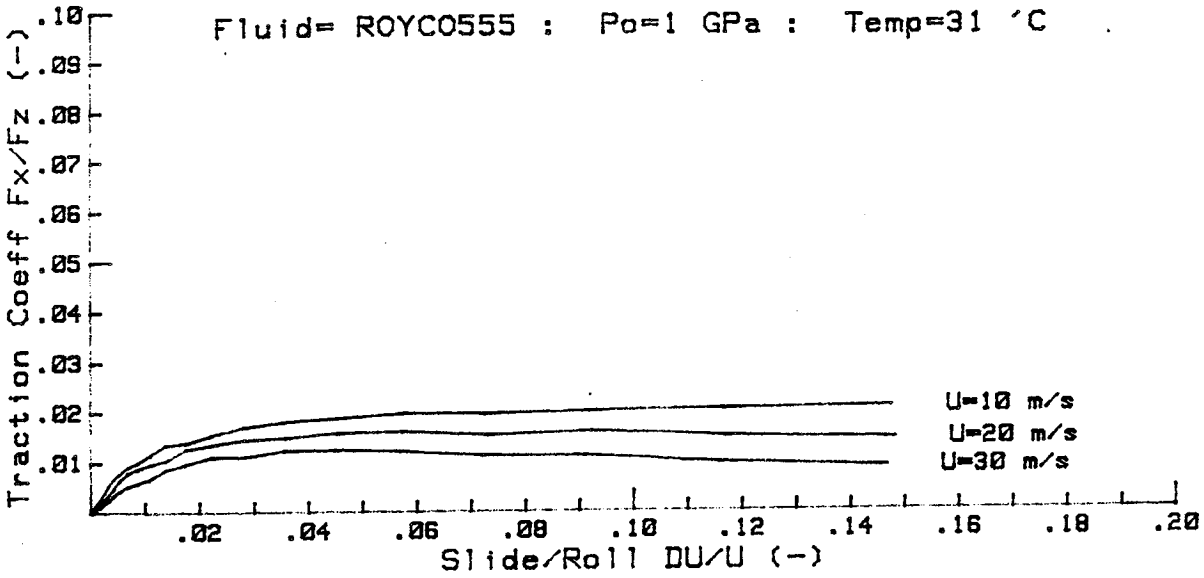
Fluid= ROYCO555 : Po=1 GPa : Temp=31 'C
Traction Coeff Fx/Fz (-)
.10
.09
.08
.07
.06
.05
.04
.03
.02
.01
U=10 m/s
U=20 m/s
U=30 m/s
.02 .04 .06 .08 .10 .12 .14 .16 .18 .20
Slide/Roll DU/U (-)

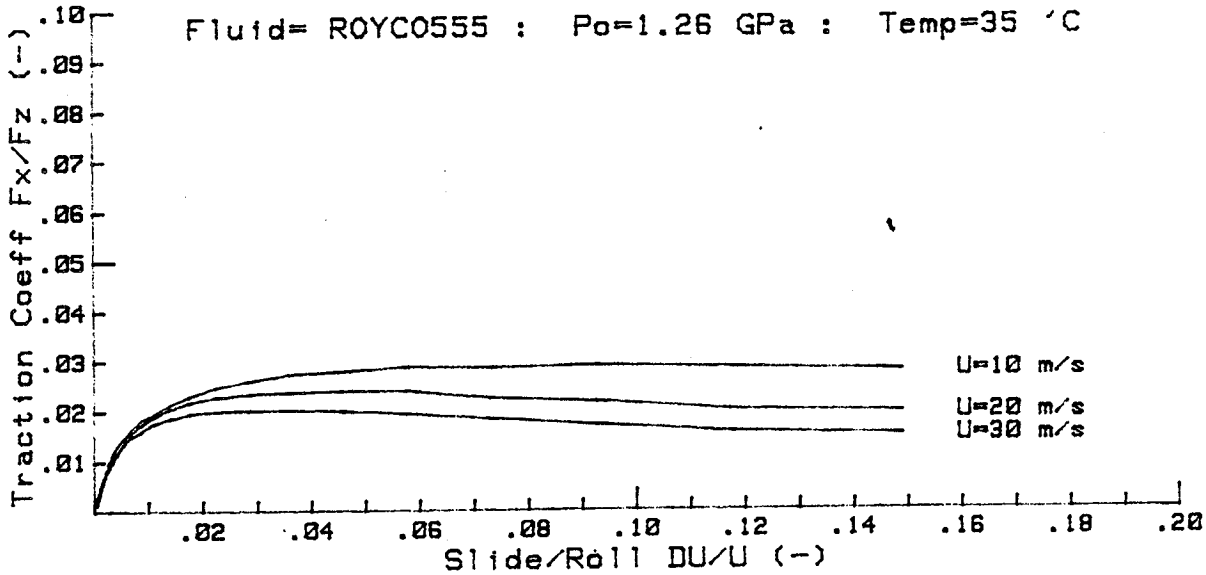
Fluid= ROYCO555 : Po=1.26 GPa : Temp=35 'C
Traction Coeff Fx/Fz (-)
.10
.09
.08
.07
.06
.05
.04
.03
.02
.01
U=10 m/s
U=20 m/s
U=30 m/s
.02 .04 .06 .08 .10 .12 .14 .16 .18 .20
Slide/Roll DU/U (-)

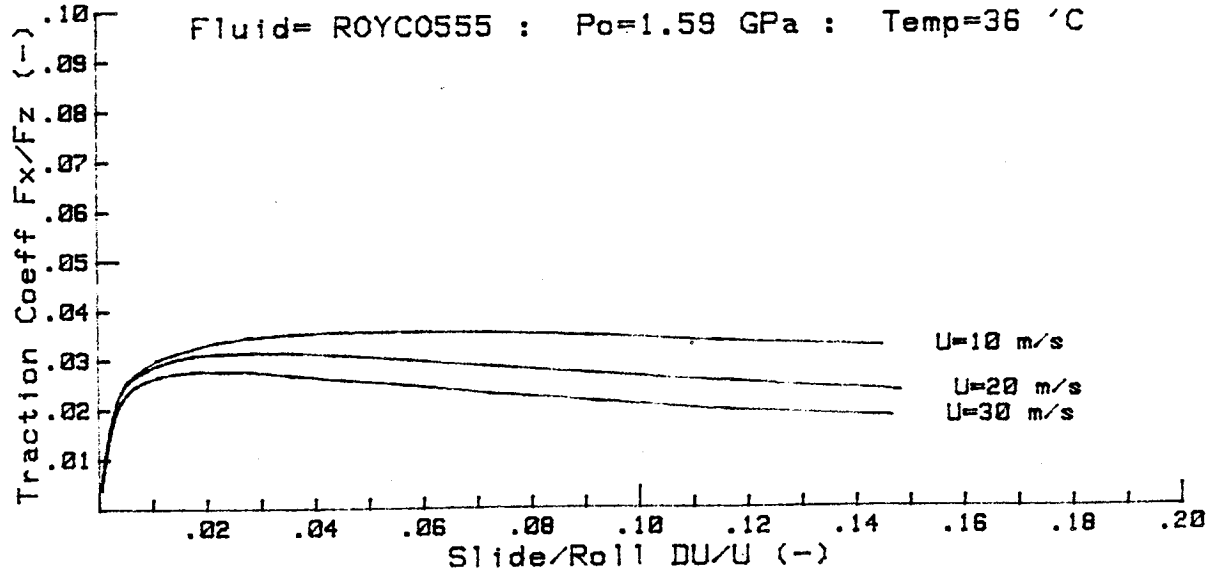
Fluid= ROYCO555 : Po=1.59 GPa : Temp=36 'C
Traction Coeff Fx/Fz (-)
.10
.09
.08
.07
.06
.05
.04
.03
.02
.01
U=10 m/s
U=20 m/s
U=30 m/s
.02 .04 .06 .08 .10 .12 .14 .16 .18 .20
Slide/Roll DU/U (-)

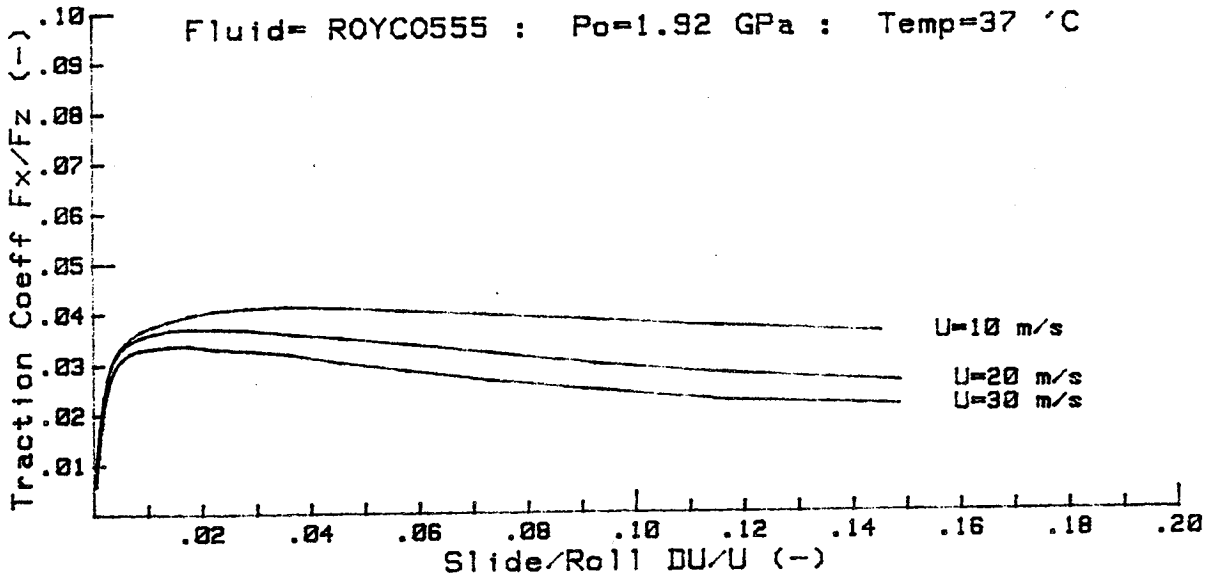
Fluid= ROYCO555 : Po=1.92 GPa : Temp=37 'C
Traction Coeff Fx/Fz (-)
.10
.09
.08
.07
.06
.05
.04
.03
.02
.01
U=10 m/s
U=20 m/s
U=30 m/s
.02
.04
.06
.08
.10
.12
.14
.16
.18
.20
Slide/Roll DU/U (-)

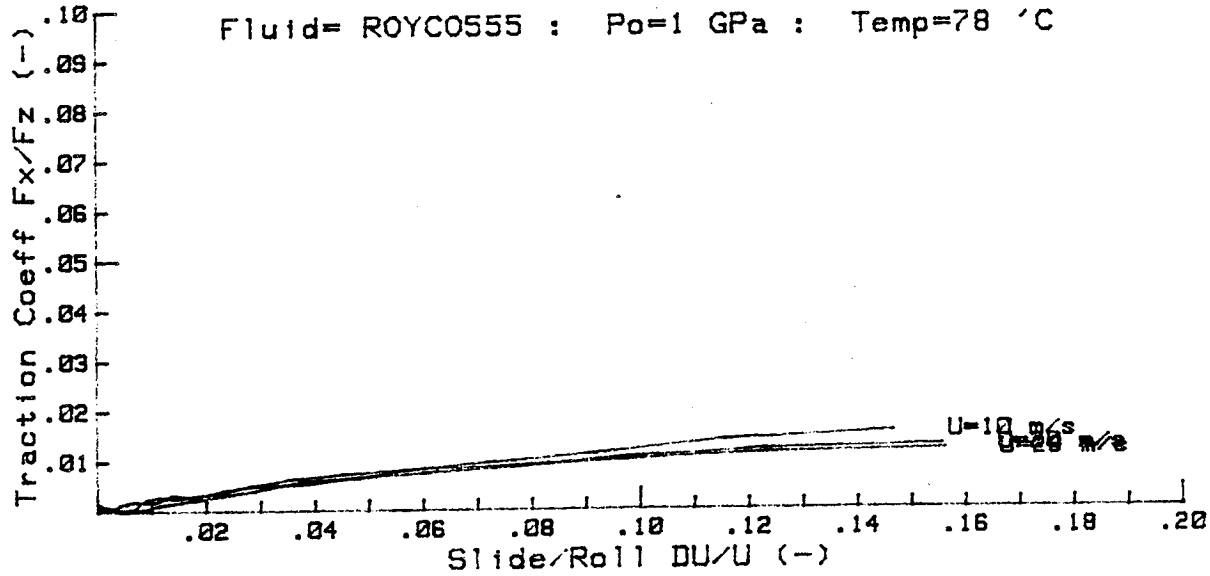
Fluid= ROYCO555 : Po=1 GPa : Temp=78 'C
Traction Coeff Fx/Fz (-)
.10
.09
.08
.07
.06
.05
.04
.03
.02
.01
U=10 m/s
U=20 m/s
.02
.04
.06
.08
.10
.12
.14
.16
.18
.20
Slide/Roll DU/U (-)

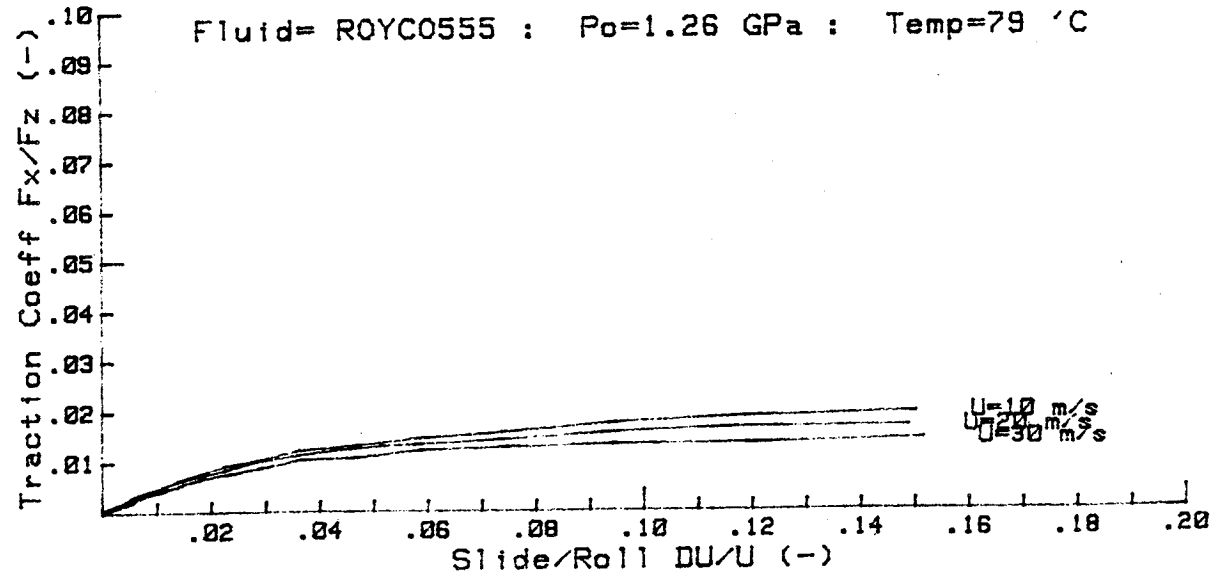
Fluid= ROYCO555 : Po=1.26 GPa : Temp=79 'C
Traction Coeff Fx/Fz (-)
.10
.09
.08
.07
.06
.05
.04
.03
.02
.01
U=10 m/s
U=20 m/s
U=30 m/s
.02
.04
.06
.08
.10
.12
.14
.16
.18
.20
Slide/Roll DU/U (-)

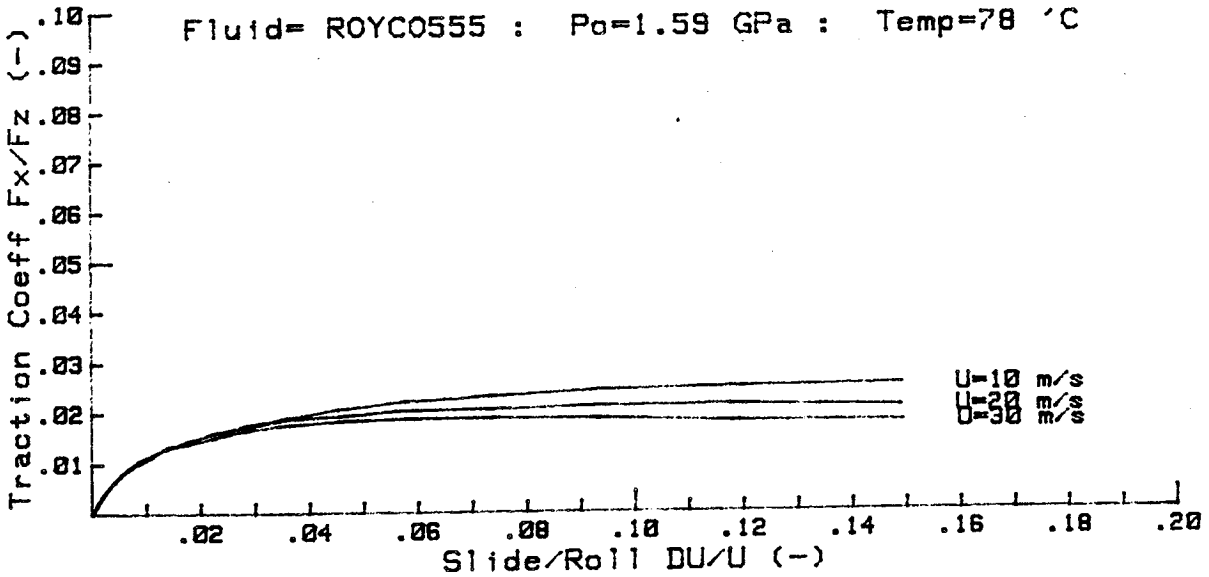
Fluid= ROYCO555 : Po=1.59 GPa : Temp=78 'C
Traction Coeff Fx/Fz (-)
.10
.09
.08
.07
.06
.05
.04
.03
.02
.01
U=10 m/s
U=20 m/s
U=30 m/s
.02
.04
.06
.08
.10
.12
.14
.16
.18
.20
Slide/Roll DU/U (-)

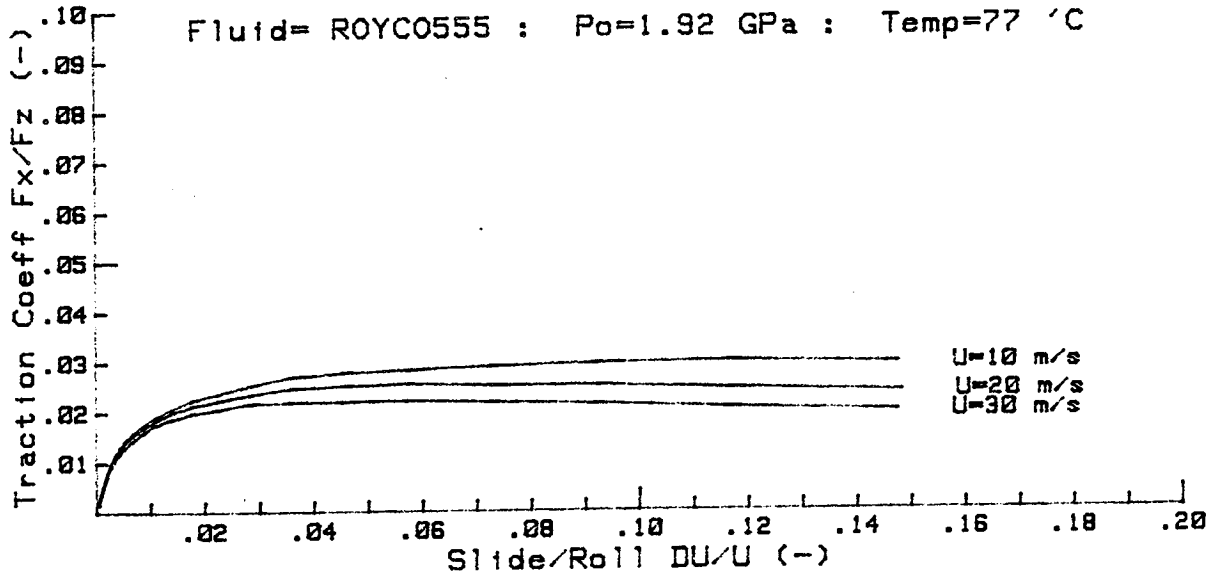
Fluid= ROYCO555 : Po=1.92 GPa : Temp=77 'C
Traction Coeff Fx/Fz (-)
.10
.09
.08
.07
.06
.05
.04
.03
.02
.01
U=10 m/s
U=20 m/s
U=30 m/s
.02
.04
.06
.08
.10
.12
.14
.16
.18
.20
Slide/Roll DU/U (-)

********** 2.08662912E+11

TRACTION CURVE DATA SUMMARY FOR TDF88 :Prog PLOTTER Rev# 1

**********01:06:25

Test # (----)	Po (GPa)	Uo (m/s)	To ('C)	Fz (N)	kk (-)	a (m)
TDF882BJBR	1.68	21.3	57	400	.9	.00036
TDF882BJCR	1.68	30.0	58	400	.9	.00036
TDF882BJDR	1.68	40.5	60	400	.9	.00036
TDF882BJ6R	2.11	22.0	69	800	.9	.00046
TDF882BJ7R	2.11	30.0	67	800	.9	.00046
TDF882BJ8R	2.11	40.5	69	800	.9	.00046
TDF882BJ1R	2.55	21.8	67	1400	.9	.00055
TDF882BJ2R	2.55	30.4	76	1400	.9	.00055
TDF882BJ3R	2.55	40.5	84	1400	.9	.00055
TDF882BJGR	1.68	21.3	79	400	.9	.00036
TDF882BJHR	1.68	30.3	82	400	.9	.00036
TDF882BJIR	1.68	40.5	85	400	.9	.00036
TDF882BJLR	2.11	23.4	100	800	.9	.00046
TDF882BJMR	2.11	31.3	97	800	.9	.00046
TDF882BJNR	2.11	40.5	98	800	.9	.00046
TDF882BJQR	2.55	22.8	106	1400	.9	.00055
TDF882BJRR	2.55	29.7	107	1400	.9	.00055
TDF882BJSR	2.55	40.5	112	1400	.9	.00055

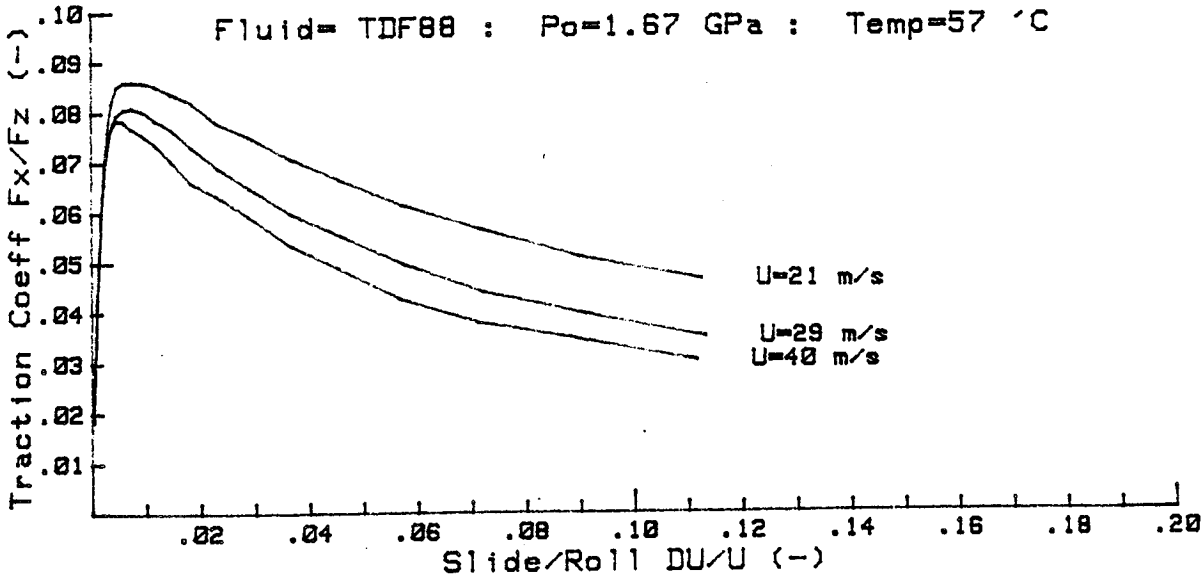
Fluid= TDF88 : Po=1.67 GPa : Temp=57 'C
Traction Coeff Fx/Fz (-)
.10
.09
.08
.07
.06
.05
.04
.03
.02
.01
U=21 m/s
U=29 m/s
U=40 m/s
.02 .04 .06 .08 .10 .12 .14 .16 .18 .20
Slide/Roll DU/U (-)

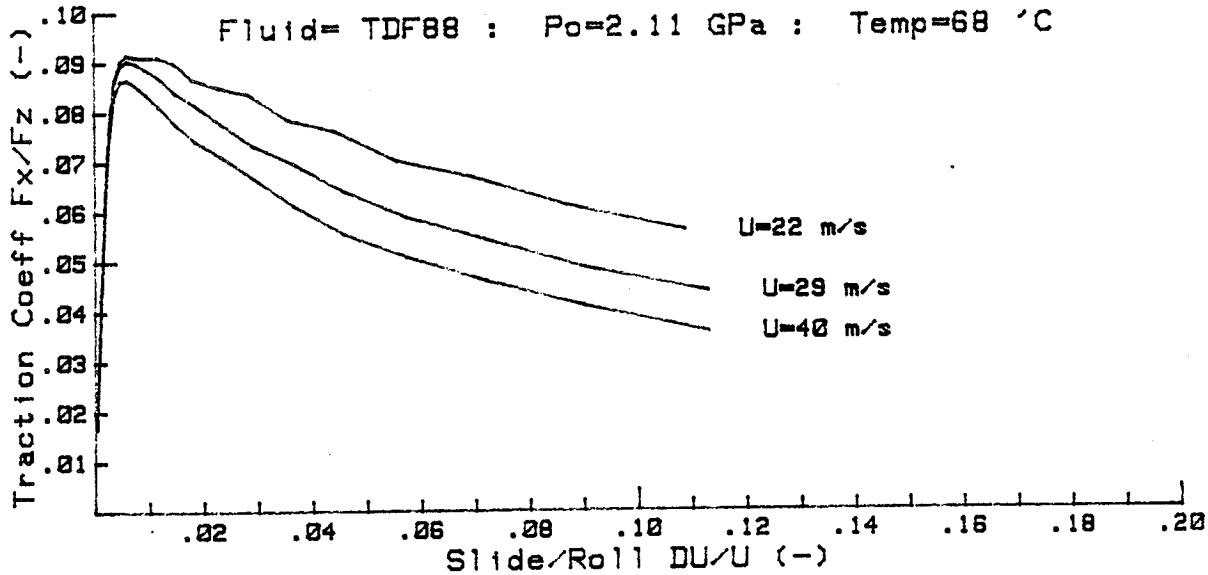
Fluid= TDF88 : Po=2.11 GPa : Temp=68 'C
Traction Coeff Fx/Fz (-)
.10
.09
.08
.07
.06
.05
.04
.03
.02
.01
U=22 m/s
U=29 m/s
U=40 m/s
.02 .04 .06 .08 .10 .12 .14 .16 .18 .20
Slide/Roll DU/U (-)

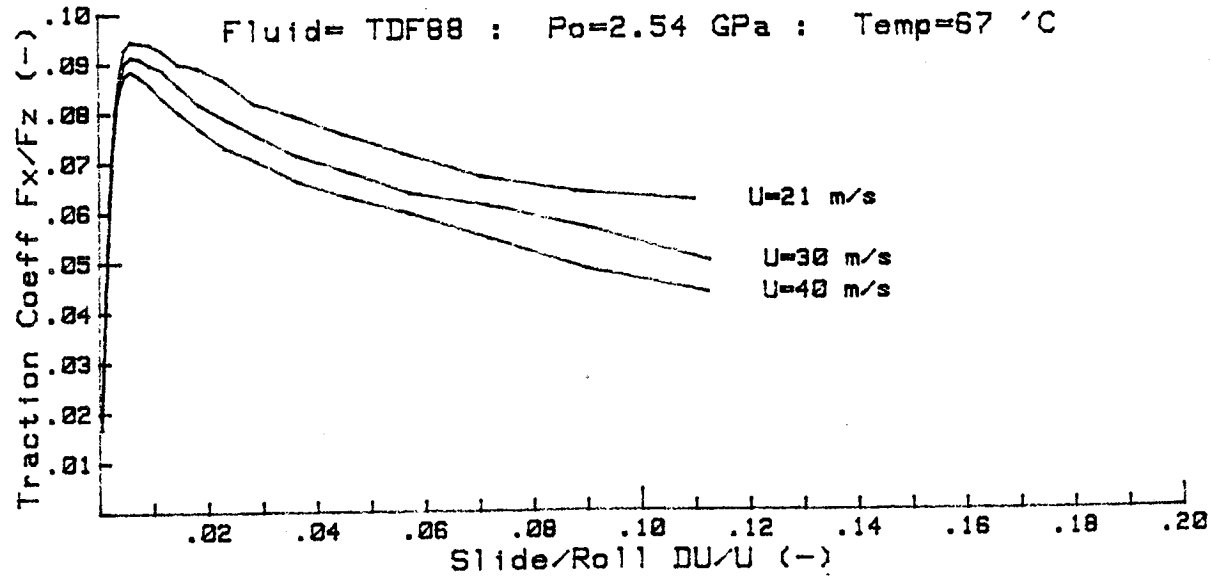
Fluid= TDF88 : Po=2.54 GPa : Temp=67 'C
Traction Coeff Fx/Fz (-)
.10
.09
.08
.07
.06
.05
.04
.03
.02
.01
U=21 m/s
U=30 m/s
U=40 m/s
.02 .04 .06 .08 .10 .12 .14 .16 .18 .20
Slide/Roll DU/U (-)

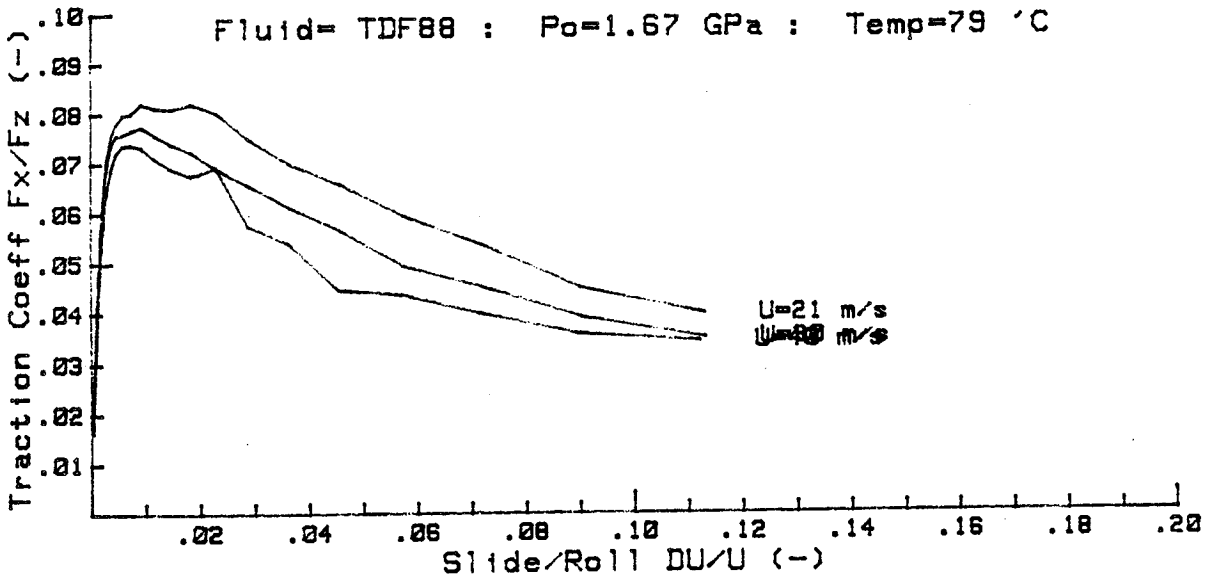
Fluid= TDF88 : Po=1.67 GPa : Temp=79 'C
Traction Coeff Fx/Fz (-)
.10
.09
.08
.07
.06
.05
.04
.03
.02
.01
U=21 m/s
.02 .04 .06 .08 .10 .12 .14 .16 .18 .20
Slide/Roll DU/U (-)

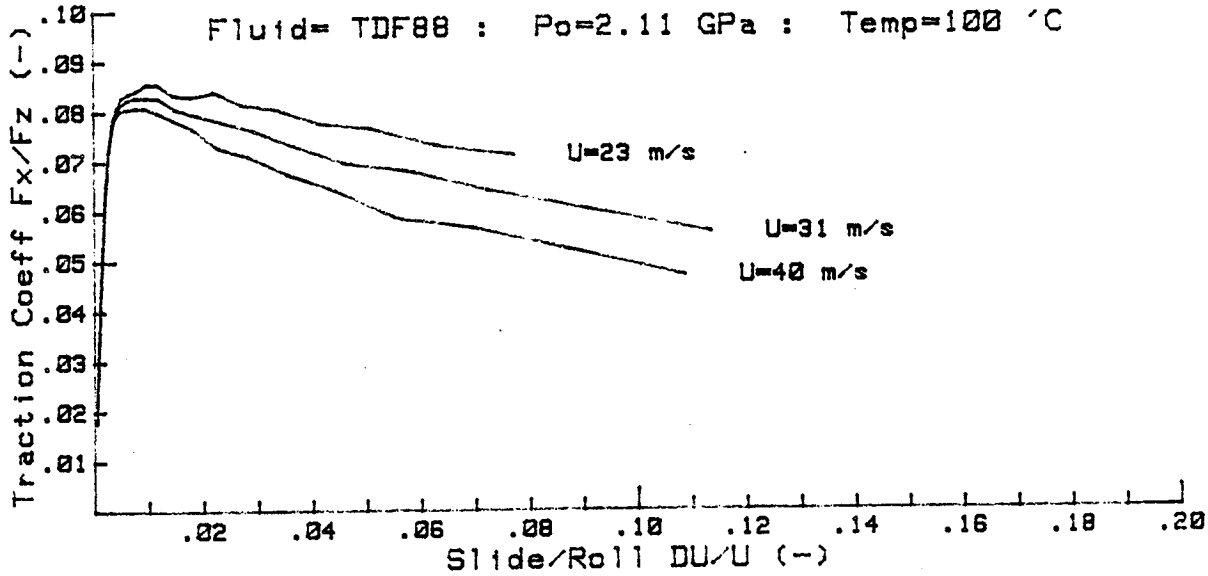
Fluid= TDF88 : Po=2.11 GPa : Temp=100 'C
Traction Coeff Fx/Fz (-)
.10
.09
.08
.07
.06
.05
.04
.03
.02
.01
U=23 m/s
U=31 m/s
U=40 m/s
.02 .04 .06 .08 .10 .12 .14 .16 .18 .20
Slide/Roll DU/U (-)

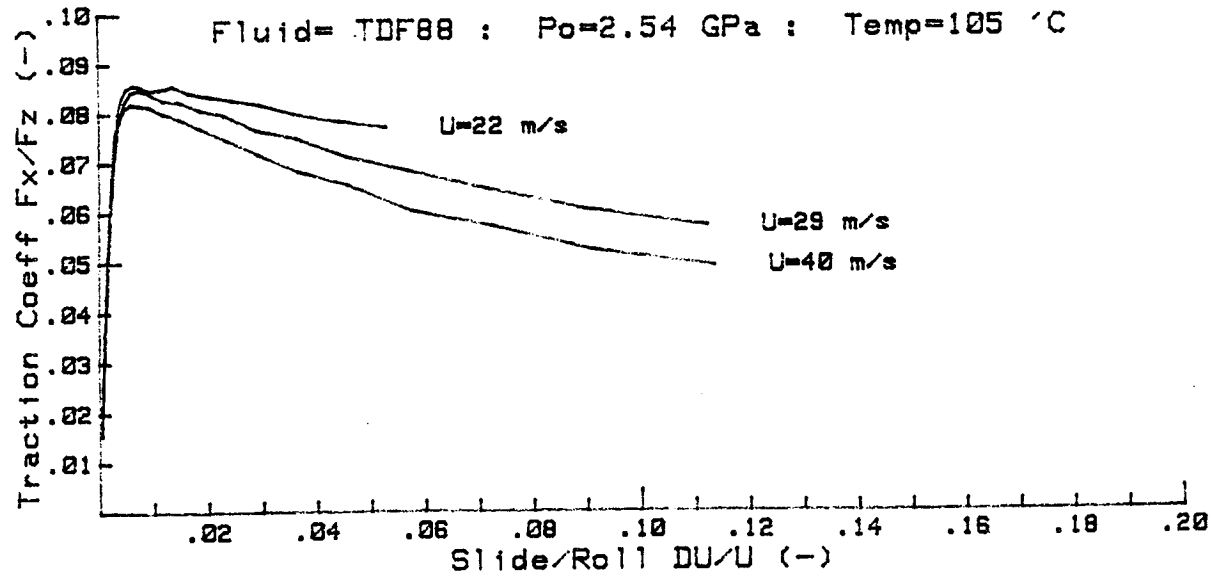
Fluid= TDF88 : Po=2.54 GPa : Temp=105 'C
Traction Coeff Fx/Fz (-)
.10
.09
.08
.07
.06
.05
.04
.03
.02
.01
U=22 m/s
U=29 m/s
U=40 m/s
.02 .04 .06 .08 .10 .12 .14 .16 .18 .20
Slide/Roll DU/U (-)

********** 2.113580736E+11

TRACTION CURVE DATA SUMMARY FOR SAN50 :Prog PLOTTER Rev# 1

**********20:50:27

Test # (----)	Po (GPa)	Uo (m/s)	To ('C)	Fz (N)	kk (-)	a (m)
SAN5044K1R	2.55	11.9	37	1400	.9	.00055
SAN5044K2R	2.55	22.9	50	1400	.9	.00055
SAN5044K3R	2.55	33.3	57	1400	.9	.00055
SAN5044K4R	2.11	11.8	38	800	.9	.00046
SAN5044K5R	2.11	23.4	40	800	.9	.00046
SAN5044K6R	2.11	32.5	44	800	.9	.00046
SAN5044K7R	1.68	32.7	41	400	.9	.00036
SAN5044K8R	1.68	21.4	37	400	.9	.00036
SAN5044K9R	1.68	11.4	34	400	.9	.00036
SAN5044JDR	1.68	11.8	69	400	.9	.00036
SAN5044JER	1.68	21.3	67	400	.9	.00036
SAN5044JFR	1.68	31.1	69	400	.9	.00036
SAN5044JGR	2.11	12.2	72	800	.9	.00046
SAN5044JHR	2.11	22.8	74	800	.9	.00046
SAN5044JIR	2.11	34.0	78	800	.9	.00046
SAN5044JJR	2.55	32.7	87	1400	.9	.00055
SAN5044JKR	2.55	22.9	90	1400	.9	.00055
SAN5044JLR	2.55	11.4	91	1400	.9	.00055

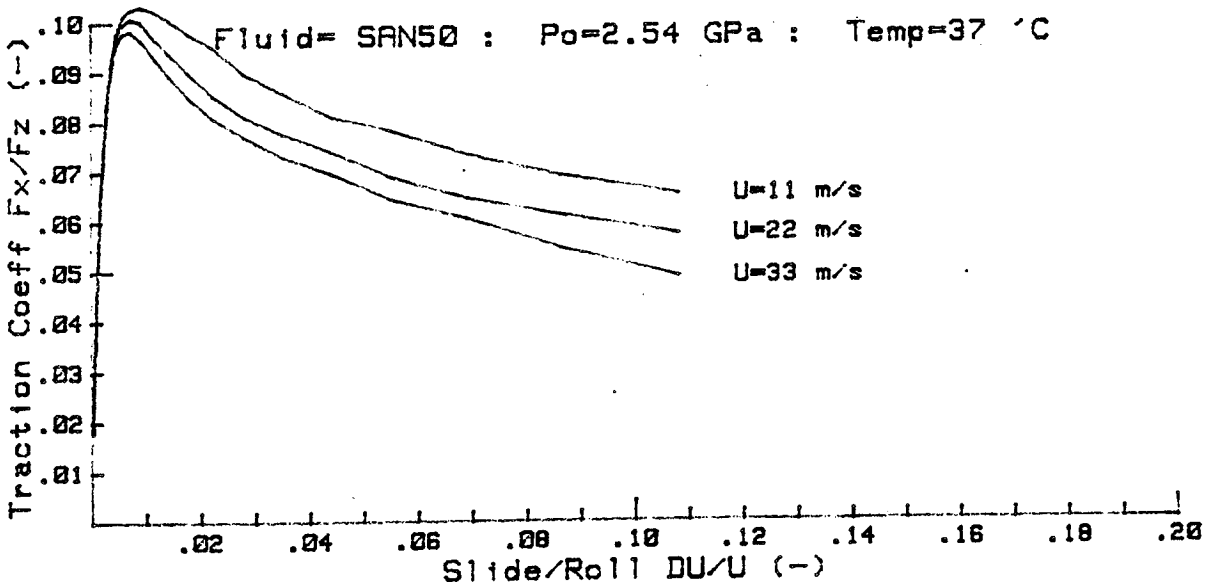
Fluid= SAN50 : Po=2.54 GPa : Temp=37 'C
U=11 m/s
U=22 m/s
U=33 m/s
Traction Coeff Fx/Fz (-)
.10
.09
.08
.07
.06
.05
.04
.03
.02
.01
.02 .04 .06 .08 .10 .12 .14 .16 .18 .20
Slide/Roll DU/U (-)

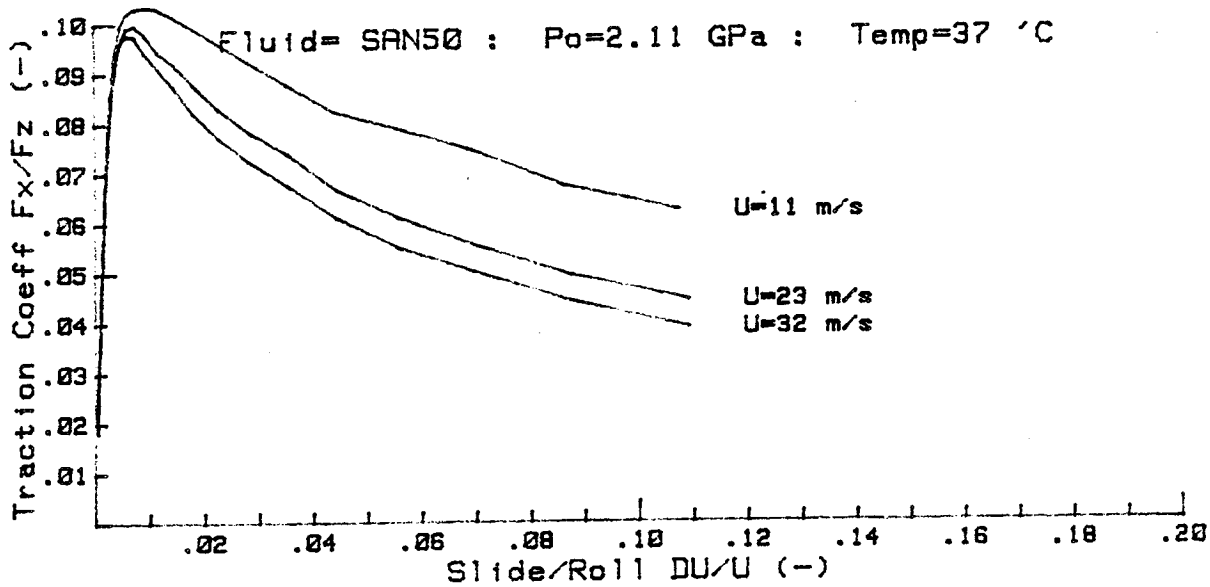
Fluid= SAN50 : Po=2.11 GPa : Temp=37 'C
U=11 m/s
U=23 m/s
U=32 m/s
Traction Coeff Fx/Fz (-)
.10
.09
.08
.07
.06
.05
.04
.03
.02
.01
.02 .04 .06 .08 .10 .12 .14 .16 .18 .20
Slide/Roll DU/U (-)

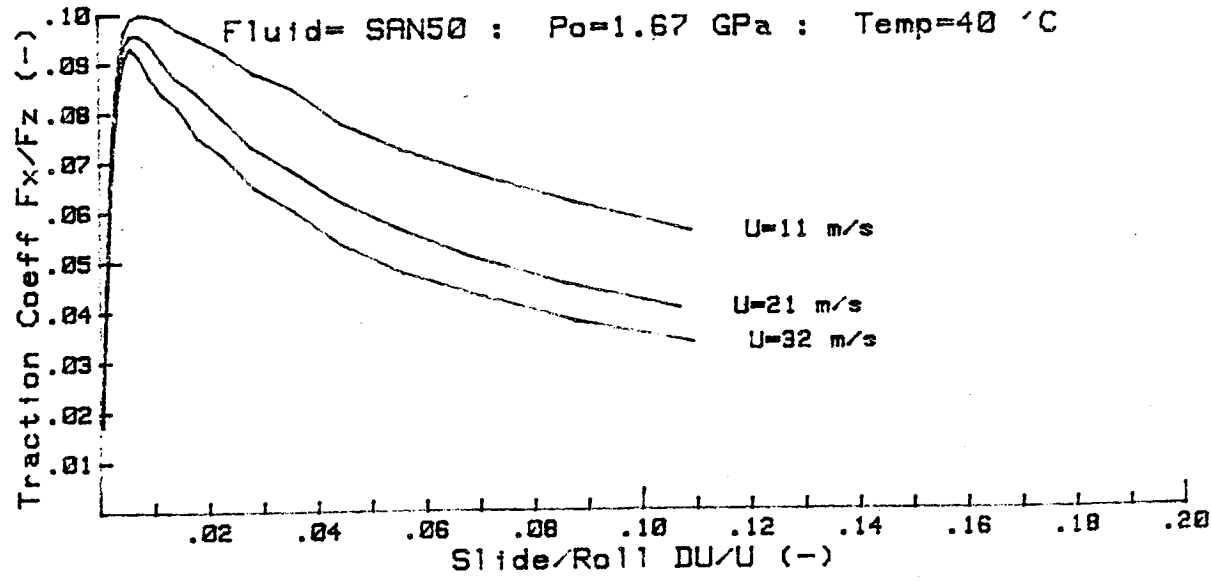
Fluid= SAN50 : Po=1.67 GPa : Temp=40 'C
U=11 m/s
U=21 m/s
U=32 m/s
Traction Coeff Fx/Fz (-)
.10
.09
.08
.07
.06
.05
.04
.03
.02
.01
.02 .04 .06 .08 .10 .12 .14 .16 .18 .20
Slide/Roll DU/U (-)

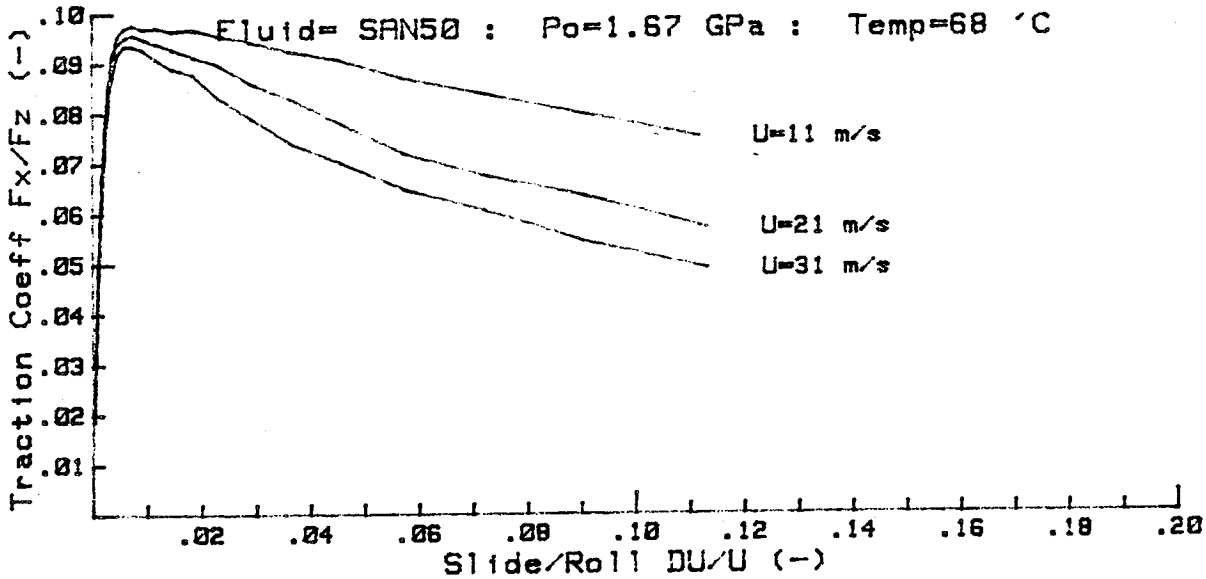
Fluid= SAN50 : Po=1.67 GPa : Temp=68 'C
U=11 m/s
U=21 m/s
U=31 m/s
Traction Coeff Fx/Fz (-)
.10
.09
.08
.07
.06
.05
.04
.03
.02
.01
.02 .04 .06 .08 .10 .12 .14 .16 .18 .20
Slide/Roll DU/U (-)

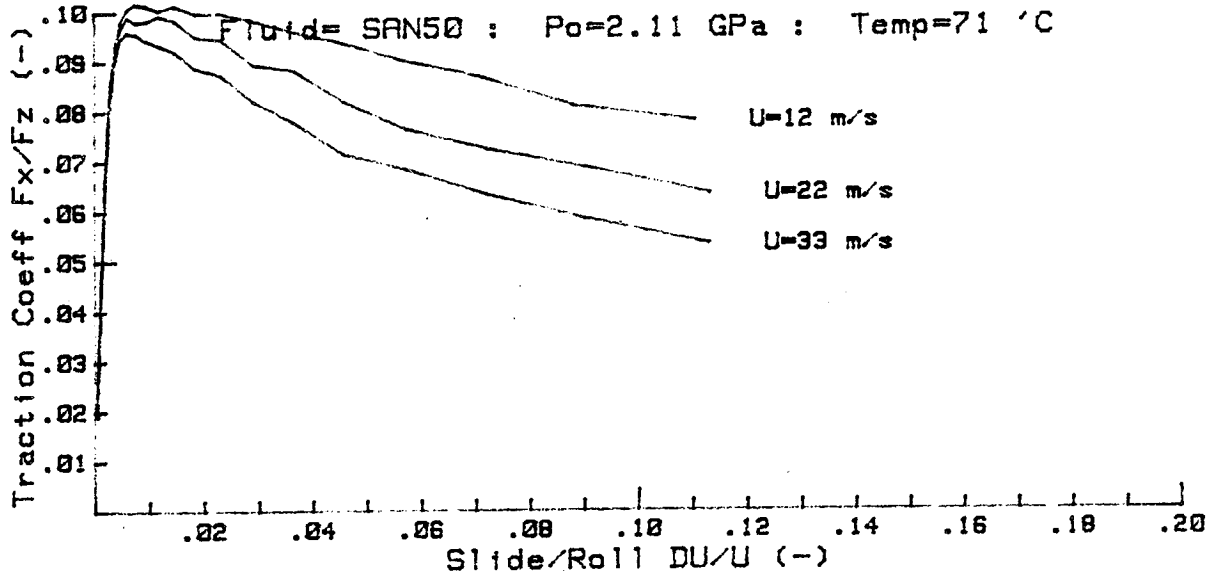
Fluid= SAN50 : Po=2.11 GPa : Temp=71 'C
U=12 m/s
U=22 m/s
U=33 m/s
Traction Coeff Fx/Fz (-)
.10
.09
.08
.07
.06
.05
.04
.03
.02
.01
.02 .04 .06 .08 .10 .12 .14 .16 .18 .20
Slide/Roll DU/U (-)

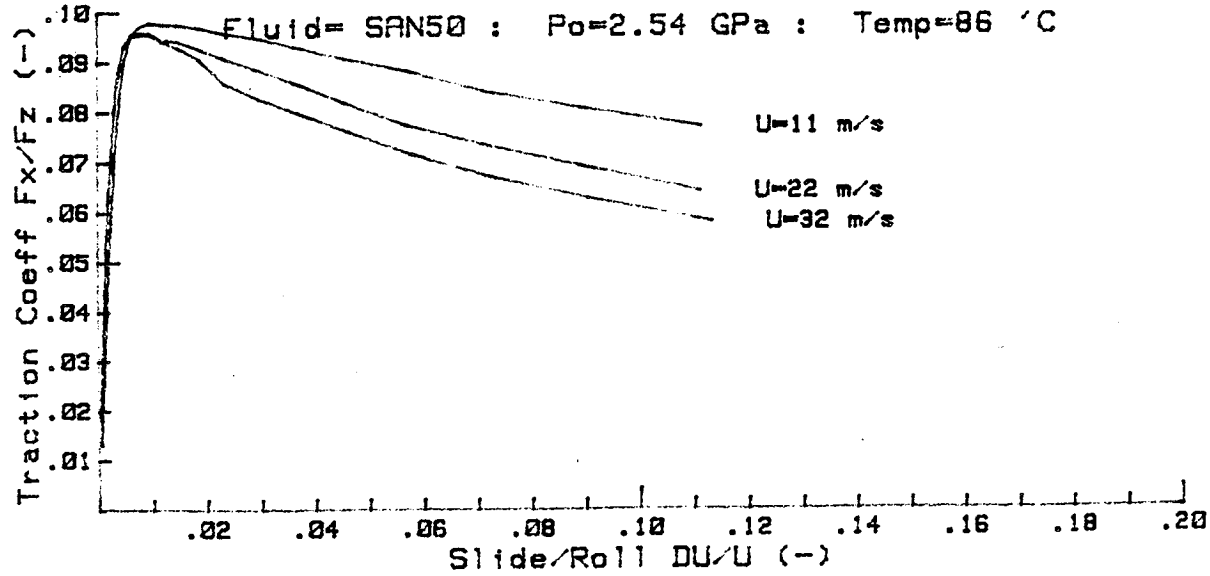
Fluid= SAN50 : Po=2.54 GPa : Temp=86 'C
U=11 m/s
U=22 m/s
U=32 m/s
Traction Coeff Fx/Fz (-)
.10
.09
.08
.07
.06
.05
.04
.03
.02
.01
.02 .04 .06 .08 .10 .12 .14 .16 .18 .20
Slide/Roll DU/U (-)

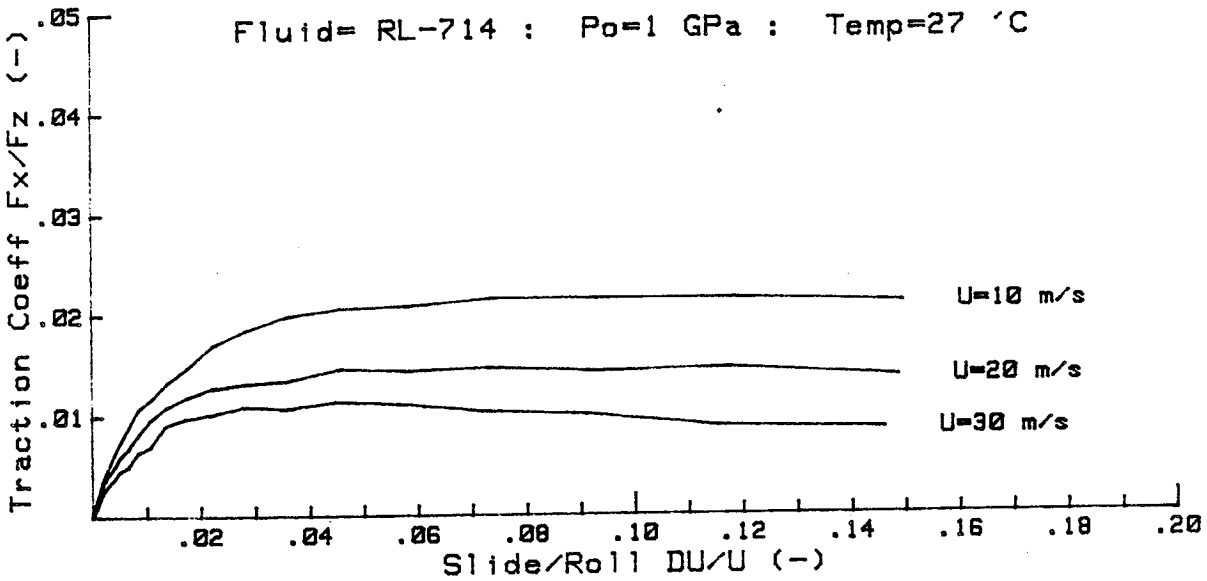
Fluid= RL-714 : Po=1 GPa : Temp=27 'C
Traction Coeff Fx/Fz (-)
.05
.04
.03
.02
.01
U=10 m/s
U=20 m/s
U=30 m/s
.02 .04 .06 .08 .10 .12 .14 .16 .18 .20
Slide/Roll DU/U (-)

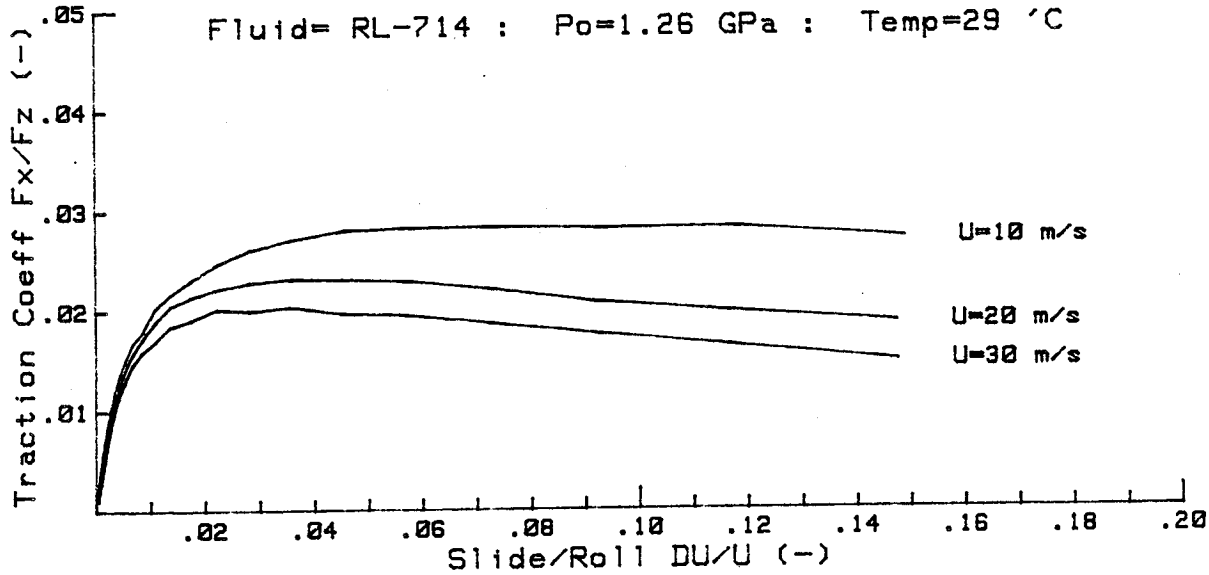
Fluid= RL-714 : Po=1.26 GPa : Temp=29 'C
Traction Coeff Fx/Fz (-)
.05
.04
.03
.02
.01
U=10 m/s
U=20 m/s
U=30 m/s
.02 .04 .06 .08 .10 .12 .14 .16 .18 .20
Slide/Roll DU/U (-)

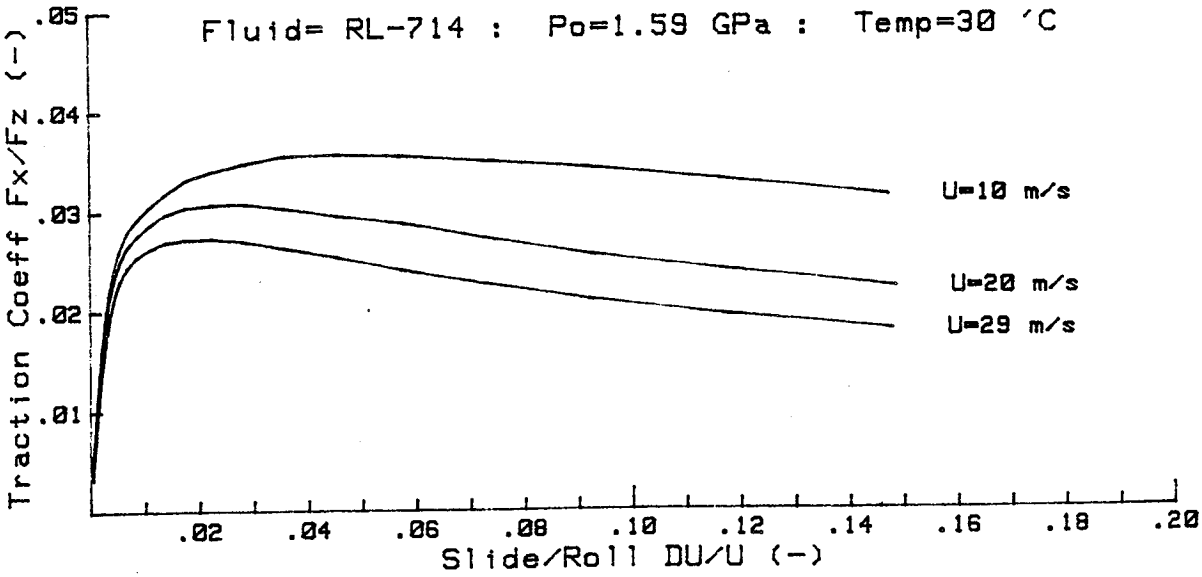
Fluid= RL-714 : Po=1.59 GPa : Temp=30 'C
Traction Coeff Fx/Fz (-)
.05
.04
.03
.02
.01
U=10 m/s
U=20 m/s
U=29 m/s
.02 .04 .06 .08 .10 .12 .14 .16 .18 .20
Slide/Roll DU/U (-)

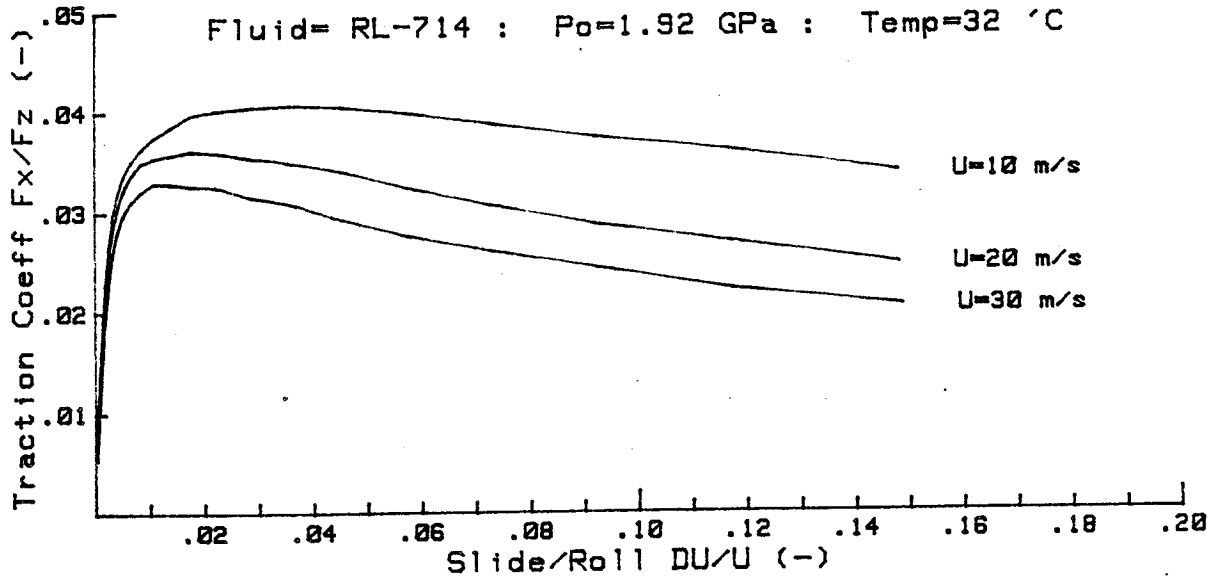
Fluid= RL-714 : Po=1.92 GPa : Temp=32 'C
Traction Coeff Fx/Fz (-)
.05
.04
.03
.02
.01
U=10 m/s
U=20 m/s
U=30 m/s
.02 .04 .06 .08 .10 .12 .14 .16 .18 .20
Slide/Roll DU/U (-)

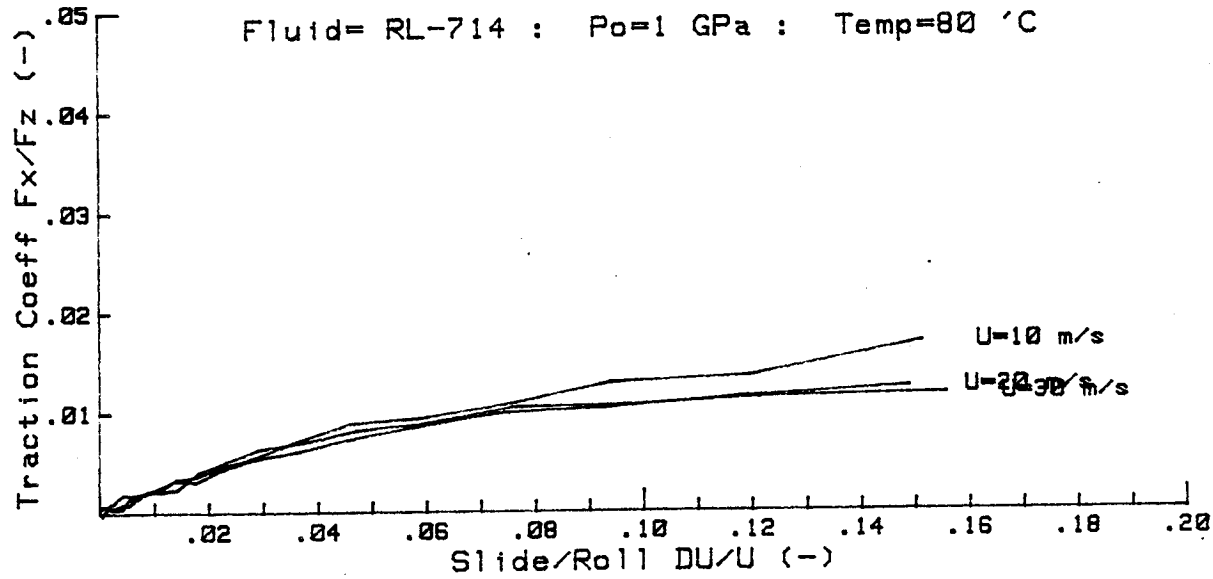
Fluid= RL-714 : Po=1 GPa : Temp=80 'C
Traction Coeff Fx/Fz (-)
.05
.04
.03
.02
.01
U=10 m/s
U=20 m/s
U=30 m/s
.02 .04 .06 .08 .10 .12 .14 .16 .18 .20
Slide/Roll DU/U (-)

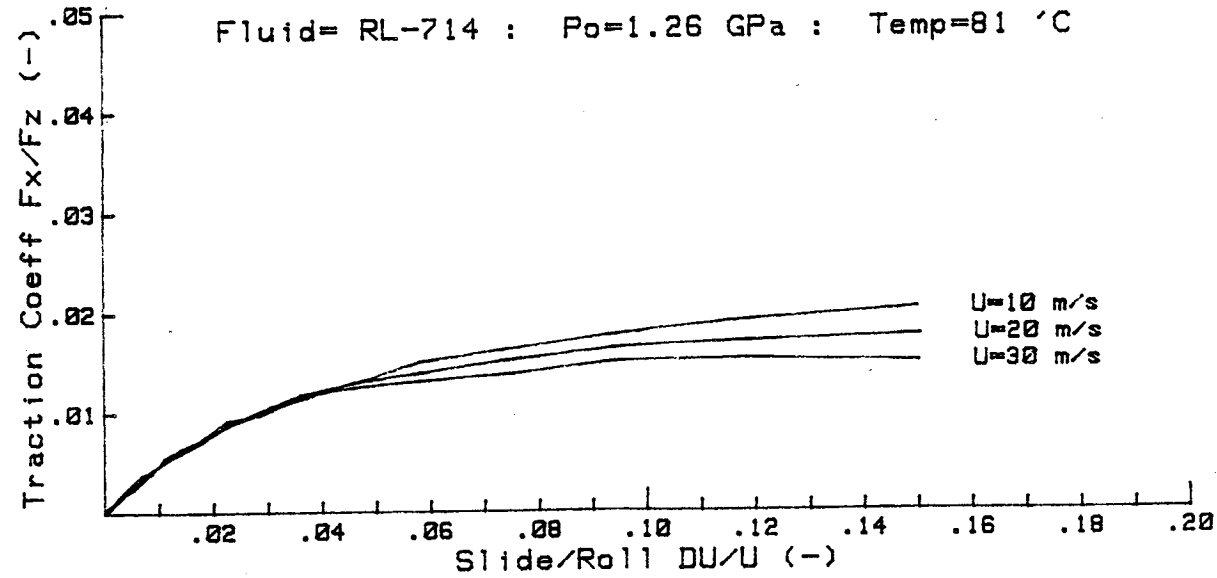
Fluid= RL-714 : Po=1.26 GPa : Temp=81 'C
Traction Coeff Fx/Fz (-)
.05
.04
.03
.02
.01
U=10 m/s
U=20 m/s
U=30 m/s
.02 .04 .06 .08 .10 .12 .14 .16 .18 .20
Slide/Roll DU/U (-)

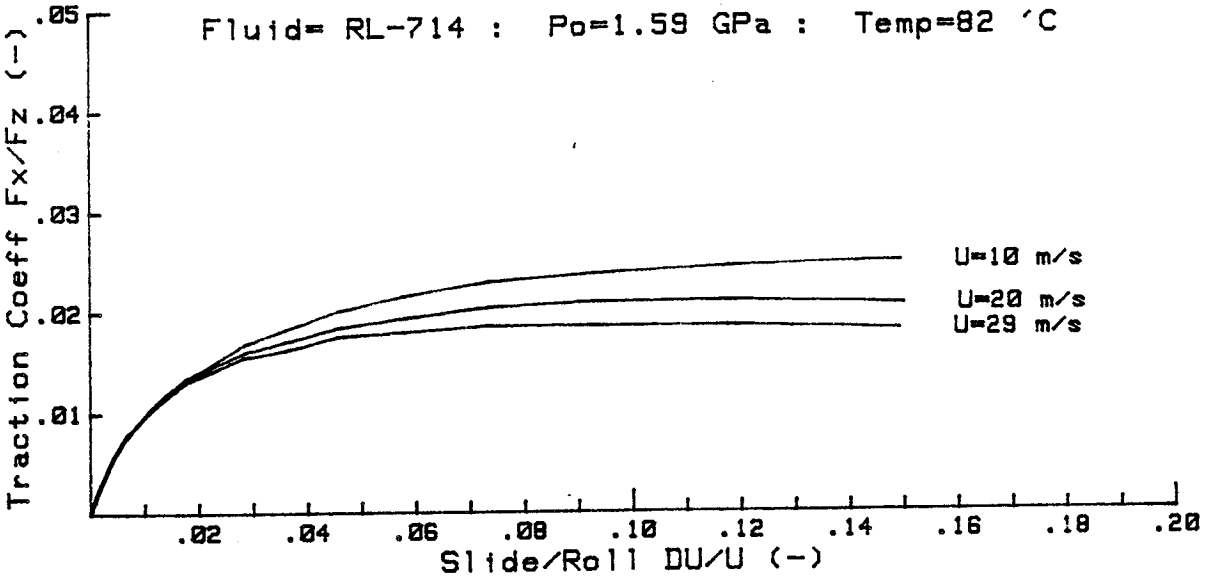
Fluid= RL-714 : Po=1.59 GPa : Temp=82 'C
Traction Coeff Fx/Fz (-)
.05
.04
.03
.02
.01
U=10 m/s
U=20 m/s
U=29 m/s
.02
.04
.06
.08
.10
.12
.14
.16
.18
.20
Slide/Roll DU/U (-)

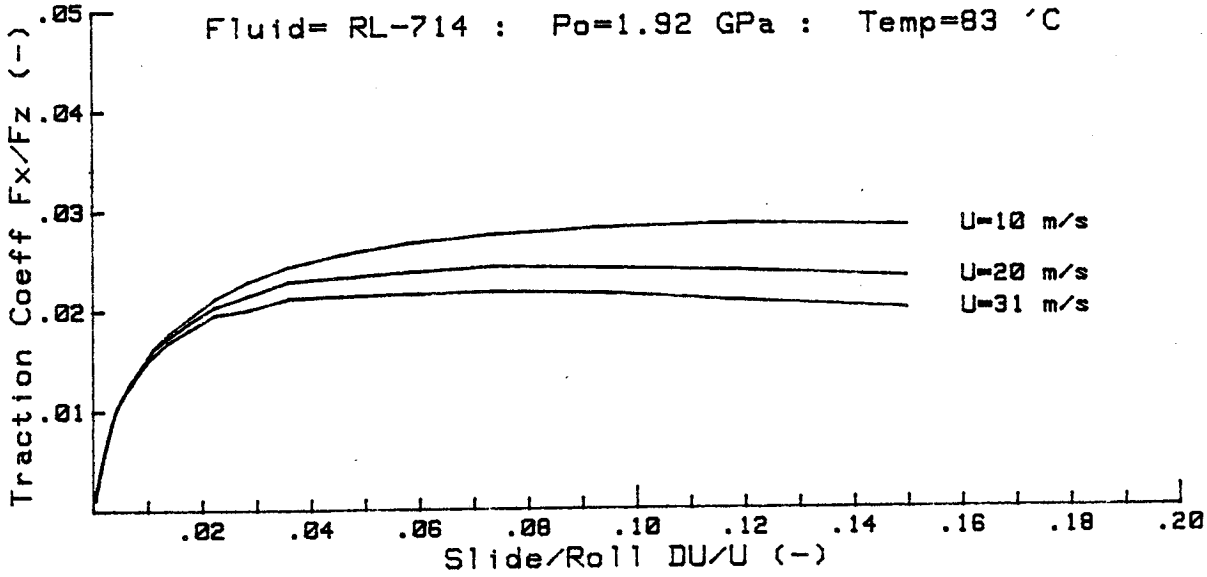
Fluid= RL-714 : Po=1.92 GPa : Temp=83 'C
Traction Coeff Fx/Fz (-)
.05
.04
.03
.02
.01
U=10 m/s
U=20 m/s
U=31 m/s
.02
.04
.06
.08
.10
.12
.14
.16
.18
.20
Slide/Roll DU/U (-)

********** 2.113580736E+11
MULTIPLE TRACTION CURVE DATA ANALYSIS FOR MOBIL2 :Prog HYPER Rev# 7.4

Data corrections:
Long. slip YES: Reduced press. YES: Inlet heating YES: Therm. Cond.YES

The following oil properties were used in the analysis:
Viscosity temperature: Av= 878.0 'C Dv=120.0 'C V0= .0000853 Pas
Viscosity Pressure : B=2448.0 'C/GPa Dp=174.0 'C
Thermal Conductivity : K'=1851.0 W/m'C K''=272.0 'C
Eyring Temperatures : Dp 174.0 'C Ds =120.0 'C
**********18:27:13

TEST INCLUDED IN THE MULTIPLE TRACTION DATA ANALYSIS

Test #	Po	Uo	To	Fz	kk	a	Pes
(----)	(GPa)	(m/s)	('C)	(N)	(-)	(m)	(-)
MOBIL5132R	1.01	19.9	33	200	1.7	.00024	5.31E+02
MOBIL5133R	1.01	30.2	35	200	1.7	.00024	8.84E+02
MOBIL5134R	1.27	10.2	34	400	1.7	.00030	1.17E+02
MOBIL5135R	1.27	20.3	35	400	1.7	.00030	3.73E+02
MOBIL5136R	1.27	30.2	37	400	1.7	.00030	6.23E+02
MOBIL5137R	1.60	10.3	35	800	1.7	.00037	7.87E+01
MOBIL5138R	1.60	20.2	36	800	1.7	.00037	2.59E+02
MOBIL5139R	1.60	29.1	38	800	1.7	.00037	4.05E+02
MOBIL513AR	1.93	10.9	37	1400	1.7	.00045	6.06E+01
MOBIL513BR	1.93	20.6	38	1400	1.7	.00045	1.88E+02
MOBIL513CR	1.93	27.8	41	1400	1.7	.00045	2.68E+02
MOBIL5149R	1.60	30.1	83	800	1.7	.00037	1.31E+02
MOBIL5148R	1.93	20.2	84	1400	1.7	.00045	4.48E+01

TYPE OF FIT IS 4

BEST FIT CONSTANTS ARE:
E0= 2.3448E-06 E1= 1.9894E-05 E2= 3.5903E-01 E3= 0.0000E+00

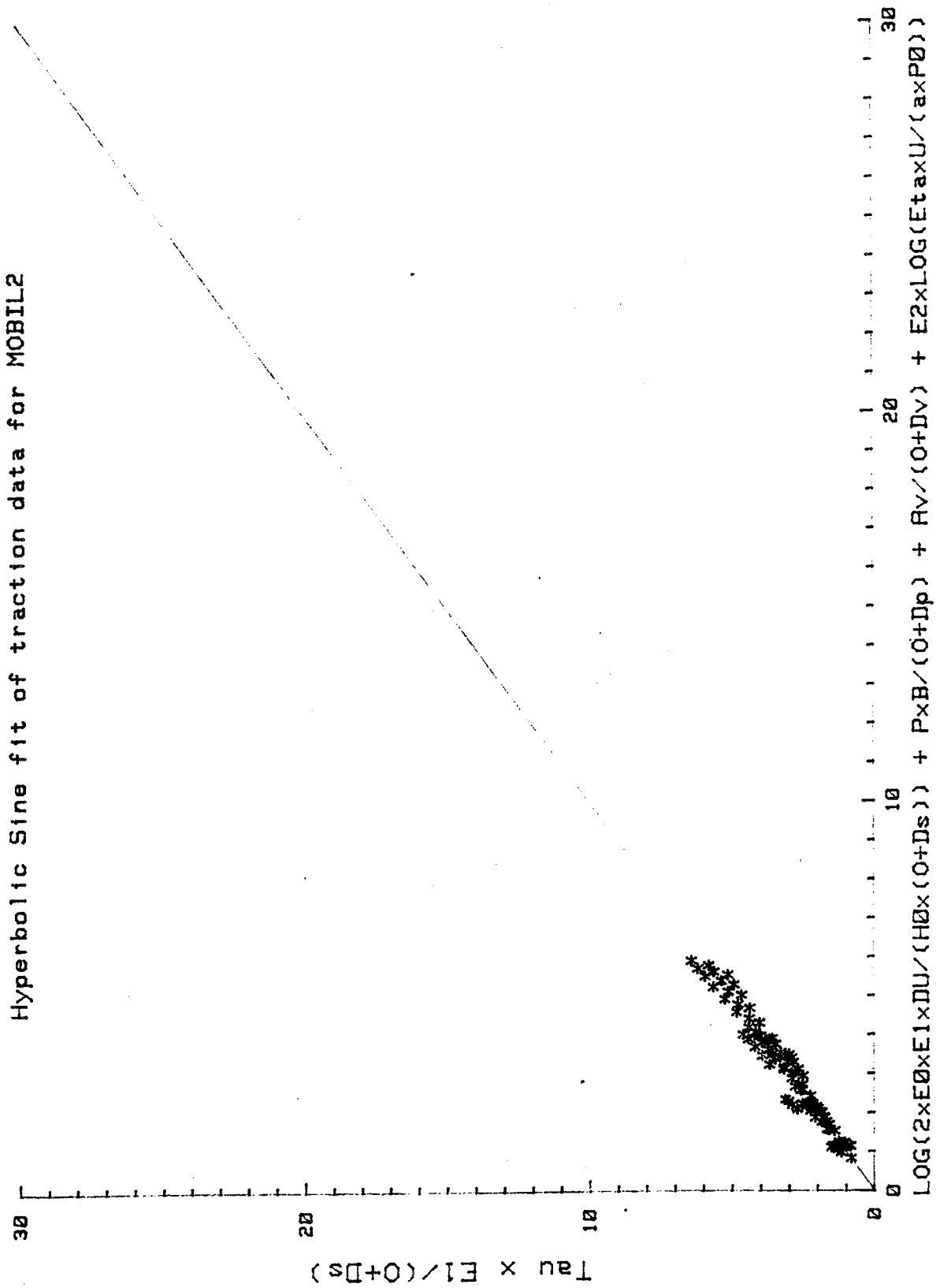
Hyperbolic Sine fit of traction data for MOBIL2
Tau x E1/(O+Ds)
LOG(2xE0xE1xDU/(H0x(O+Ds)) + PxB/(O+Dp) + Av/(O+Dv) + E2xLOG(EtaxU/(axP0)))
0
10
20
30

********** 2.113580736E+11
MULTIPLE TRACTION CURVE DATA ANALYSIS FOR NS-6774 :Prog HYPER Rev# 7.4

Data corrections:
Long. slip YES: Reduced press. YES: Inlet heating YES: Therm. Cond.YES

The following oil properties were used in the analysis:
Viscosity temperature: Av= 798.0 'C Dv=100.0 'C V0= .0000982 Pas
Viscosity Pressure : B=2788.0 'C/GPa Dp=140.0 'C
Thermal Conductivity : K'=1851.0 W/m'C K''=233.0 'C
Eyring Temperatures : Dp 140.0 'C Ds =100.0 'C
**********19:03:52

TEST INCLUDED IN THE MULTIPLE TRACTION DATA ANALYSIS

Test #	Po	Uo	To	Fz	kk	a	Pes
(----)	(GPa)	(m/s)	('C)	(N)	(-)	(m)	(-)
NS_675191R	1.01	10.2	34	200	1.7	.00024	3.96E+02
NS_675193R	1.01	29.7	38	200	1.7	.00024	1.70E+03
NS_675195R	1.27	20.3	37	400	1.7	.00030	7.81E+02
NS_675196R	1.27	30.2	40	400	1.7	.00030	1.19E+03
NS_675197R	1.60	10.2	38	800	1.7	.00037	1.84E+02
NS_675198R	1.60	20.3	39	800	1.7	.00037	5.33E+02
NS_675199R	1.60	30.2	41	800	1.7	.00037	8.44E+02
NS_67519AR	1.93	11.1	39	1400	1.7	.00045	1.46E+02
NS_67519BR	1.93	21.1	41	1400	1.7	.00045	3.97E+02
NS_67519CR	1.93	31.3	45	1400	1.7	.00045	6.20E+02
NS_67519LR	1.60	30.2	81	800	1.7	.00037	2.86E+02
NS_67519NR	1.93	21.0	84	1400	1.7	.00045	9.99E+01
NS_67519OR	1.93	30.5	83	1400	1.7	.00045	2.07E+02

TYPE OF FIT IS 4

BEST FIT CONSTANTS ARE:
E0= 3.1248E-06 E1= 2.9719E-05 E2= 1.7973E-01 E3= 0.0000E+00

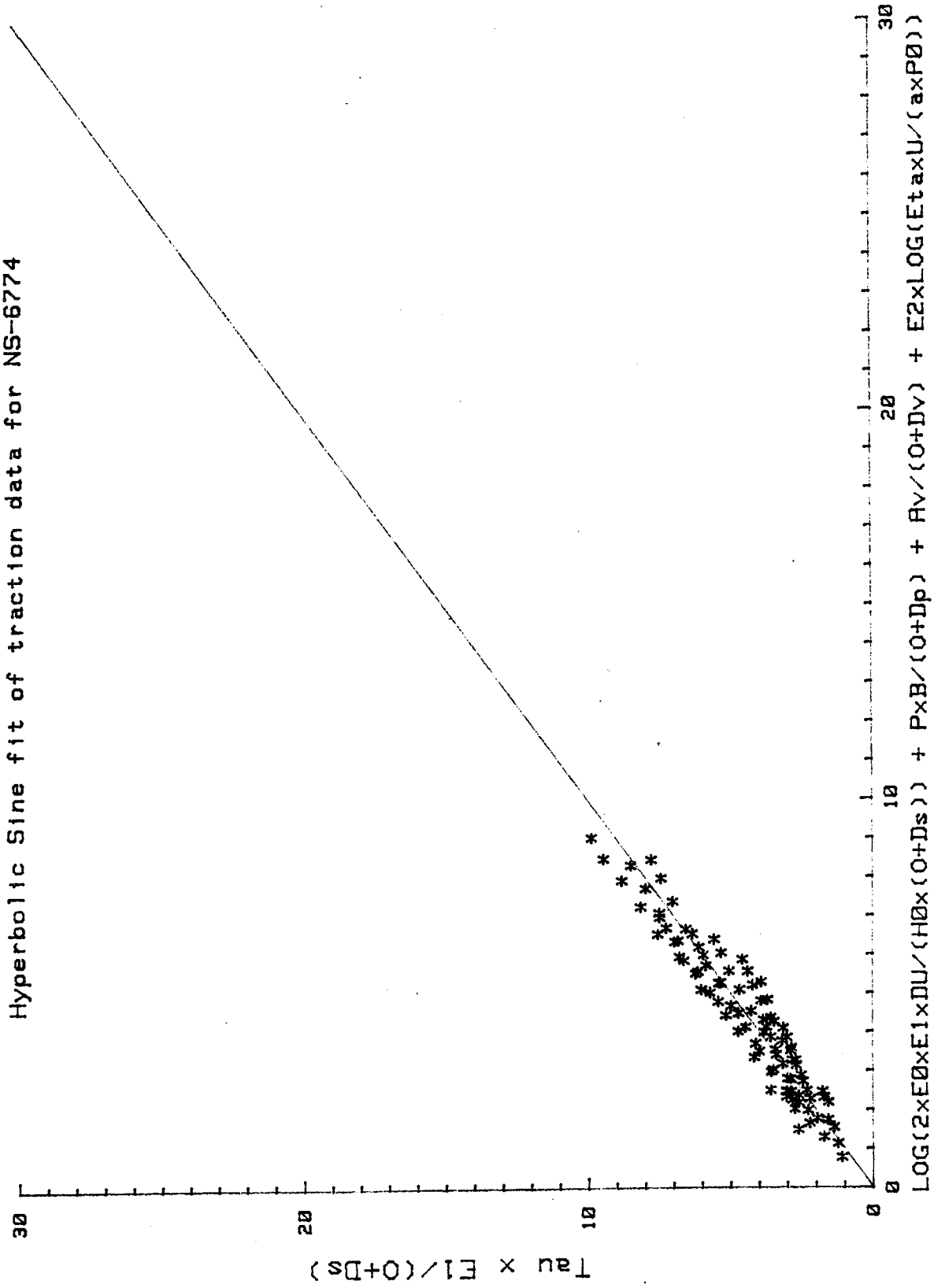
Hyperbolic Sine fit of traction data for NS-6774
Tau x E1/(O+Ds)
LOG(2xE0xE1xDU/(H0x(O+Ds)) + PxB/(O+Dp) + Rv/(O+Dv) + E2xLOG(EtaxU/(axP0))
0
10
20
30

********** 2.113580736E+11
MULTIPLE TRACTION CURVE DATA ANALYSIS FOR ATF220 :Prog HYPER Rev# 7.4

Data corrections:
Long. slip YES: Reduced press. YES: Inlet heating YES: Therm. Cond.YES

The following oil properties were used in the analysis:
Viscosity temperature: Av= 993.0 'C Dv=120.0 'C V0= .0000650 Pas
Viscosity Pressure : B=3095.0 'C/GPa Dp=182.0 'C
Thermal Conductivity : K'=1851.0 W/m'C K''=252.0 'C
Eyring Temperatures : Dp 182.0 'C Ds =200.0 'C
**********18:11:52

TEST INCLUDED IN THE MULTIPLE TRACTION DATA ANALYSIS

Test #	Po	Uo	To	Fz	kk	a	Pes
(----)	(GPa)	(m/s)	('C)	(N)	(-)	(m)	(-)
ATF224CV1R	1.01	10.2	27	200	1.7	.00024	4.79E+02
ATF224CV2R	1.01	20.2	28	200	1.7	.00024	1.26E+03
ATF224CV3R	1.01	30.2	30	200	1.7	.00024	1.89E+03
ATF224CV4R	1.01	20.2	30	200	1.7	.00024	1.19E+03
ATF224CV5R	1.01	10.0	29	200	1.7	.00024	4.24E+02
ATF224CV6R	1.27	9.8	29	400	1.7	.00030	3.19E+02
ATF224CV7R	1.27	20.0	30	400	1.7	.00030	8.73E+02
ATF224CV8R	1.27	30.0	31	400	1.7	.00030	1.38E+03
ATF224CV9R	1.60	10.2	30	800	1.7	.00037	2.15E+02
ATF224CVAR	1.60	20.2	31	800	1.7	.00037	6.36E+02
ATF224CVBR	1.60	30.2	33	800	1.7	.00037	9.80E+02
ATF224CVCR	1.93	10.9	32	1400	1.7	.00045	1.42E+02
ATF224CVDR	1.93	20.6	33	1400	1.7	.00045	4.53E+02
ATF224CVER	1.93	30.5	35	1400	1.7	.00045	7.37E+02
ATF225133R	1.01	25.3	84	200	1.7	.00024	3.34E+02
ATF225134R	1.01	30.1	85	200	1.7	.00024	4.41E+02
ATF225137R	1.27	30.0	82	400	1.7	.00030	3.44E+02
ATF225138R	1.60	10.5	82	800	1.7	.00037	3.06E+01
ATF225139R	1.60	20.3	82	800	1.7	.00037	1.25E+02
ATF22513AR	1.60	30.1	84	800	1.7	.00037	2.54E+02
ATF22513BR	1.93	20.9	83	1400	1.7	.00045	9.40E+01
ATF22513CR	1.93	25.7	83	1400	1.7	.00045	1.40E+02
ATF22513DR	1.93	10.9	81	1400	1.7	.00045	2.58E+01

TYPE OF FIT IS 4

BEST FIT CONSTANTS ARE:
E0= 2.9401E-06 E1= 3.3432E-05 E2= 4.3173E-01 E3= 0.0000E+00

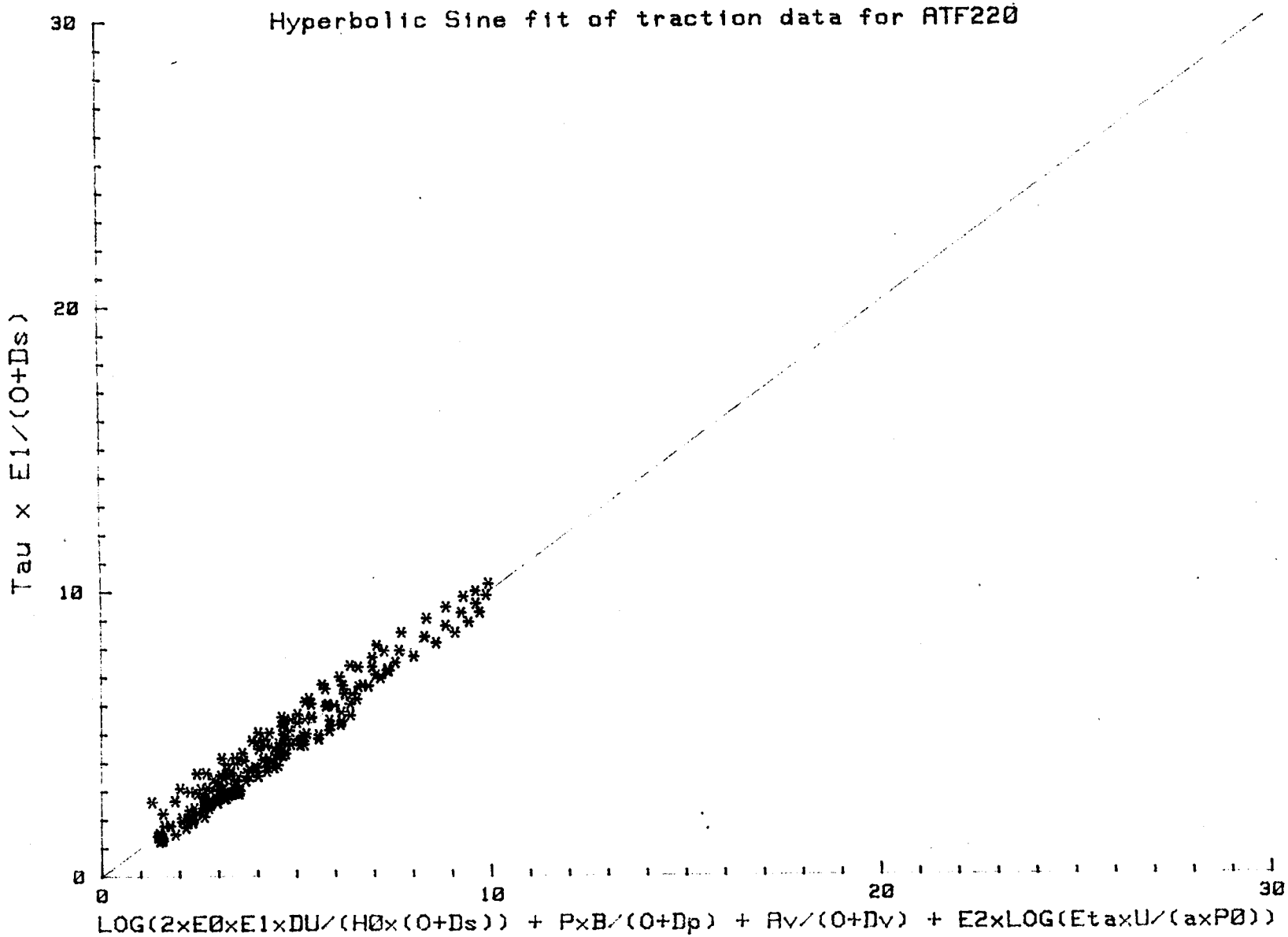
Hyperbolic Sine fit of traction data for ATF220
Tau x E1/(O+Ds)
30
20
10
0
0
10
20
30
LOG(2xE0xE1xDU/(H0x(O+Ds)) + PxB/(O+Dp) + Av/(O+Dv) + E2xLOG(EtaxU/(axP0))

********** 2.113580736E+11
MULTIPLE TRACTION CURVE DATA ANALYSIS FOR ROYCO555 :Prog HYPER Rev# 7.4

Data corrections:
Long. slip YES: Reduced press. YES: Inlet heating YES: Therm. Cond.YES

The following oil properties were used in the analysis:
Viscosity temperature: Av= 865.0 'C Dv=110.0 'C V0= .0000865 Pas
Viscosity Pressure : B=2823.0 'C/GPa Dp=225.0 'C
Thermal Conductivity : K'=1851.0 W/m'C K''=221.0 'C
Eyring Temperatures : Dp 225.0 'C Ds =110.0 'C
**********18:42:17

TEST INCLUDED IN THE MULTIPLE TRACTION DATA ANALYSIS

Test #	Po	Uo	To	Fz	kk	a	Pes
(----)	(GPa)	(m/s)	('C)	(N)	(-)	(m)	(-)
ROYCO5142R	1.01	20.3	34	200	1.7	.00024	8.42E+02
ROYCO5143R	1.01	30.1	36	200	1.7	.00024	1.26E+03
ROYCO5145R	1.27	20.3	36	400	1.7	.00030	5.77E+02
ROYCO5146R	1.27	30.6	39	400	1.7	.00030	8.84E+02
ROYCO5147R	1.60	10.2	36	800	1.7	.00037	1.41E+02
ROYCO5148R	1.60	20.1	38	800	1.7	.00037	3.82E+02
ROYCO5149R	1.60	30.1	40	800	1.7	.00037	6.19E+02
ROYCO514AR	1.93	10.5	37	1400	1.7	.00045	1.04E+02
ROYCO514BR	1.93	20.4	40	1400	1.7	.00045	2.83E+02
ROYCO514CR	1.93	30.2	43	1400	1.7	.00045	4.41E+02
ROYCO514LR	1.60	30.1	79	800	1.7	.00037	2.36E+02
ROYCO514NR	1.93	20.2	79	1400	1.7	.00045	8.19E+01
ROYCO514OR	1.93	30.1	81	1400	1.7	.00045	1.66E+02

TYPE OF FIT IS 4

BEST FIT CONSTANTS ARE:
E0= 1.0050E-06 E1= 1.7647E-05 E2= 4.9829E-01 E3= 0.0000E+00

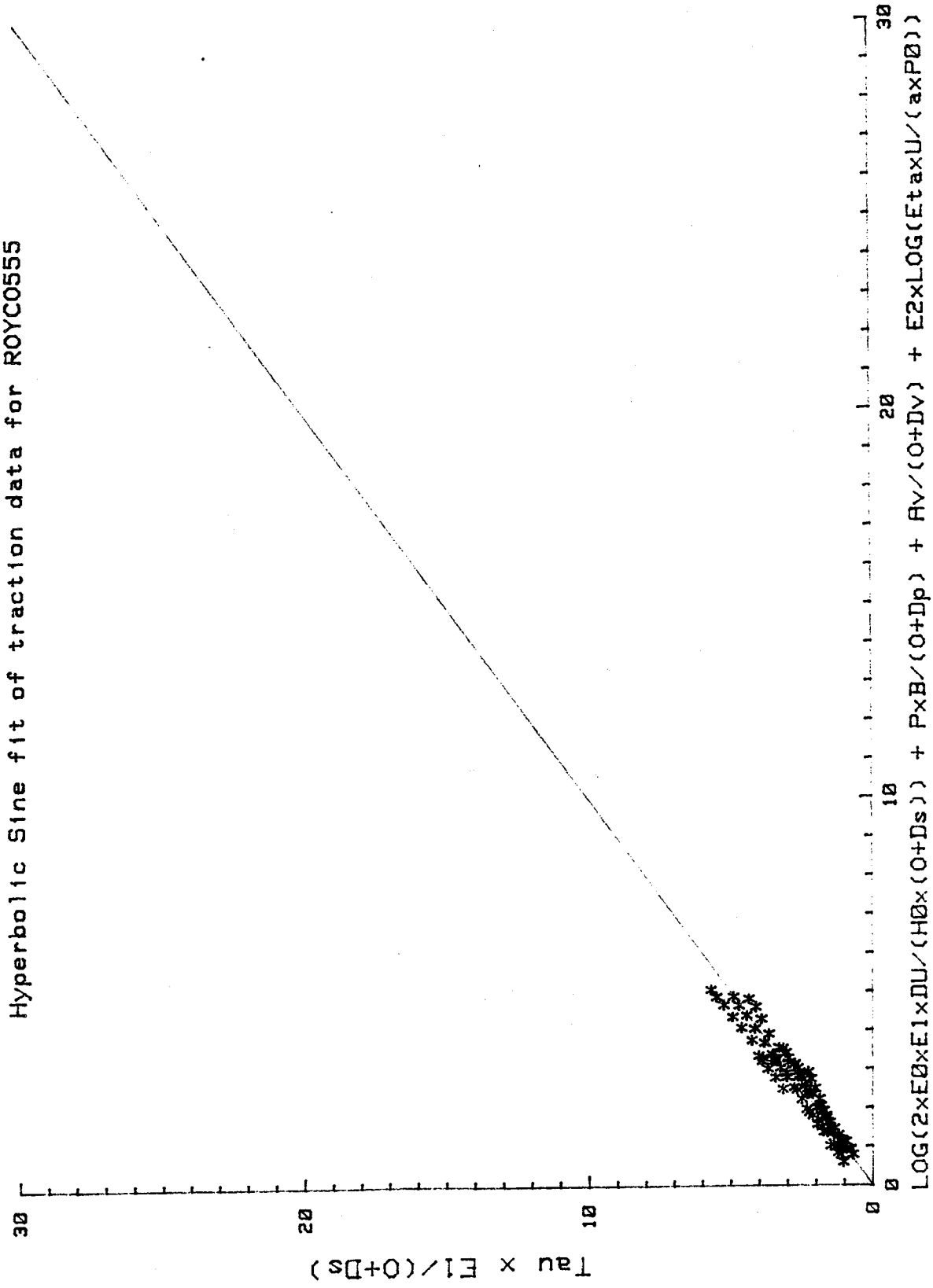
Hyperbolic Sine fit of traction data for ROYC0555
Tau x E1/(O+Ds)
LOG(2xE0xE1xDU/(H0x(O+Ds)) + PxB/(O+Dp) + Av/(O+Dv) + E2xLOG(EtaxU/(axP0))
0
10
20
30

********** 2.113580736E+11
MULTIPLE TRACTION CURVE DATA ANALYSIS FOR SAN50 :Prog HYPER Rev# 7.4

Data corrections:
Long. slip YES: Reduced press. YES: Inlet heating YES: Therm. Cond.YES

The following oil properties were used in the analysis:
Viscosity temperature: Av= 596.0 'C Dv= 65.0 'C V0= .0001816 Pas
Viscosity Pressure : B=3298.0 'C/GPa Dp= 65.0 'C
Thermal Conductivity : K'=1506.0 W/m'C K''=160.0 'C
Eyring Temperatures : Dp 65.0 'C Ds = 65.0 'C
**********20:19:02

TEST INCLUDED IN THE MULTIPLE TRACTION DATA ANALYSIS

Test #	Po	Uo	To	Fz	kk	a	Pes
(----)	(GPa)	(m/s)	('C)	(N)	(-)	(m)	(-)
SAN5044JDR	1.68	11.8	69	400	.9	.00036	1.94E+02
SAN5044JER	1.68	21.3	67	400	.9	.00036	7.12E+02
SAN5044JFR	1.68	31.1	69	400	.9	.00036	1.31E+03
SAN5044JGR	2.11	12.2	72	800	.9	.00046	1.13E+02
SAN5044JHR	2.11	22.8	74	800	.9	.00046	4.52E+02
SAN5044JIR	2.11	34.0	78	800	.9	.00046	9.42E+02
SAN5044JJR	2.55	32.7	87	1400	.9	.00055	4.78E+02
SAN5044JKR	2.55	22.9	90	1400	.9	.00055	1.70E+02
SAN5044JLR	2.55	11.4	91	1400	.9	.00055	3.30E+01
SAN5044K1R	2.55	11.9	37	1400	.9	.00055	4.97E+02
SAN5044K2R	2.55	22.9	50	1400	.9	.00055	9.21E+02
SAN5044K3R	2.55	33.3	57	1400	.9	.00055	1.33E+03
SAN5044K4R	2.11	11.8	38	800	.9	.00046	6.81E+02
SAN5044K5R	2.11	23.4	40	800	.9	.00046	1.68E+03
SAN5044K6R	2.11	32.5	44	800	.9	.00046	2.45E+03
SAN5044K7R	1.68	32.7	41	400	.9	.00036	3.22E+03
SAN5044K8R	1.68	21.4	37	400	.9	.00036	2.18E+03
SAN5044K9R	1.68	11.4	34	400	.9	.00036	1.15E+03

TYPE OF FIT IS 4

BEST FIT CONSTANTS ARE:
E0= 1.0160E-03 E1= 2.8533E-05 E2= 2.7131E-01 E3= 0.0000E+00

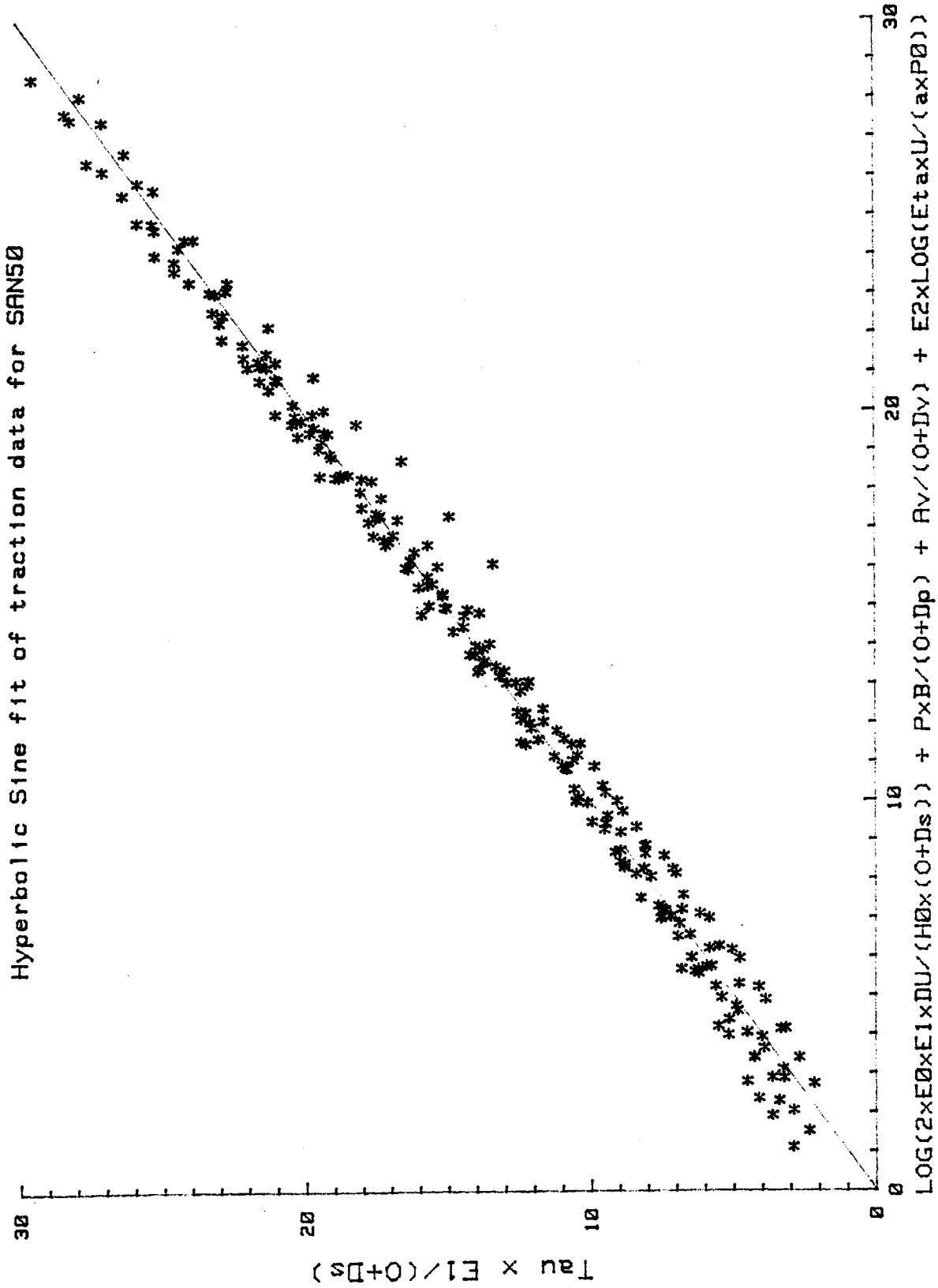
Hyperbolic Sine fit of traction data for SAN50
Tau x E1/(O+Ds)
LOG(2xE0xE1xDU/(H0x(O+Ds)) + PxB/(O+Dp) + Av/(O+Dv) + E2xLOG(EtaxU/(axP0))
0
10
20
30

********** 2.113580736E+11
MULTIPLE TRACTION CURVE DATA ANALYSIS FOR TDF88 :Prog HYPER Rev# 7.4

Data corrections:
Long. slip YES: Reduced press. YES: Inlet heating YES: Therm. Cond.YES

The following oil properties were used in the analysis:
Viscosity temperature: Av= 899.3 'C Dv= 85.0 'C V0= .0001489 Pas
Viscosity Pressure : B=2975.0 'C/GPa Dp= 84.0 'C
Thermal Conductivity : K'=1506.0 W/m'C K''=160.0 'C
Eyring Temperatures : Dp 84.0 'C Ds = 85.0 'C
**********17:43:57

TEST INCLUDED IN THE MULTIPLE TRACTION DATA ANALYSIS

Test #	Po	Uo	To	Fz	kk	a	Pes
(----)	(GPa)	(m/s)	('C)	(N)	(-)	(m)	(-)
TDF882BJ1R	2.55	21.8	67	1400	.9	.00055	2.61E+02
TDF882BJ2R	2.55	30.4	76	1400	.9	.00055	3.84E+02
TDF882BJ3R	2.55	40.5	84	1400	.9	.00055	4.94E+02
TDF882BJ6R	2.11	22.0	69	800	.9	.00046	3.38E+02
TDF882BJ7R	2.11	30.0	67	800	.9	.00046	6.24E+02
TDF882BJ8R	2.11	40.5	69	800	.9	.00046	9.94E+02
TDF882BJBR	1.68	21.3	57	400	.9	.00036	6.91E+02
TDF882BJCR	1.68	30.0	58	400	.9	.00036	1.17E+03
TDF882BJDR	1.68	40.5	60	400	.9	.00036	1.60E+03
TDF882BJGR	1.68	21.3	79	400	.9	.00036	3.19E+02
TDF882BJHR	1.68	30.3	82	400	.9	.00036	5.58E+02
TDF882BJIR	1.68	40.5	85	400	.9	.00036	8.67E+02
TDF882BJLR	2.11	23.4	100	800	.9	.00046	1.97E+02
TDF882BJMR	2.11	31.3	97	800	.9	.00046	2.98E+02
TDF882BJNR	2.11	40.5	98	800	.9	.00046	4.86E+02
TDF882BJQR	2.55	22.8	106	1400	.9	.00055	9.33E+01
TDF882BJRR	2.55	29.7	107	1400	.9	.00055	1.52E+02
TDF882BJSR	2.55	40.5	112	1400	.9	.00055	2.79E+02

TYPE OF FIT IS 4

BEST FIT CONSTANTS ARE:
E0= 2.0059E-03 E1= 2.5249E-05 E2=-1.7702E-01 E3= 0.0000E+00

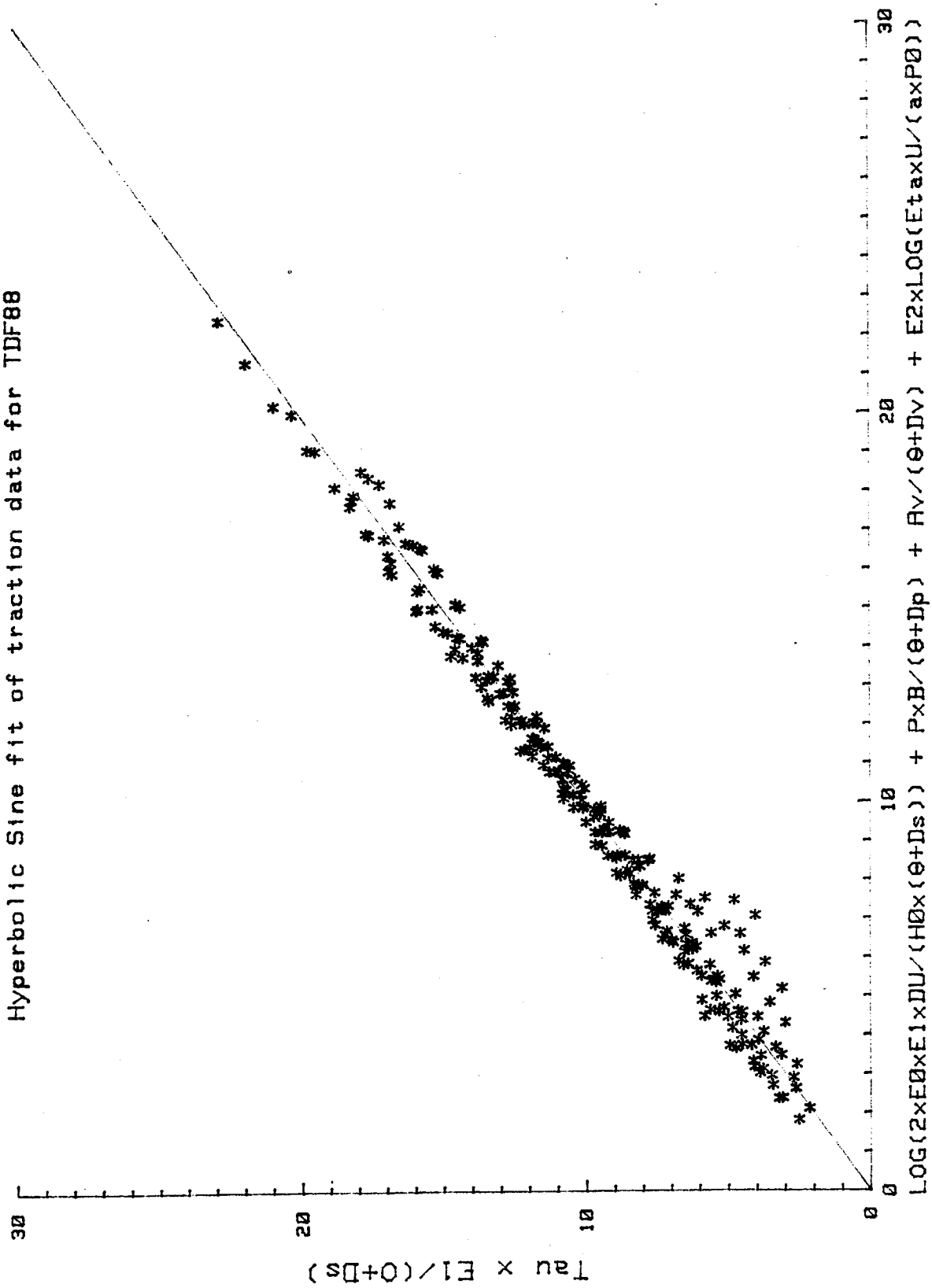
Hyperbolic Sine fit of traction data for TDF88
Tau x E1/(Θ+Ds)
LOG(2xE0xE1xDU/(H0x(Θ+Ds)) + PxB/(Θ+Dp) + Av/(Θ+Dv) + E2xLOG(EtaxU/(axP0)))
0
10
20
30
0
10
20
30

********** 2.113580736E+11
MULTIPLE TRACTION CURVE DATA ANALYSIS FOR RL-714 :Prog HYPER Rev# 7.4

Data corrections:
Long. slip YES: Reduced press. YES: Inlet heating YES: Therm. Cond.YES

The following oil properties were used in the analysis:
Viscosity temperature: Av= 756.0 'C Dv=100.0 'C V0= .0000967 Pas
Viscosity Pressure : B=3363.0 'C/GPa Dp=210.0 'C
Thermal Conductivity : K'=1851.0 W/m'C K''=263.0 'C
Eyring Temperatures : Dp 210.0 'C Ds =100.0 'C
**********19:21:02

TEST INCLUDED IN THE MULTIPLE TRACTION DATA ANALYSIS

Test #	Po	Uo	To	Fz	kk	a	Pes
(----)	(GPa)	(m/s)	('C)	(N)	(-)	(m)	(-)
RL_715182R	1.01	20.3	29	200	1.7	.00024	7.64E+02
RL_715183R	1.01	30.2	31	200	1.7	.00024	1.20E+03
RL_715184R	1.27	10.2	30	400	1.7	.00030	1.82E+02
RL_715185R	1.27	20.2	32	400	1.7	.00030	5.10E+02
RL_715186R	1.27	30.2	33	400	1.7	.00030	8.18E+02
RL_715187R	1.60	10.2	30	800	1.7	.00037	1.31E+02
RL_715188R	1.60	20.2	32	800	1.7	.00037	3.68E+02
RL_715189R	1.60	30.0	35	800	1.7	.00037	5.86E+02
RL_71518AR	1.93	10.6	32	1400	1.7	.00045	9.30E+01
RL_71518BR	1.93	20.7	35	1400	1.7	.00045	2.76E+02
RL_71518CR	1.93	30.5	38	1400	1.7	.00045	4.18E+02
RL_71518NR	1.93	20.9	84	1400	1.7	.00045	5.48E+01
RL_71518OR	1.93	31.1	84	1400	1.7	.00045	1.18E+02

TYPE OF FIT IS 4

BEST FIT CONSTANTS ARE:
E0= 2.7050E-07 E1= 2.4535E-05 E2= 4.9818E-01 E3= 0.0000E+00

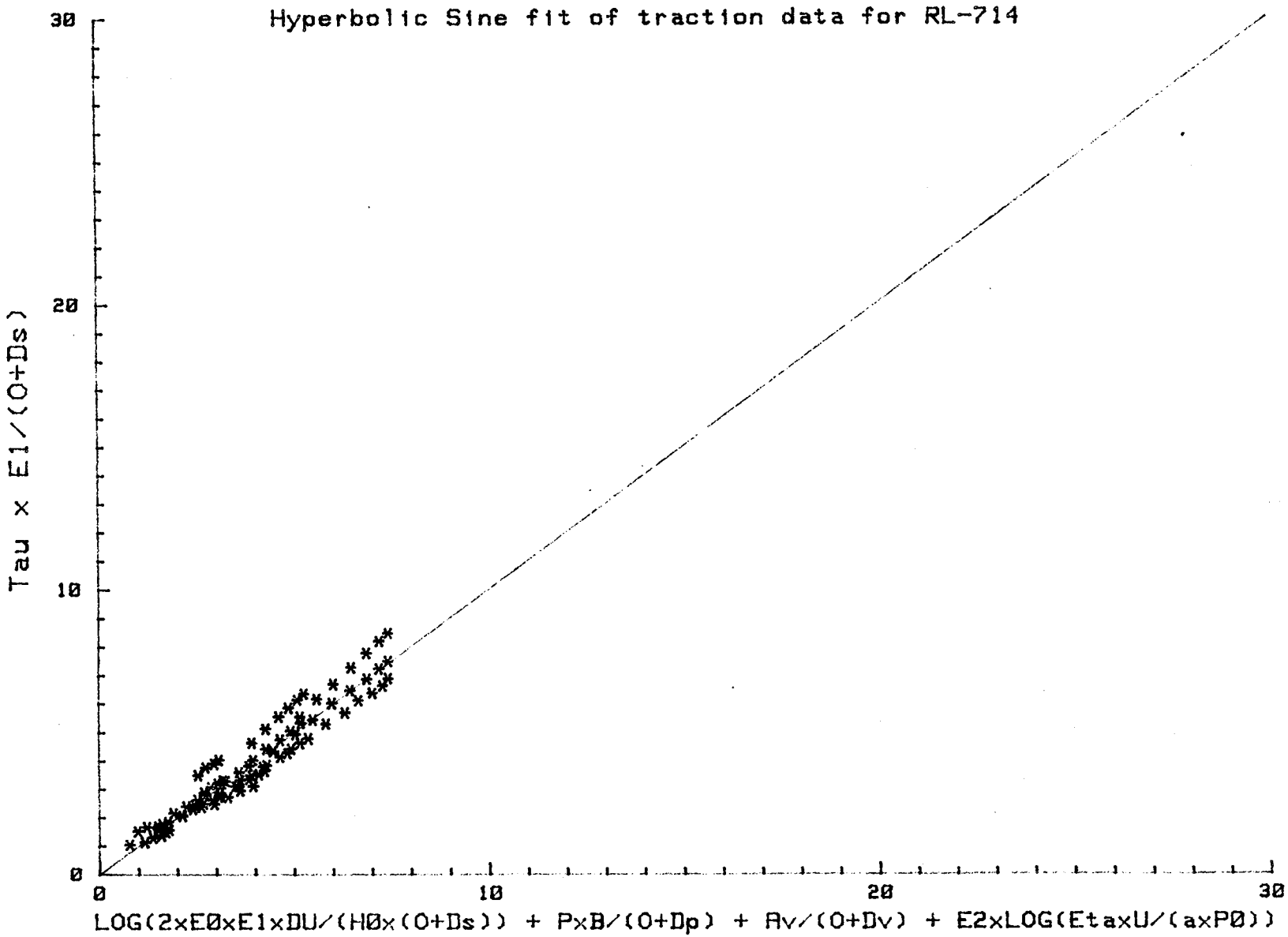
Hyperbolic Sine fit of traction data for RL-714
Tau x E1/(O+Ds)
30
20
10
0
0
10
20
30
LOG(2xE0xE1xDU/(H0x(O+Ds)) + PxB/(O+Dp) + Av/(O+Dv) + E2xLOG(EtaxU/(axP0))